THE UNIVERSITY OF MICHIGAN

INDUSTRY PROGRAM OF THE COLLEGE OF ENGINEERING

THE USE OF NUCLEAR REACTOR RADIATION TO PROMOTE CHEMICAL REACTIONS

George H. Miley

A dissertation submitted in partial fulfillment
of the requirements for the degree of
Doctor of Philosophy in the
University of Michigan
1958

December, 1958

IP-346

Doctoral Committee:

Professor Joseph J. Martin, Chairman
Professor Leigh C. Anderson
Assistant Professor Kenneth F. Gordon
Associate Prefessor Wayne W. Weinke
Professor Robert R. White

TABLE OF CONTENTS

TABLE OF CONTENTS (CONT'D)

LIST OF TABLES

LIST OF FIGURES

LIST OF FIGURES (CONT'D)

LIST OF FIGURES (CONT'D)

NOMENCLATURE

a	a constant, defined as the ratio of the volume average residence time to the actual residence time.
A_g	the number of neutron absorptions per unit mass per second, gm^{-1} sec^{-1}.
A_{SAT}	the saturated activity for gold foil irradiation, counts/sec.
A'_{SAT}	the specific saturated activity, counts/sec 100 mg.
A^{th}_{SAT}	the saturated activity due only to thermal neutrons, counts/sec.
C_g	the number of neutron scattering collisions per unit mass per second, gm^{-1} sec^{-1}.
C.R.	the cadmium ratio
D	the total radiation dose received, kiloreps.
D.R.	the total dose rate due to all forms of radiation, rep/min.
D_γ	the dose rate due to gamma radiation only, rep/min.
E	energy, Mev.
ΔE	the loss of energy by a neutron due to a scattering collision, or alternately the energy band width on a 100-channel analyzer, Mev.
E_g^s	the slow neutron contribution to the total energy absorbed per unit mass per second, Mev/gm sec.
E_g^f	the fast neutron contribution to the total energy absorbed per unit mass per second, Mev/gm sec.
E_g^γ	the gamma radiation contribution to the total energy absorbed per unit mass per second, Mev/gm sec.
$E_g^{e_1-e_2}$	the contribution to the total energy absorption due to neutrons in the energy interval $e_1 - e_2$, Mev/gm sec.
e	the base of the Naperian system of logarithms, 2.71828.

NOMENCLATURE (CONT'D)

F_n	the flow rate for run number n, liters/hr.
G	the total number of feed molecules reacting per 100 ev of radiation energy absorbed.
G(x)	the number of molecules of compound "x" formed per 100 ev of radiation energy absorbed.
g	the foil weight, grams.
h	the pulse height from a 100-channel analyzer.
L	distance, cm.
N_{H_2}	the number of hydrogen atoms per cc.
P	reactor power level, kilowatts.
T	absolute temperature, °R.
t_1	the time a sample or foil is irradiated, minutes.
t_2	the time lapse between irradiating a foil and counting its activity, minutes.
Δt	the foil counting time, seconds.
V	the volume of the reaction vessel, liters.
V_0	the total volume of the system, cm^3.
ϵ	the fraction of the total gamma energy released during a neutron capture reaction which is actually transferred to the chemical system.
λ	the decay constant for a radioactive substance.
μ_γ	the gamma radiation energy absorption coefficient, cm^2/gm.
ρ	density, gm/cm^3.
$\sigma_{s,avg}^{H_2}(e_1-e_2)$	the average microscopic scattering cross-section for hydrogen over the energy range $e_1 - e_2$, barns.

$\Sigma_a^{H_2}$	the macroscopic absorption cross-section for hydrogen, cm^{-1}.
τ	the residence time for a flow system averaged over the actual residence time distribution, minutes.
$\tau_{n,Avg}$	the average residence time for run n calculated by dividing the reaction vessel volume by the flow rate, minutes.
$\varphi_s(\vec{r})$	the slow neutron flux at a point $\vec{r}$, n/cm^2 sec.
φ_s	the slow neutron flux averaged over the reaction system volume, n/cm^2 sec.
$\varphi_F(\vec{r},E)$	the fast neutron flux at point $\vec{r}$ with energy E, n/cm^2 sec.
$\bar{\varphi}_F(E)$	the fast neutron flux of energy E averaged over the reaction system volume, n/cm^2 sec.
$\bar{\varphi}_{Avg}(e_1-e_2)$	the average neutron flux in the reaction system volume in the energy range $e_1 - e_2$, n/cm^2 sec.
$\Phi(>E)$	the total neutron flux above the energy level E, n/cm^2 sec.

I. INTRODUCTION

A. Objectives

The following general objectives were set forth for the present investigation of nuclear reactor radiation effects on chemical reactions:

1) The design and construction of an apparatus suitable for high temperature and pressure flow irradiation experiments in the Ford Nuclear Reactor,

2) the formulation of safe operating procedures for this apparatus, and

3) an exploratory study of several different organic chemical reactions.

Exploratory work, it was hoped, would not only provide preliminary reaction data but also be a test of the operation of experimental equipment and procedures.

B. Long-Range Objectives

The present work is considered to be the initial step in a long-range research program aimed at the development of an integrated chemical plant and nuclear reactor. Such a plant is visioned by the McKinney Panel[15] "as a complex and highly integrated unit. At the heart of the process is an atomic reactor. Nuclear heat will drive endothermic chemical reactions that will probably be catalyzed by atomic radiation. By-product power to operate the plant equipment will be derived from the nuclear-fired process-steam boilers. Fission products may be recovered for sale for tracers or other applications."

Such a plant, in fact, may not be too far from reality. The Standard Oil Company of New Jersey, long-time holders of a basic patent

covering the use of pile radiation to promote chemical reactions[6], has just recently released the details of a proposed reactor design which would serve to both irradiate a process stream and produce process steam.[49] Preliminary estimates for this reactor indicate irradiation costs are much lower than those for a Co^{60} source or a linear electron accelerator.

In addition to the more immediate practical aspect, research in the area of radiation-induced chemical reactions is apparently leading toward a better understanding of the mechanism of certain chemical reactions. Already, many basic theories concerned with the nature of thermal cracking of organics have been drastically changed or revised as the result of radiation research.[40]

C. Interaction of Reactor Radiation and Organic Systems

Radiation energy is transferred to a chemical system placed in a nuclear reactor through the interaction of both gamma photons and neutrons with the system. The mechanism and quantitative description of the promotion of chemical reactions by gamma radiation have been covered in a number of articles, and a selected list of references is included in the bibliography.[7,8,29,35,44]

On the other hand, the promotion of chemical reactions with neutrons has received less attention, and will be briefly reviewed. The entire literature dealing with nuclear reactor physics is concerned with the interaction of neutrons and matter[24]; however, the actual mechanisms by which such interactions lead to chemical reactions have been discussed in only a few articles.[9,10,50]

For the purposes of this discussion, attention is mainly confined to the irradiation of organic systems, and neutrons are divided into two classes, fast and slow.

(1) Slow Neutrons

Since most organic compounds have bond energies of about 4 ev, neutrons possessing less energy than this cannot produce a bond rupture by a simple scattering mechanism and hence are termed "slow neutrons". The energy region included in this definition is broader than that usually associated with thermal neutron (average energy of 0.025 ev).

However, slow neutrons may transfer energy to a system through absorption. Although, in general, free radicals and ions may be produced in numerous secondary events as well as the primary neutron capture[50], the main source of ionization in pure organic materials is due to the 2.17 Mev gammas given off when the neutrons are captured by hydrogen.[10] Hydrogen has a relatively large thermal absorption cross-section (0.33 barns as compared to 0.0032 barns for carbon), so that the resulting gamma intensity can be quite high. The energy-input due to this mechanism may be estimated by noting that A_g, the number of absorptions per unit mass per second, is given by

$$A_g = \bar{\Phi}_s \frac{\Sigma_a^{H_2}}{\rho} \qquad (1)$$

where $\Sigma_a^{H_2}$ is the macroscopic absorption cross-section for hydrogen, ρ is the density of the material, and $\bar{\Phi}_s$ is defined as the thermal flux averaged over the reaction vessel volume. Thus

$$\bar{\Phi}_s = \frac{1}{V}\int \Phi_s(\vec{r})\, dV \qquad (2)$$

where $\Phi_s(\vec{r})$ represents the thermal flux at a point r in a reaction system with volume V. If all of the gamma energy thus produced were absorbed in the system, Expression (1) might simply be multiplied by the energy of the gamma's, E_γ, to obtain the energy input. However, some correction must be made for gamma leakage, so that E_g^s, the energy input per unit mass per second due to the thermal neutron flux, $\bar{\Phi}_s$, is given by

$$E_g^s = \bar{\Phi}_s \frac{\Sigma_a^{H_2}}{\rho} E_\gamma \epsilon \qquad (3)$$

where ϵ is a probability factor representing the fraction of the total gamma energy released which is actually transferred to the system. is, then, a function of the geometry of the system, and $\epsilon \to 1$ as the size of the system approaches infinity. For an actual case, the evaluation of ϵ is complicated; however, for the present work an order of magnitude approximation will be made by assuming that

$$\epsilon = \left(1 - e^{-\mu_\gamma \rho L}\right) \qquad (4)$$

where L is some characteristic length of the system, μ_γ is the energy absorption coefficient for gamma radiation of energy E_γ, and e is the base for the Naperian system of logarithms. A conservative estimate for L may be obtained for many systems by computing the radius of a sphere of volume equal to the volume of the experimental vessel.

Two assumptions are inherent in Equation (4). Radiation re-entering the system due to back-scattering from surroundings is neglected.

Also, radiation entering the system due to neutron absorptions external to the system is not considered. The latter assumption deserves special attention. The use of Equation (4) assumes the point of view that the energy of interest is that which would be transferred to the system if it were suspended in space with a neutron flux $\bar{\Phi}_S$ passing through it. Thus, gamma radiation entering the system as the result of thermal neutron capture in the vessel wall or nuclear reactor water is not differentiated from gammas originating with the fission products in the reactor core.

(2) Fast Neutrons

Although fast neutrons also undergo some capture reactions, by far the greatest energy transfer in organic systems occurs as the result of hydrogen recoils.[10] In slowing down, the fast neutrons undergo numerous elastic scattering collisions, primarily with the nuclei of hydrogen atoms which then recoil and are ejected as fast-moving protons. These protons interact with electrons in the surrounding matter, producing ionization and excitation.

C_g, the number of scattering collisions occurring per unit mass per second is given by

$$C_g = \int_E \bar{\Phi}_F(E) \frac{\Sigma_s^{H_2}(E)}{\rho} dE \qquad (5)$$

The integration is performed over all energies greater than thermal. $\Sigma_s^{H_2}(E)$ represents the scattering cross-section for hydrogen for neutrons of energy E, and $\bar{\Phi}_F$ is the fast neutron flux of energy E

averaged over the reaction vessel volume, such that

$$\overline{\Phi}_F(E) = \frac{\int_V \Phi_F(\vec{r}, E)\, dV}{V} \tag{6}$$

where $\Phi_F(\vec{r}, E)$ is the neutron flux of energy E at a point $\vec{r}$ in the volume under consideration, V.

It can be shown[24], that the average fractional energy lost by a neutron during an elastic scattering with hydrogen, $\frac{\Delta E}{E}$, is given by

$$\frac{\Delta E}{E} = 1 - \frac{1}{e} \tag{7}$$

where e is base for the Naperian system of logarithms.

Equations (5) and (7) may now be combined to obtain E_g^F, the energy per unit mass per second transferred to the chemical system through hydrogen scatter collisions.

$$E_g^F = \left(1 - \frac{1}{e}\right) \int_E \overline{\Phi}_F(E)\, \frac{\Sigma_s^{H_2}(E)\, E\, dE}{\rho} \tag{8}$$

The exact evaluation of E_g^F from Equation (8) requires a knowledge of the fast neutron spectrum throughout the chemical system of interest. However, an order of magnitude approximation of Expression (8) which simplifies calculations, may be obtained by dividing the fast neutron energy region into a series of small energy ranges, $e_1 - e_2$, $e_2 - e_3$, ..., in which the flux and cross section do not change rapidly. Then, average values for the flux and cross-section may be used for each energy

range, and Equation (8) is fairly well approximated by a sum such as

$$E_g^F = E_g^{e_1 - e_2} + E_g^{e_2 - e_3} + E_g^{e_3 - e_4} + \cdots \qquad (9)$$

where

$$E_g^{e_1-e_2} = \overline{\Phi}_{AVg}(e_1-e_2)\ \sigma_{s,AVg}^{H_2}(e_1-e_2)\ \frac{N_{H_2}\ E_{AVg}^{e_1-e_2}}{\rho}\left(1 - \frac{1}{e}\right) \qquad (10)$$

$E_g^{e_1-e_2}$ is the energy input per unit mass per second due to neutrons in the energy range e_1-e_2, and $\overline{\Phi}_{AVg}(e_1-e_2)$, $\sigma_{s,AVg}^{H_2}(e_1-e_2)$ and $E_{AVg}^{e_1-e_2}$ represent average values in this energy range for the neutron flux, microscopic hydrogen scattering cross-section, and neutron energy respectively. N_{H_2} is the number of hydrogen atoms per cubic centimeter, and it will be noted that the product $N_{H_2}\sigma_{s,AVg}^{H_2}(e_1-e_2)$ is equivalent to an average macroscopic hydrogen scattering cross-section. Equation (8) shows that the energy transfer due to fast neutrons is a direct function of the neutron energy spectrum. Thus, this energy transfer depends on the nuclear characteristics of the pile and also the actual position under consideration in the piles.

The scattering cross-section changes rapidly with energy, especially at low energies.[24,33] For example, at neutron energies around 10 ev, $\sigma_s^{H_2}$ is about 20 barns, but it increases to 80 barns for very slow neutrons. At 1 Mev, $\sigma_s^{H_2}$ is about 4.5 barns.

A very high energy neutron ($>$0.5 Mev) can transfer a large amount of energy to the system during each scattering collision. However, because the scattering cross-section decreases with energy and

because the fast flux drops off rapidly with energy[32], the total energy transfer due to neutrons of energies above 0.5 Mev is not much larger than that due to lower energy neutrons.[10]

(3) Combined Absorption Energy

If D_γ represents the gamma dose rate in rep/min, then E_g^γ, the energy absorbed per unit mass per unit time may be obtained by a simple conversion factor. Therefore, E_g^γ in Mev per gram per sec is given by

$$E_g^\gamma = 9.6 \times 10^5 D_\gamma \tag{11}$$

The total energy absorbed per unit mass per second, E_g, can now be calculated by adding the individual energy contributions given by Equations (3), (8) and (11). Therefore,

$$E_g = E_g^S + E_g^F + E_g^\gamma$$

$$= \bar{\Phi}_S \frac{\Sigma_a^{H_2}}{\rho} E_\gamma \left(1 - e^{-\mu_\gamma \rho L}\right)$$

$$+ \sum_{4ev}^{10Mev} \bar{\Phi}_{Avg} \frac{\sigma_{S,Avg}^{H_2} N_{H_2} E_{Avg}}{\rho} \left(1 - \frac{1}{e}\right)$$

$$+ 9.6 \times 10^5 D_\gamma \tag{12}$$

In order to obtain a feeling for the relative magnitude of these quantities, consider the case where

$$D_\gamma = 30{,}000 \text{ R/min}$$

$$\bar{\Phi}_S = 1 \times 10^{11} \text{ n/cm}^2 \text{ sec}$$

$$\bar{\Phi}_F = 1 \times 10^{10} \text{ n/cm}^2 \text{ sec } (\geq 0.5 \text{ Mev})$$

These are reasonable values for a location 2 inches from the face of the Ford Nuclear Reactor at 100 kw (see Chapter III). To simplify the fast neutron calculation, it will be assumed that 40% of the fast neutron energy is absorbed in the range 0.01 to 0.5 Mev and 60% in the range 0.5 Mev to 1.0 Mev. This is a fairly good assumption for a graphite-reflected, water-cooled reactor.[10]

In addition, a 5.3 ℓ. reaction vessel containing pure n-heptane is assumed. The value of μ_γ is approximated by using the coefficient for water.[21,22] Then, directly substituting into Equation (12) (see Appendix B for the details of this calculation)

$$E_g = E_g^S + E_g^F + E_g^\gamma$$

$$= (7.9 \times 10^8 + 1.6 \times 10^{10} + 2.9 \times 10^{10}) \text{ Mev/gm sec}$$

$$= 4.6 \times 10^{10} \text{ Mev/gm sec}$$

$$= 2.9 \times 10^6 \text{ R/hr}$$

It is seen that E_g^S, the contribution due to slow neutrons, is approximately 1.7% of the total energy transferred while the fast neutron contribution, E_g^F, is about 35% and the gamma contribution is about 63% of the total.

It should be emphasized that the percentages calculated above are only intended to indicate the order of magnitude of the various

contributions. The actual percentages vary greatly with location within a reactor. In a swimming pool type reactor, such as the Ford Reactor, the thermal neutron flux drops off much more rapidly with distance from the core face than does the gamma flux. The fast neutron flux decreases even more rapidly than the thermal flux. As a result, for distances greater than 2 inches from the core, the neutron contribution to the total radiation energy transferred to a system is much less than indicated in the above calculation and can be neglected altogether for distances greater than one foot.

However, if a large fast neutron flux is available, as is the case in some types of nuclear reactors, the energy transfer due to fast neutrons may even be greater than that due to gamma radiation. For example, calculations and also calorimetric measurements for the ORNL Graphite Reactor indicate the following energy breakdown for materials of composition $(CH_2)_n$:[10,56,57]

% of Total Energy	Source
65 - 70	Fast Neutrons
25 - 30	Gammas
2 - 10	Thermal Neutrons

Thus, fast neutrons can account for a sizable portion of the energy transferred to a chemical system, and this method of transfer must not be overlooked in nuclear reactor experiments.

In addition to the size of the energy transfer, it should be emphasized that, as already discussed, the mechanism of interaction

with a chemical system for fast neutrons is different from that for either slow neutrons or gamma radiation. Slow neutrons produce ionization as the result of secondary gamma radiation emitted when such a neutron is absorbed by a hydrogen atom. Hence, chemical reaction effects due to slow neutrons should be equivalent to those produced by gamma radiation. On the other hand, fast neutron interactions result in ionization due to fast-moving recoil protons. This mechanism is completely different from that in the case of gamma radiation, and although the end results of all interactions are the same (ionization and excitation), the difference in ionization trace density could conceivably affect chemical yields. Thus, the question of correspondence of over-all chemical effects (that is, correspondence of "G" values and product distribution) cannot be resolved without resort to experiment.

D. Previous Work Pertaining to the Radiation Chemistry of Organic Systems

Although the radiation chemistry of organic compounds is still a relatively new field, the literature pertaining to this field is extensive. Hence, the present survey must be limited to a consideration of some general or survey articles and comments about experimental work in areas of particular interest, i.e., the radiation decomposition of hydrocarbons and the utilization of reactor radiation.

(1) General Articles

The literature contains a number of survey articles concerned with the room-temperature irradiation of organic system. Lemmon and Tolbert have published one of the most complete summaries.[38] In it,

"G" values, along with references, are listed for about one hundred compounds. Collision and Swallow[18] are authors of a similar summary entitled "The Action of Ionizing Radiation on Organic Compounds" but arrange their material under the headings of various reactions studied, i.e., polymerization, oxidation, dehydrogenation, etc. Sachs[52] arranges his article according to the type of radiation used, i.e., alpha, beta, gamma, and X-rays. Radical yields obtained in the radiolysis of many hydrocarbons have been tabulated.[68]

Radiation-induced polymerization has received much interest, and a number of articles have appeared dealing specificly with this subject. Included among these are review articles by Martin[46], Manowitz[42], the Rock Island Arsenal Lab Staff[51], and Wahl[67]. Extensive work has been reported, mainly by Charlesby at Harwell[11,12,13,14], on the cross-linking and degradiation of long-chain polymers.

(2) Specific Systems

If consideration is limited to the radiation decomposition of organic compounds, the experimental variables which may affect results include:

a. The system, i.e., the type and purity of organic compounds as well as the amount and type of dissolved gases such as oxygen, etc.

b. Temperature.

c. Pressure.

d. Phase, i.e., liquid, gas, two phase, etc. (This variable is, of course, not independent but is determined by variables a through c).

e. Type of radiation, i.e. electrons, neutrons, gamma rays, alpha particles, etc.

f. Energy level of the radiation, i.e., fast neutrons versus slow, X-rays as gamma rays, etc.

g. Radiation intensity.

h. Total radiation dose.

i. Mixing in the system.

j. The presence of a catalyst as well as radiation, i.e., the addition of some catalyst such as platinum to the reaction vessel, etc. (The reaction vessel wall itself, as well as dissolved air, may serve as a catalyst in some systems.)

Although all of the variables listed may not be important for a particular experiment, it is still apparent that the large number of possible variables lead to a very complex situation. To present, a complete study of radiation decomposition as a function of these many variables has not been performed. It appears that much more experimental data will have to be accumulated in many of these areas before a comprehensive theory can be formulated.

The effect of temperature on radiation decomposition has only recently received attention. Most of the work reported in the literature has been at room temperature and pressure, and the status of the results from eight types of organic compounds is summarized in the table below taken from Reference 38.

TABLE I

SUMMATION OF RADIATION CHANGES IN ORGANIC COMPOUNDS (FROM REFERENCE 38)

System	Major "G" Values Determined[a]
Saturated hydrocarbons	$-M$[b], 4-9; H_2, 2-6; CH_4, 0.06-1
Unsaturated aliphatic and alicyclic hydrocarbons	Polymer[c], 10-2000; cross-link, 6-14; $H_2 \sim 1$; CH_4, 0.1-4.0
Aromatic hydrocarbons	Polymer, ~ 1; H_2, 0.04-0.4; CH_4, 0.001-0.08
Halides	$1/2I_2$, 2-4; HI, 0; 1/2Br, 0-0.5; HBr, 0-15; $1/2Cl_2$, 0; HCl ~ 4
Alcohols	-M, 3-12; H_2, 1-3.5; hydrocarbons, 0.5-1.5 carbonyl, 1-2; vic-alycol, 0.5-1.5
Carboxylic acids	-M, > 0.3; CO_2, 0.5-4; CO, < 0.5; H_2, 0.5-2
α-Amino acids	-M, 3-10; $NH_3 \sim 1$; $CO_2 \sim 1$; amine ~ 1
Quaternary ammonium salts	-M, 1-1000; amine, 1-1000

[a] G value $\equiv$ number of a specified ion, atom, radical, or molecule involved in the radiation process/100ev. of energy absorbed.

[b] "M" represents the starting material that is permanently altered.

[c] G (polymer) is calculated as though it were for the reaction G(M nonvolatile products)

As shown in Table I, the principle products from the low-temperature radiation decomposition of the saturated hydrocarbons are hydrogen and traces of light hydrocarbons. With the exception of long chain polymerization reactions, all "G" values are low (< 10).

Most studies, as those summarized in the above table, are concerned with the analysis of the gaseous products from irradiated organics. N-hexane is one of the few compounds for which both liquid and vapor analyses have been published. Dewhurot[19] used partition chromatography to study the liquid products resulting from the cobalt-60 irradiation of μ-hexane (total dose, 1.5×10^8 Rep). A total of 16 products is reported, from which n-pentane, 3-methyl pentane, n-dodecane, isomoric dodecanes, and hexane have been positively identified. Krenz[37] has determined the following G values for the gaseous products from the cobalt-60 irradiation of n-hexane:

$$G(H_2) = 4.89 \pm 0.2$$

$$G(CH_4) = 0.41 \pm 0.1$$

$$G(C{=}C) = 4.0 \pm 0.2$$

$$G(C_2H_6) = 0.69 \pm 0.1$$

Traces of three, four, and five carbon compounds were noted in addition to the above compounds.

Recently, a few experiments dealing specifically with high-temperature cracking have been described.[17,40,58]

Snow, Uhl, and Lewis[58] have studied the effect of gamma radiation on the cracking of normal-heptane in the temperature range 620°F to 900°F. All runs were at 1000 p.s.i.g. and the mole ratio of hydrogen to

heptane in the feed varied from 0 to 8. Doses up to 10^5 rep were obtained. Snow, et al., conclude from this work that "under the conditions and radiation doses used, radiation-induced reactions are of small magnitude compared to thermally-induced reactions."

Perhaps the most significant study in the field of high-temperature radiation chemistry is the work performed by Baeder, et al.[40] They used both cobalt-60 and nuclear reactor sources to study the radiation-induced cracking of n-hexadecane, methylayclohexane, and some crude oil stocks in the temperature range 600°F to 950°F. All runs were at atmospheric pressure. In sharp contrast to the low temperature work already described (G's < 10), radiation yields (i.e. G values) as high as 10^5 - 10^6 are reported for the gamma irradiation of Texas crude and methylcyclohexane from 850 to 950°F and 10^3 - 10^4 from the pile irradiation of n-hexadecane from 600 to 850°F. These extremely high G values indicate a surprisingly long chain reaction, a mechanism which had not previously been expected. The product distribution, instead of being predominantly hydrogen as in low temperature work, was found to resemble the distribution for thermal cracking. Baeder, et al., propose that these results can be explained by assuming the Rice-Herzfeld radical mechanism applies. It is predicted that the G value will switch from an increasing to a decreasing function of temperature at very high temperatures.

Colichman and Gerche[17] have performed polyphenyl irradiations with 1-Mev electrons at 86, 527, and 662°F. They found that the G(gas) increased with temperature, e.g., about a four-fold increase over the temperature range for p-terphenyl.

A typical set of data is shown below. As indicated, there is a slight decrease in hydrogen yield and corresponding increase in light hydrocarbons as the temperature is increased.

TABLE II

SUMMARY OF DATA FROM 1-MEV ELECTRON BOMBARDMENT OF p-TERPHENYL (REFERENCE 17)

Compound	Temp. (°C)	Energy Input (Watt hr/gm)	Gas Yield (Moles x 10^5)	Composition, % by Volume							
				H_2	CH_4	C_2H_6	C_2H_4	C_2H_2	C_3H_8	(1)	(2)
p-terphenyl	30	99	3.42	92.2	2.9	0.4	-	0.9	-	0.3	3.3
	350	99	13.8	86.1	5.3	2.0	1.2	2.3	0.7	0.5	1.9

Notes: (1) Benzene

(2) Undetermined

At the other end of the temperature scale, a few low-temperature irradiations have been carried out. Charlesby[14], while studying the decomposition of polyisobutylene, found that 45 ev are required per fracture at -196°C, 20 ev at room temperature, and 11 ev at 70°C. In an effort to explain this temperature effect, Charlesby has postulated a two-stage energy-absorption and disintegration process. Due to the possibility of trapping free radicals, added emphasis has recently been given to low-temperature work. For example, Mesrobian and co-workers[48] found that no polymerization took place until samples of acrylamide monomer were brought to room temperature after cobalt-60 irradiation at -18°C.

The importance of the dose received by a system has been demonstrated in experiments. Honig[31] has shown vividly that the possible

reconversion of products after prolonged exposure can drastically effect results. The graph reproduced below shows the reconversion of products in methane irradiation.

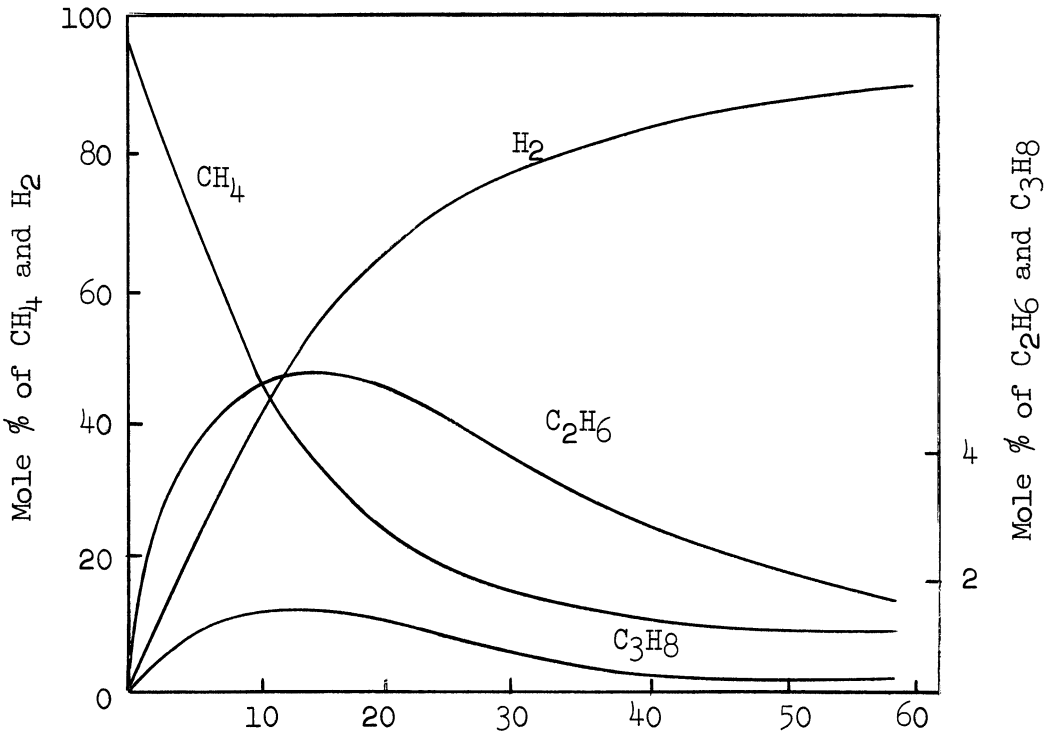

Figure 1. Reconversion in Methane Bombardments from Data by Honig[31].

The graph represents an analysis of the gaseous phase only, thus the disappearing hydrocarbons have polymerized to form liquid products. If radiation were continued long enough, the gas phase would contain only hydrogen.

It is interesting to note a similar phenomenon observed by Charlesby[12] in the irradiation of long chain paraffins. A typical graph is shown below

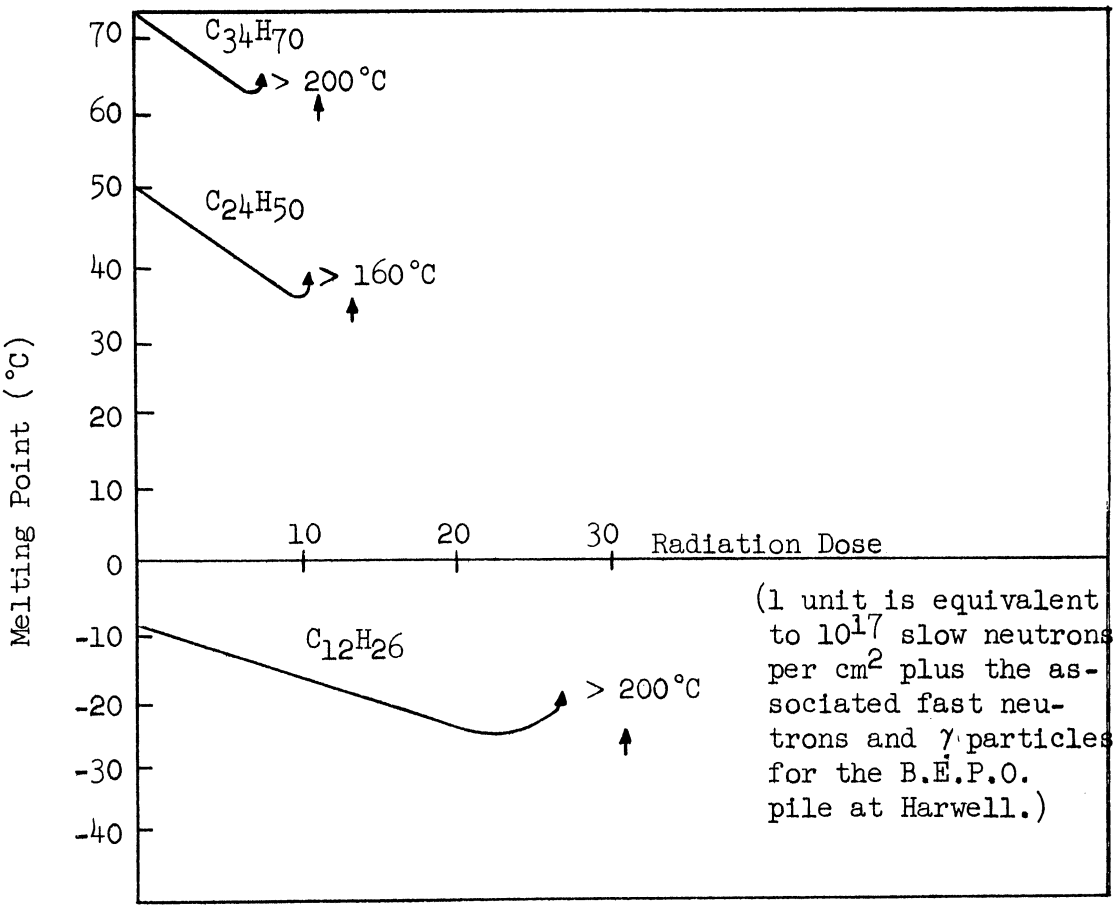

Figure 2. Change of Melting Point for the Irradiation of Long Chain Paraffins. From Data by Charlesby.[12]

The decrease in melting point of the hydrocarbon is attributed to the fracture of the main paraffin chain, which produces lower paraffins. The sudden alteration in melting point corresponds to the formation of a "gel" by cross linking, the theoretical molecular weight of the gel being infinite. Colichman and Gercke[17] found that the total G value for gas formed in the irradiation of polyphenyls decreased with increasing dose in the temperature range 30°C to 350°C.

The dependence of results upon the type of radiation used has received some experimental attention, but more work appears necessary before a comprehensive theory can be formulated. Evidence cited by Henley, et al.,[30] indicates that radiation-induced chemical reactions in solution are dependent on the rate of energy loss of the radiation and therefore upon the type of radiation. A typical example of such a reaction is the decomposition of 0.8 N Sulfuric Acid solution which has been studied with radiations ranging from CO-60 gamma rays to the heavy particle recoils from the $B^{10}(n, \alpha)\ Li^{7}$ reaction. A marked increase in molecular products was noted along with a corresponding decrease in radical yields with increasing rate of energy loss.

On the other hand, a number of experiments with hydrocarbon irradiation indicate that hydrocarbon decomposition reactions, as opposed to solution reactions, are less dependent upon the type of radiation used. Hydrogen yields from cyclohexane irradiated with 2 Mev electrons have been found to be comparable with yields from 35 Mev alpha particle irradiations.[54] Honig and Sheppard[31] performed exhaustive studies comparing the effects of deuterons and alpha particles on methane. They concluded that, although results do not confirm complete identity of the

chemical effects, "sufficient agreement is shown to indicate that the deuteron beam is a valuable adjunct to other natural radioactive sources." Keenam[36] has studied the radiolytic decomposition of liquid hydrocarbons (cyclohexane, methylayclohexane, 2,4-dimethypentane and n-heptane) with 1 Mev electrons, reactor radiation, and recoil particles from the $\beta^{10}(n, \alpha)$ Li^7 reaction. The same products were obtained from all irradiations; however, the heavy recoil particles caused a shift in product distribution which is attributed to a molecular process associated with the track effect. Data from experimental work by Colichman and Gercke[17], and Marion and Burton[43], show equivalent effects for reactor radiation and electron irradiation of toluene. Equivalent gas yields from polyphenyl irradiation were also obtained. On the other hand, these same workers point out that yields from benzene, where ring rupture is important, show no correspondence between reactor and electron irradiation, possibly due to "knock-on" interactions with neutrons.

Also, radiation-damage work on plastics and elastomers show no effect due to changes in the rate of energy loss.[12,56,57]

Hartech and Dondes[27] have performed a series of experiments using fission fragments directly to induce nitrogen fixation. In these experiments, enriched uranium was placed in the reaction vessel and irradiation carried out in a nuclear reactor. The radiation efficiency is increased in this manner to the point where "commercial usefulness of the process may be possible." This increased efficiency is mainly due to the high intensity of highly ionizing fragments produced directly in the system. The data presented does not clearly establish whether or not the actual G value for the reaction is altered by using fission fragments.

E. Choice of Systems and Range of Variables

In light of the high temperature and pressure design of the pilot unit, used in the present experiments, a major effort seemed logical in the area of the effect of radiation on the thermal-cracking of organic compounds. Normal heptane was chosen for this work for two reasons. First, thermal-cracking data are readily available. And, secondly, n-heptane had been used in the only high-temperature radiation experiment reported in the literature(58) up to the time when this choice was made. Since the latter work was performed with gamma radiation, this presented an opportunity to compare pure gamma-and pile-radiation effects.

In addition to cracking studies, high-temperature experiments with the following systems were selected for exploratory work: water saturated with benzene, nitrogen-oxygen, and nitrogen-hydrogen.

The benzene-water system has been proposed as a reliable chemical dosimeter(34), and it was, in fact, used for dosimetry measurements in this work. Since the temperature effect on this reaction had not been determined, it was chosen for experiments in the range 70°F to 212°F. In fact, very little information has been published about the effect of temperature on radiation-induced solution reactions.

The nitrogen-oxygen system has been studied with good results in batch experiments, but the present experimental apparatus offered a chance to try the reaction in a short-residence time-flow system.

The temperature and pressures possible in the pilot unit used in the present work are of the same order as those used in commercial ammonia plants. Thus, although little success had been reported for using radiation in this reaction, it appeared most interesting and was chosen for exploratory work.

Originally, experiments were planned to cover the entire design range of the equipment, i.e., 1000 psi and 900°F maximum. However, after careful consideration of the experiment, the Ford Reactor Safety Committee (Professors Gomberg, Osborn, Wiedenbeck, Ricker, Whipple, Emmons, and Edmonson) recommended that maximum conditions of temperature and pressure be set at 500°F and 250 psi for these exploratory experiments.(61) The permissible temperature range was increased to 750°F several weeks later, and the maximum pressure limit was eventually raised to 500 psi.(62) A better understanding of the concern for safe experimental operation can be obtained by reading the safety report submitted to the Reactor Advisory Committee (see Appendix C).

II. DESCRIPTION OF THE FORD NUCLEAR REACTOR FACILITY AND FLOW APPARATUS USED IN BEAM PORT EXPERIMENTS

A. Brief Description of the Ford Nuclear Reactor

A detailed description of the facility in handbook form is available through the Michigan Memorial Phoenix Project[64]. Other available literature is listed in the bibliography[63,65,66].

The Ford Nuclear Reactor (often referred to as a "pile" to avoid confusion with a chemical reactor) is of the swimming pool type similar to the Oak Ridge Bulk Shielding Facility. A general view of the reactor is shown in Figure 3, and the details of the core and mobile bridge assembly are shown in Figure 4. A standard fuel element measures approximately 3 inches in cross section and 35 inches in length. Under normal operation, the center portion of the core will contain 16 or more fuel elements, while the outer rows of the grid plate are filled with reflector elements. The latter elements are the same size as the fuel elements but are constructed of graphite clad in aluminum. The present A.E.C. licencse does not cover operation of the reactor with a bare core, i.e., without the outer row of reflector elements. However, the Cook Electric Company, under an Air Force contract, recently obtained a fission-plate assembly and a special operating license for its use in the Ford Nuclear Reactor. By placing the fission plate on the outer face of the core, an increased fast-neutron flux similar to that possible with a bare core can be obtained[63, p. 106]. The overall dimensions of this plate are 13" x 13" x 3" and it is designed to fit into the grid plate in place of four standard elements.

Some technical specifications for the pile are listed in Table 3.

The experimental work described here-in was performed shortly after the Ford Reactor first went critical, and the reactor power level

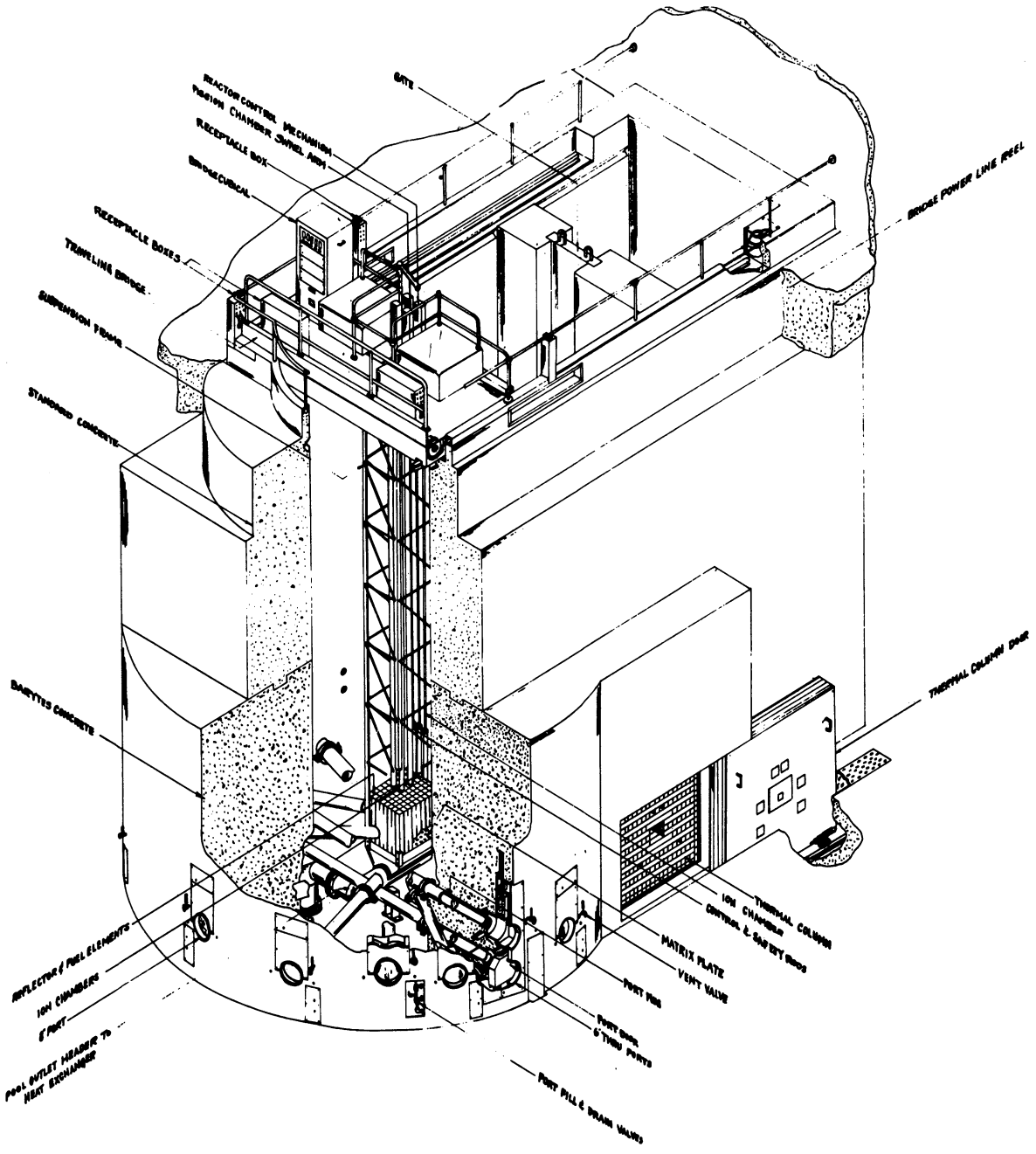

Figure 3. Isometric View of the Ford Nuclear Reactor

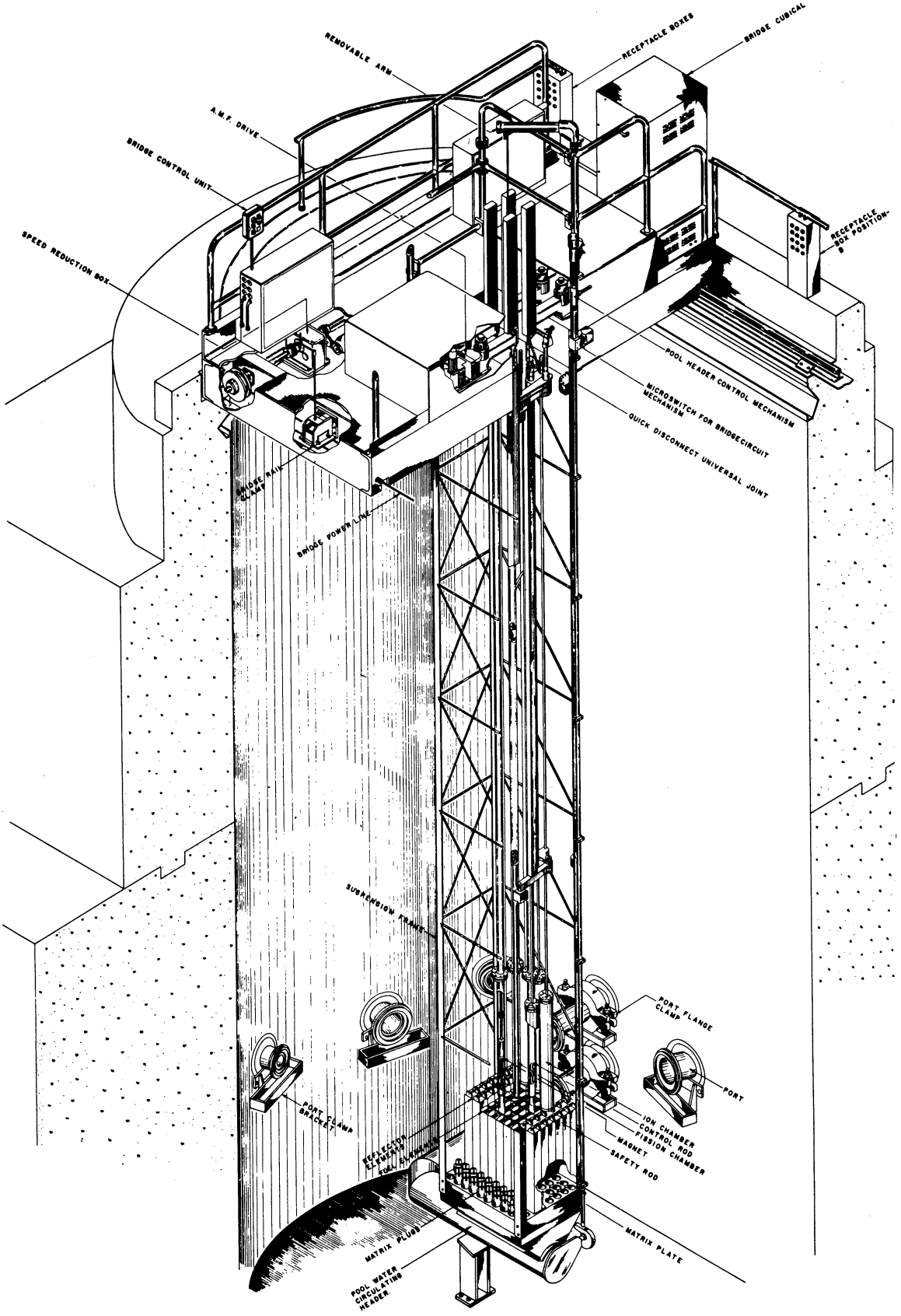

Figure 4. Isometric View of the Reactor Bridge and Core

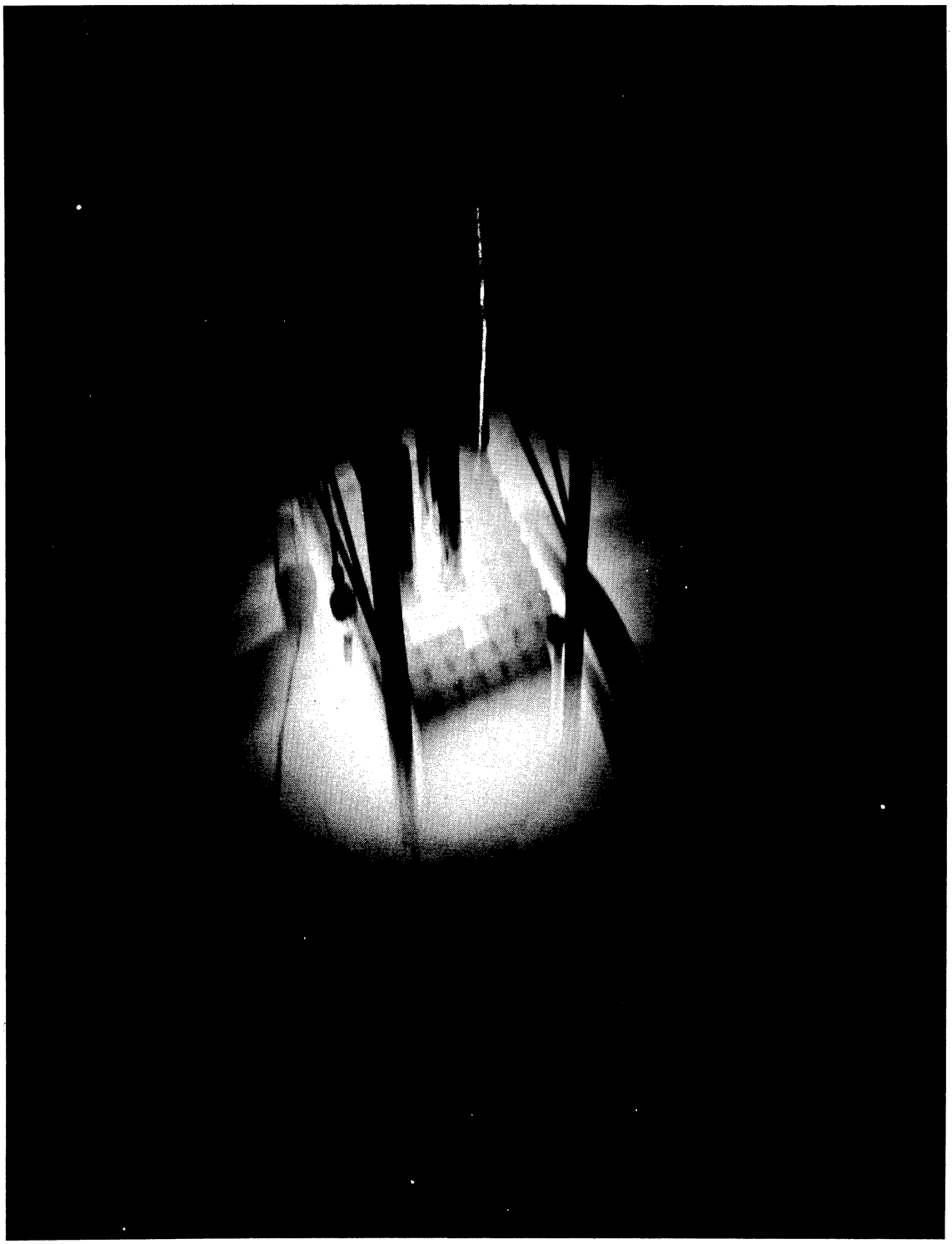

Figure 5. Cerenkov Radiation Emitted from the Reactor Core at 100 KW

TABLE III

TECHNICAL SPECIFICATIONS FOR THE FORD NUCLEAR REACTOR

Power Rating	1 Megawatt
Average thermal flux at 1 megawatt	1 x 10^{13} n/cm^2 sec
Uranium inventory	3.5 kg.
Core dimensions	approx. a 2 ft. cube
Depth of pool	27 ft.
Volume of pool water	41,000 gal.
Pool water temperature	100°F max.
Thickness of shield	5.6 ft. (Barytes concrete at base).

was still restricted by the A.E.C. to a maximum of 100 kilowatts. Hence, the available flux was lower than the design flux at 1 megawatt by a factor of ten.

Figure 5 is a photograph showing the Cerenkov radiation emitted from the reactor core at 100 kilowatts.

B. Considerations in Choice of a Beam-Port for Experimental Studies

Sample irradiation in the proximity of the reactor core may be accomplished by one of three methods.

1. The sample enclosed in a waterproof container may be dropped down through the pool water next to the core by the use of a rope or wire. This approach is, for obvious reasons, referred to as "fishing".

2. Small samples may be placed in position by the core by means of the pneumatic tube system which is built into the reactor (see Figure 3).

3. The sample may be inserted through one of fourteen beam-ports which run to or past the core.

The thermal column presents a fourth method of sample irradiation, but it is restricted to slow neutron studies.

For the present work, the pneumatic tube system and thermal column methods of irradiation were immediately eliminated. The high temperatures and pressures desired are impossible in the pneumatic tubes, and gamma and fast-neutron effects were of greater interest than slow-neutron work with the thermal column.

The remaining two irradiation methods differ in one major respect from the point of view of this study. Namely, the beam-port approach is best suited to a flow apparatus, while the "fishing" method lends itself best to batch work. Batch work in a beam-port would be extremely difficult due to the complexity of loading and unloading the port (see Appendix E). Likewise it would be difficult to place a flow system directly in the pool water due to safety considerations, danger of pool water contamination, lack of space for pumps and other external equipment on the control room floor, and the problem of passing all utility leads down through the water.

Actually, chemical reaction kinetic data and yields can be obtained from either a flow or a batch system. However, for the high-temperature and pressure reactions considered here, the flow system has several advantages. First, it eliminates many radioactive handling problems, since the reaction vessel, once placed in position by the pile core, can be left indefinitely. In contrast, batch irradiation would necessitate frequent removals of reaction vessels from the pile. Unfortunately, the use of high-pressure and temperature conditions make it necessary to construct the vessel of a high strength metal. All such metals have a high induced radioactivity, although

some, such as aluminum, have reasonably short half-lives. But, of course, the pressure vessel would have an extremely thick wall if it were constructed of aluminum. A second advantage of a flow system is that temperature control and installation are simplified, since direct contact with pool water does not occur in a beam-port.

In view of these considerations, it was decided to utilize a beam-port in conjunction with a flow system.

The Ford Reactor has a total of fourteen beam-ports, 2 eight-inch and 12 six-inch ports. Of the latter, two are through ports; that is, they extend from the east side of the reactor shield, through the water by the face of the core, and out the opposite or west shield of the reactor. All other beam-ports simply lead up to the core face (see Figures 3 and 6).

The through ports appear to be best suited to chemical reaction work. The reason is that a cylindrical reaction vessel in one of these ports would receive a high radiation level all along the wall facing the core. In contrast, a similar vessel placed in one of the other ports would only receive this high radiation level at the end of the vessel nearest the core. In addition, shielding problems are simplified in the through ports since, unlike the other ports, they do not face directly into the core and hence do not present a straight radiation path outward from the core.

Unfortunately, due to scheduling problems, the through ports could not be obtained for this work. Of the remaining ports, either of the eight-inch ports appeared preferable, simply to gain maximum space for the pressure vessel. "G" port (see Figure 6) was chosen in preference to "J" because of the larger floor space available for equipment around the port

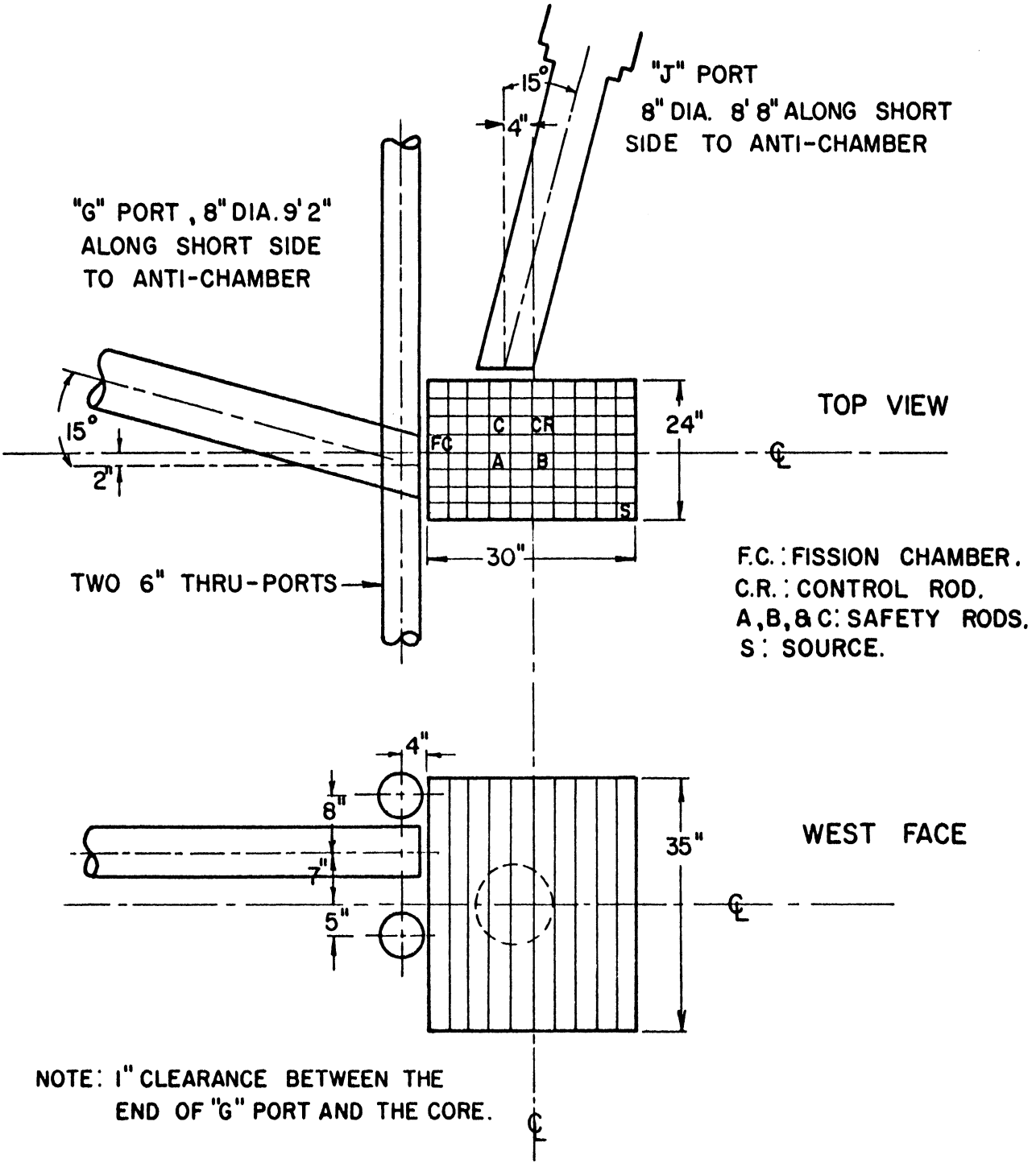

Figure 6. General Positioning of the 8-inch Beam-Ports and Through-Ports.*

*Details of the Ford Reactor and exact dimensions may be obtained from the design blueprints, Babcock and Wilcox Co., Job No. GM-46429.

entrance. Also, this position places the experiment further away from the doorway frequented by vistors.

Since the initial selection of "G" port several disadvantages connected with its use have shown-up and should be noted for future work. First, the presence of the fission chamber (see Figures 6 and 19) in front of "G" port prevents insertion of the fission plate at this location. Secondly, as indicated, "G" port ends about 7 inches above the core-center line. Since the radiation flux peaks at the core-center line, slightly lower radiation levels are available in "G" port, as compared to several other ports such as "J" which are closer to the center line. Fortunately, an assembly designed for "G" port can also be used in "J" port, despite the fact that "J" is six inches shorter.

C. Description of the Experimental Apparatus

(1) Preliminary Remarks

Two major goals of this experimental program were the design and construction of the flow system and the development of safe operating procedures.

The apparatus may be thought of as consisting of two major sections -- pieces of equipment such as pumps, etc. which are external to the pile; and the internal reaction vessel and shielding. Each section is considered later in detail. The external section (pictured in Figure 9 and discussed in Section II-C2) is based on the following general design philosophy:

1. The apparatus should be as general as possible, so that a continuing series of exploratory experiments covering a wide range of reactions can be performed with it.

2. It should be easily movable and compact.

3. It should have generous safety factors.

4. It should be constructed for long operation and be considered a permanent part of a long series of future experiments. The internal section (see Section III-C3) on the other hand is not of conventional design. Thus, unlike the external section, it is not considered a permanent part of the apparatus. Rather, it is intended to be a preliminary effort which will be improved upon in future experiments.

(2) Description of the Pilot Plant

(a) General Description

A detailed flow diagram (Figure 7) and a simplified diagram (Figure 8) of the pilot plant are shown on pages 34 and 35 respectively. The schematic illustration outlines the major sections of the apparatus; namely, the feed storage and pump, reaction vessel, and product separation system. For ordinary operation, liquid feed stored in tank I-1 is forced into the system by either pump P-1 (3.2 gals/hr max) or pump P-2 (225 ml/hr max). Both pumps are of the positive displacement, variable feed rate, metering type and rated at over 2500 psi. Feed rates are determined by use of liquid level gauge L-1 in conjunction with T-1 or alternately by spot check feeding from burette T-6. Possible variations of this basic feed system are: feed entirely from burette T-6; maintain a nitrogen blanket and positive pressure over the liquid in feed tank T-1; by-pass the pumps by means of valve 22 while maintaining a nitrogen pressure on the feed; meter two liquids into the system by feeding from T-6 through the left piston of pump P-1 and from T-1 through the right piston (1.6 gals/hr max per side).

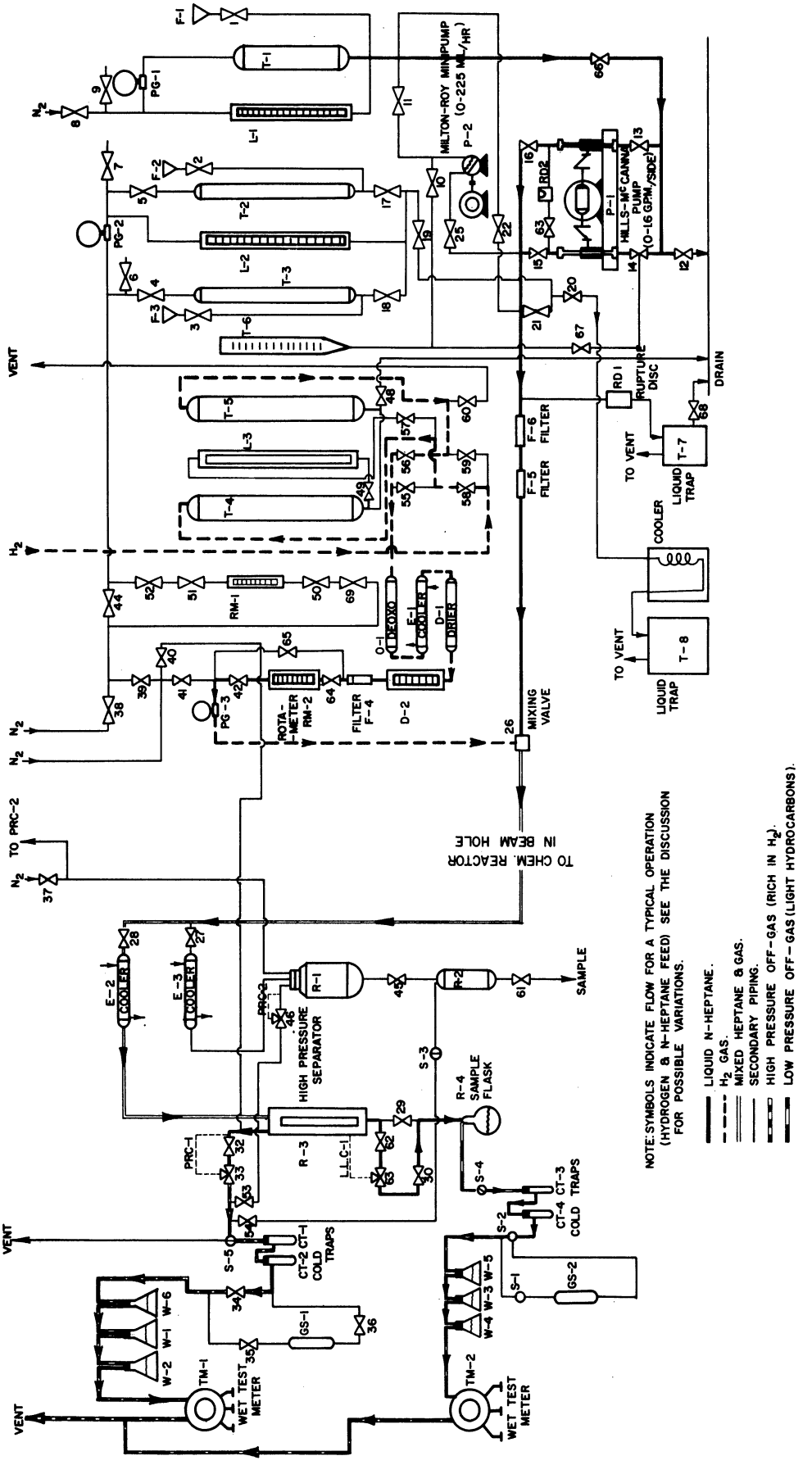

Figure 7. Flow Diagram for the Pilot Plant Used for Studies of Nuclear Reactor Radiation Effects on Chemical Reactions

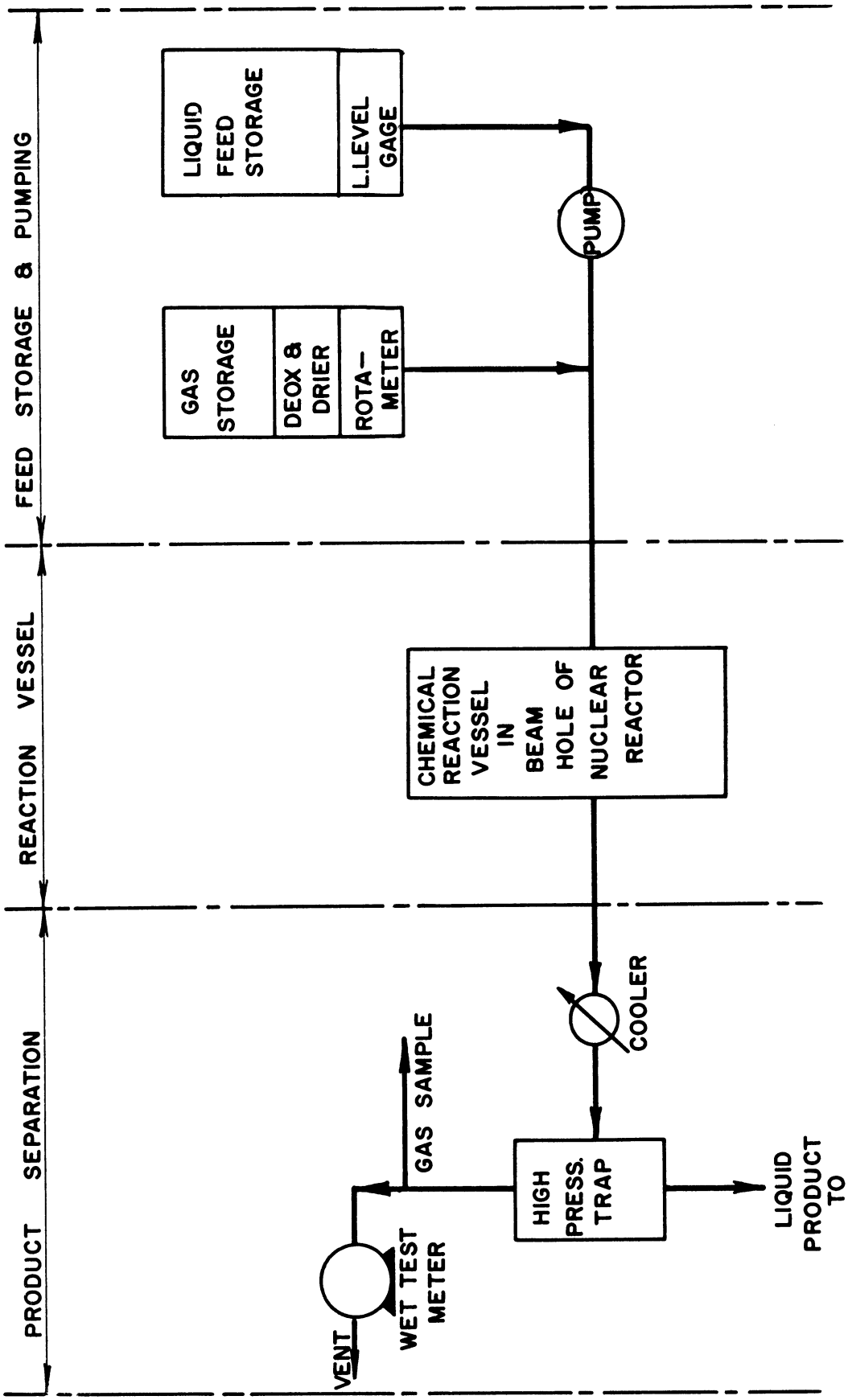

Figure 8. A Simplified Illustration of the Flow Diagram for the Pilot Plant

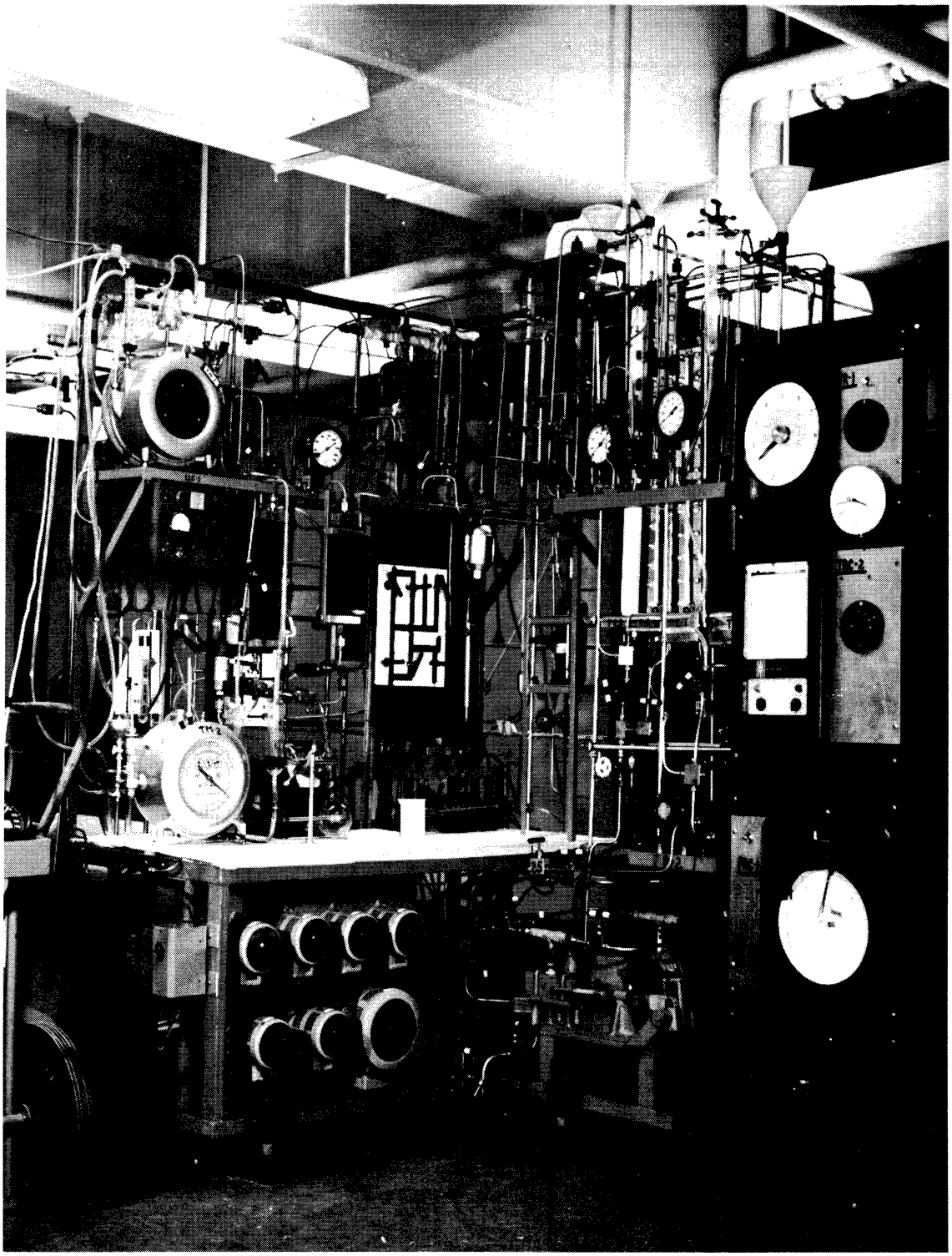

Figure 9. General View of the Pilot Unit

TABLE IV

EQUIPMENT LIST FOR PILOT PLANT

Symbol on Flow Diagram	Description
C-1	Keleket Radiation Monitor, Model K-900, Serial No. 134.
CT-1 through CT-4	Cold traps, 50 cc., glass construction.
D-1	Drier, 1/2" S.S. pipe packed with silica-gel and wrapped with a heating element.
D-2	Jerguson high pressure sight glass filled with alternate layers of indicating silica-gel and palladium deoxo catalyst.
E-1 through E-3	Coolers, constructed of 2 feet of 3/8" S.S. tubing and jacketed with cooling water.
E-4	Cooler, constructed of 20 feet of copper tubing coiled in a 5 gallon drum.
F-1 through F-3	Glass filling funnels.
F-4, F-5	Filters, Autoclave type 5C-A.
F-6	Filter, 3/8" pipe packed with glass wool.
GS-1, GS-2	250 ml gas sample tubes.
L-1	Liquid Level gauge, Strahman type 100A, rated at 1200 psi at 100°F, 26 inches long.
LLC-1	Liquid level controller, Niagara Electron Labs thermocap relay type 114-13-T.
O-1	Deoxo unit, 2 inch stainless pipe filled with palladium deoxo catalyst and electrically heated.
P-1	Pump, Hills-McCanna variable stroke type UM-2F, 1/2 H.P., 3500 psi, 1.6 G.P.H. per side, serial no. 17910.
P-2	Pump, Milton Roy Minipump, 1/5 H.P., 3000 psi, 250 ml/hr, serial no. 15809.
PG-1	Pressure Gauge, Helicoid, 0-500 psia, 5 lb. subdivisions.
PG-2	Pressure Gauge, Duragauge, 0-1500 psia, 10 lb. subdivisions.
PRC-1	Foxboro proportional pressure controller, Model 40, 0-1200 psi, serial no. 355219. Used with a Masoneilan air-to-close #8206 regulating valve.
PRC-2	Masoneilan recording pressure controller, Model 2110, 0-2000 psi, serial no. B-2871. Used with a Research air-to-open #75 regulating valve.
R-1	High pressure trap for radioactive materials, stainless steel, 1.5 liter, lead covered.
R-2	Low pressure trap for radioactive materials, stainless steel, 1.5 liter, lead covered.
R-3	High pressure trap and level indicator, 12-inch Jerguson gauge.
R-4	Liquid sample flask, 500 ml.
RD-1, RD-2	Autoclave rupture disc assemblies.
RM-1	Rotameter, Jerguson type 15-T-20, rated at 1000 psi at 50°F.
RM-2	Rotameter, Jerguson type A4413, rated at 3000 psi at 100°F.
T-1	Feed tank, stainless steel, 0-500 psi, 500 cubic inches.
T-2	Feed tank, monel, 0-3000 psi, 1.5 liter.
T-3	Feed tank, monel, 0-3000 psi, 1.5 liter.
T-4, T-5	Gas holders, stainless steel, 0-3000 psi, 7.5 liter.
T-6	Burette, 250 ml.
TR-1	Temperature indicator, Leeds and Northrup Speedomax H, 11 points, serial no. 5639669-1-1.
TRC-2	Temperature recorder and controller, Leeds and Northrup Speedomax H and Series 60 controller, serial no. 354165.

Tanks T-2 and T-3, along with liquid level guage L-2, compose an entirely independent means of feeding a liquid into the system. Liquid is first forced from T-2 by nitrogen pressure and metered into the system through needle valve 19. When T-2 empties, feeding is continued from T-3, while T-2 is isolated from the system and refilled. Since the setting of needle valve 19 is not changed, a uniform flow rate is maintained, but the feed tanks are continually switched and refilled. Liquid level gauge L-2 automatically records the level in the tank which is being used for feed.

The liquid feed tanks are filled by means of funnels F-1 thru F-3 while venting through valves 6, 7, and 9.

The main gas feed system is composed of feed tanks T-4 and T-5 in conjunction with liquid level gauge L-3. To start a run, one of the tanks, T-4 for example, is filled with water and the other, T-5, is filled with the desired gas such as hydrogen. Then hydrogen from a gas-cylinder pressure regulator set-up is fed into the top of T-4, the water filled tanks. Thus water is slowly forced from T-4 into T-5 which, in turn, forces the hydrogen out of T-5 into the system. When 90% of the water has been transferred to T-5, appropriate valves (55 through 59) are switched and the process reversed, so that hydrogen tank pressure is placed over the water in T-5 in order to force gas out of T-4 and into the system. This method of feeding is used to obtain a more accurate measurement of the gas fed than is possible with a rotameter. The liquid level gauge, L-3, affords easy measurement of the volume of gas displaced by the water, which combined with pressure and temperature readings can be converted to standard cubic feet of gas fed to the system with reasonable accuracy. The gas flow-rate

is set by adjusting the mixing valve 26 as well as valves 42, 64 and 65. Rotameter RM-2 affords a rough visual means of setting the flow-rate but is not used for accurate determinations. The deoxo unit, O-1 contains a palladium catalyst which operates at 300 - 400°F and converts those amounts of oxygen in the main hydrogen stream into water. The gas is then cooled back to room temperature and dried by means of silica-gel, packed in D-1. Next, the gas passes into vessel D-2 which consists of a high pressure sight glass packed with a layer of indicating silica-gel, a layer of palladium deoxo catalyst and then a final layer of silica-gel. This affords a visual check on the operation of D-1 and O-1 for if the first layer of silica-gel changes color drier D-1 needs regeneration, and if the second layer changes then the palladium catalyst in O-1 is not functioning properly. D-2 is followed by a filter, F-2, and by a rotameter RM-2, the function of which has already been described. Pressure gauge PG-3 indicates the gas pressure entering the system at mixing valve 26 where gas and liquid are brought together, ready to pass into the reaction vessel.

If necessary, it is possible to feed a second gas into the system at the same time if tanks T-3 and T-2 are not used for liquid feed. This gas rate would be monitored by rotameter RM-1 as it passes from the gas cylinder, through valve 38, and 44 into T-2 or T-3. Valves 19 and 44 would be used for flow control and PG-2 to indicate pressure. Gas volume measurement by this method is, of course, not as accurate as by the first method, utilizing the water level technique.

Following mixing valve 26 gas and liquid flow into the chemical reaction pressure vessel located in the pile beam-port. A detailed description of this plug and assembly is given in Section II-C3.

Products and unreacted feed leave the reaction vessel, are cooled in passing heat exchanger E-2, and drop into the high-pressure trap R-3. (The system now described is duplicated by the set-up consisting of heat exchanger E-3 and high and low pressure receivers R-1 and R-2. The latter system, however, is shielded with sheet lead and is only used in case radioactive product is obtained. Ordinarily, neutrons will not cause an induced activity in pure H.C.'s, but impurities in the feed, rust in the system, etc. can create a severe problem.) Trap R-3 serves to separate gas and liquid streams - the liquid level is maintained automatically by liquid level control LLC-1 or by manual operation of valve 29. Liquid product is collected in sample flask R-4. As the liquid is collected, a certain portion of the lighter ends will flash off due to the sharp pressure reduction. These off gases pass through two cold traps, CT-4 and CT-3, usually placed in a dry ice-alcohol bath, and then through two water saturators, W-3 and W-4, which saturate the gas before it is measured by wet test meter TM-2. Exit gases from TM-2 are passed into the building forced-circulation vent system. Periodically, stopcocks S-1 and S-2 are switched so as to divert the gas flow through the gas sample bulb GS-2.

The pressure maintained in R-3 is automatically controlled by a pressure-recorder-controller PRC-1. Unreacted feed gas along with gaseous products pass through control valve 33 and then through a cold trap, a gas sample, and wet test meter system which is identical to that already described.

Thus, the following product samples are obtained from the unit

1) Liquid product --- R-4

2) Two cold trap samples from liquid product off-gas --- CT-3, CT-4

3) Two cold trap samples from high pressure trap off-gas --- CT-1, CT-2

4) Gas samples of liquid product off-gas --- GS-2

5) Gas samples of high pressure trap off-gas --- GS-1

At the completion of a run, it is imperative that the reaction vessel be immediately cleaned of hydrocarbon in order to prevent coking. (Coking can arise through the decomposition of hydrocarbon left for long periods in the reaction vessel which remains at elevated temperatures for a number of hours after the heaters are cut off.) To accomplish this, first, the pressure setting for PRC-1 is lowered, so that much of the hydrocarbon in the reaction vessel is flushed out into R-3. Then, valve 32 is closed and nitrogen forced into R-3 through valve 40. This sets up a reverse nitrogen purge which is the most efficient method for cleaning small amounts of reactant out of the reaction vessel. The reverse purge gas follows the system back to mixing valve 26 and then is directed through valves 21 and 20 to a cooler where the hydrocarbon is condensed out and forced into a collection drum T-8. Off-gases from this drum pass to the vent system.

Detailed operating instructions for the pilot plant are given in Appendix D.

(b) Special Features of the Pilot Plant

The following summarizes the special features of this unit which distinguish it from many similar units.

1) All equipment external to the pile is built on casters to aid movement between the radiation positions and beam parts used in various experiments.

2) Stainless steel construction is used throughout to prevent corrosion and the resulting hazard of radioactive product.

3) The design of the in-pile shielding and reaction vessel is based on many factors unique to the use of a research nuclear pile as a radiation source. These aspects are discussed in detail in Section II-C3.

4) During operation, the product stream and collection flask are continuously monitored for possible radioactivity. A "Keleket Radiation Monitor" is provided for this purpose.

5) A second lead-shielded product separation system is provided to handle contaminated products.

6) The design is as general as possible in order to handle a large variety of chemical systems. For example, three separate methods for feeding liquid reactants and two independent gas feed systems are available. The various feed systems are designed to cover a wide range of feed rates and may be used in various combinations. That is, a single liquid, a liquid and a gas, two liquids, two liquids and a gas, etc. may be fed.

7) A reverse purge system for the reaction vessel is provided to minimize coking at the end of a run.

8) Generous safety factors are used for pressure equipment, many parts being rated at 10,000 psi and a few at 3000 psi.

(3) Description of the Pressure Vessel and Shielding

The design and construction of a chemical reaction vessel for in-pile experimentation presents many unique problems, and this is perhaps the key section of the experimental apparatus. Reference 53 is recommended for a discussion of the general design criteria for in-pile reaction vessels.

The vessel described here is designed to handle organic systems such as heptane and hydrogen at pressures up to 1000 psi and temperatures up to 900°F. The space available in the beam-port restricts the size and shape of the vessel.

A picture of the general arrangement of the reaction vessel and shielding plug is shown on page 44 along with a close-up view of the vessel on page 45 . A detailed drawing of the vessel appears on page 46, and a sketch showing the general arrangement of the thermocouples and heaters is shown on page 49.

(a) Choice of Materials of Construction

The selection of type 304 stainless steel for the construction of the pressure vessel was based on the following considerations:

1) high mechanical strength

2) good creep strength properties

3) corrosion resistance

4) resistance to radiation damage

5) small catalytic effect upon the reaction.

The absolute necessity for safety and, hence, proper selection of materials from a mechanical strength point of view cannot be overemphasized (see

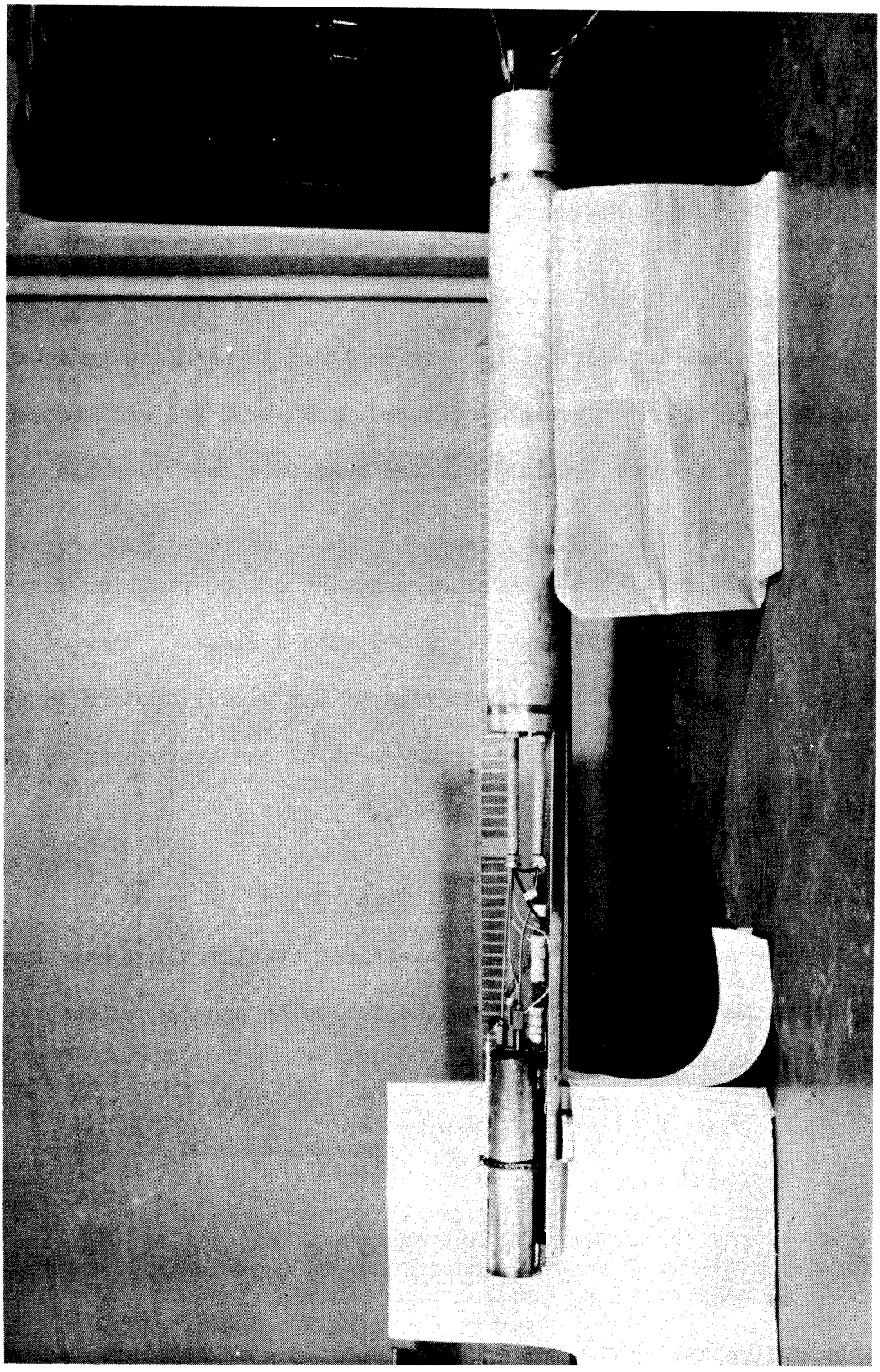

Figure 10. General View of the Reaction Vessel and Shielding Plug

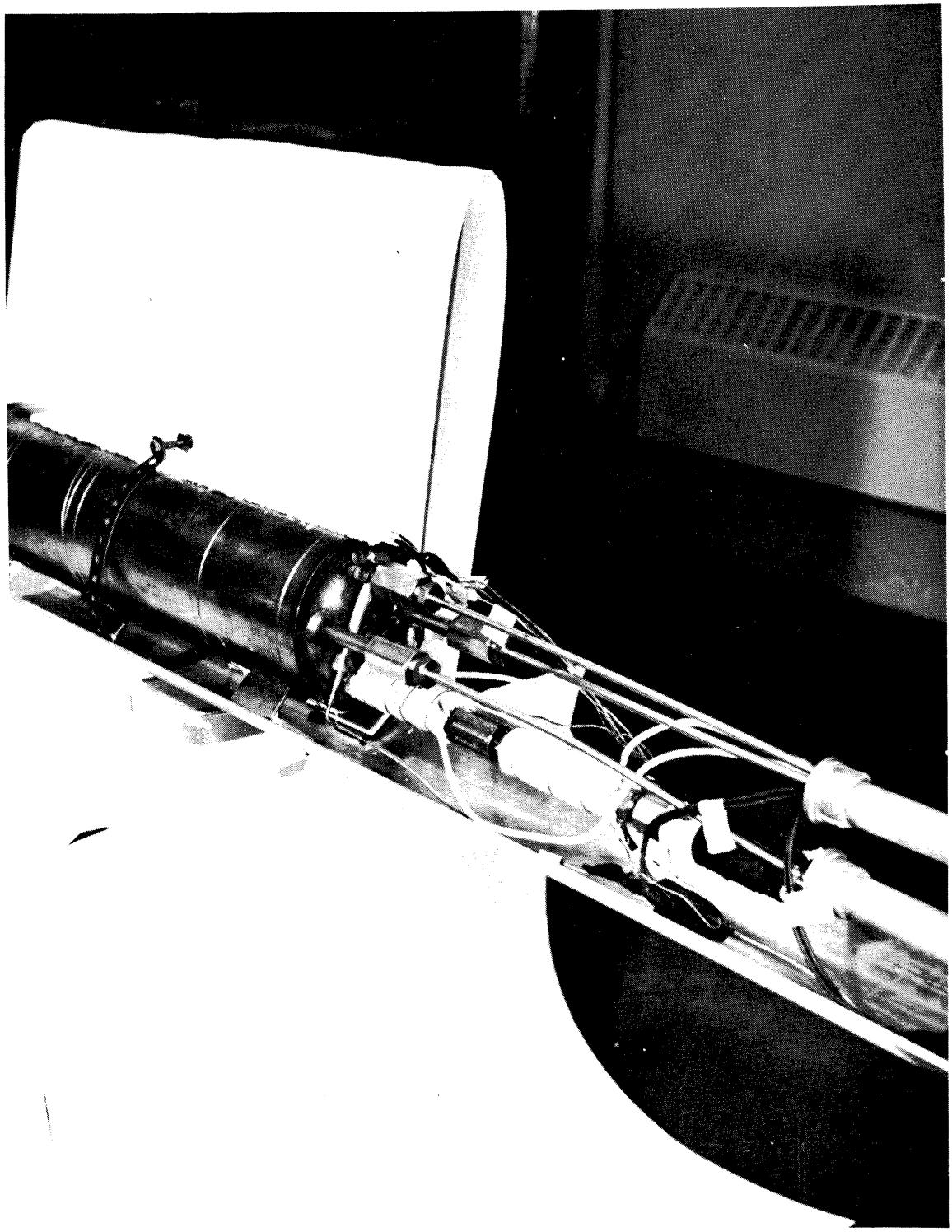

Figure 11. Close-Up View of the Reaction Vessel

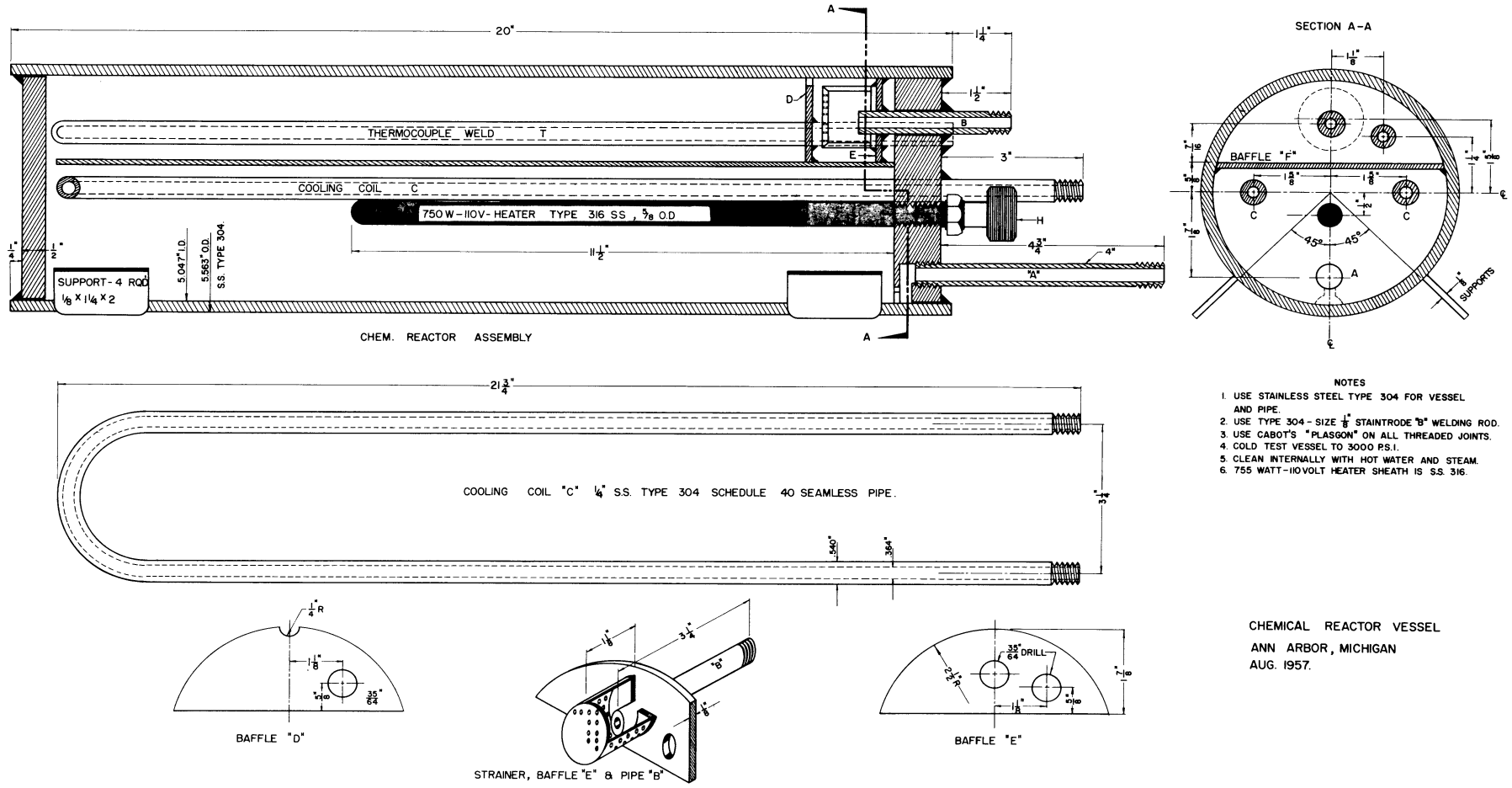

Figure 12. Detailed Drawing of the Reaction Vessel

Appendix C for a hazards analysis). A number of materials, such as aluminum and graphite, which are frequently used in reactor experiments to minimize induced radioactivity, were not considered because of the mechanical strength requirements.

Induced radioactivity is not included in the list of factors considered in the final selection of a material of construction. Certainly, it is an important consideration in any operation requiring the movement or handling of the vessel. But fortunately, the Phoenix Memorial Laboratory has a large lead handling coffin which makes the transferral of even an extremely radioactive vessel possible (see Section II-D) and hence this is not a limiting factor. Maintenance operations on the vessel are also effected by induced radioactivity, but all of the high strength metals in the stainless class have too high an induced activity to consider maintenance without a special hot cell facility. Hence, the vessel is considered expendable from this point of view, i.e., if something such as a plug occurs, the vessel must be discarded.

Although induced activity was not found to be important for this experiment, it might be for other work, and several points should be noted. A fairly complete mechanical design for the vessel, based on each material of interest, must be made to determine the weight of the metal required. For example, Schoeder, et al.[53], found that for one reactor design only 9 lbs. of A-286 steel was required, as compared to 45 lbs. of Type 316. But this advantage is partially overcome by the fact that for a given radiation exposure A-286 has a much higher induced activity than Type 316 on a pound-per-pound basis.

A major portion of the long-lived activity from stainless steel is from 5.3 yr Co-60. Yet, the cobalt content of stainless steel is extremely low (0.01-0.05%) and, in general, is not accurately known. Hence, at present it appears desirable to rely on experimental data rather than estimating activity from chemical analysis. Bopp and Sisman[5] present data for many materials.

(b) General Design Considerations and Description

A reaction vessel for in-pile work must be designed to:

1) be compact in order to fit into the beam-port;

2) make maximum utilization of the available flux;

3) have sufficient strength for safe operation;

4) have efficient and uniform heating;

5) have some method for cooling;

6) be capable of long operation without plugging.

The radiation flux drops off quite rapidly with distance from the core end of the beam-port (the thermal neutron flux decreases by a factor of 6 in 20 inches in "G" port when dry), so that any design should pass all of the reactants as close to the core end of the port as possible. As shown in Figure 12, the present design accomplishes this by means of a baffle which divides the upper and lower sections of the vessel. This arrangement forces the reactants to flow upwards past the core end of the vessel and also creates turbulent mixing at this point.

The preheaters, RH-2 and RH-2A, shown in Figure 13, bring the feed within several hundred degrees of reaction conditions. The main heater, RH-1, is a calrod heater located near the center of the vessel,

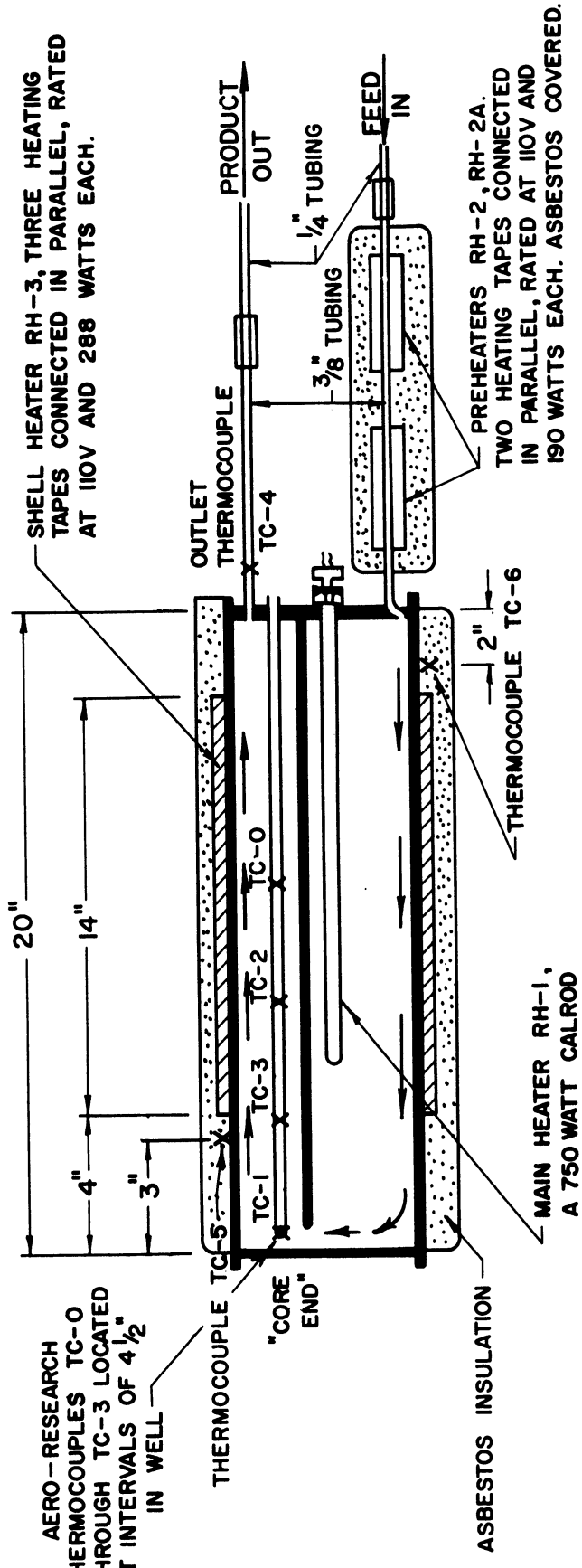

SUMMARY OF HEATER RATINGS

Shell heater	864 watts
Main heater	750 watts
Preheater	380 watts
Total	1,994 watts

Figure 13. Sketch of the Reaction Vessel Cross-Section Showing the Heater and Thermocouple Locations

just below the dividing baffle and in the lower or feed inlet section. Due to its location and direct contact with the fluid, this heater is most efficient. In addition, the vessel is wrapped with heating tape and asbestos insulation to minimize heat losses through the walls and to flatten the temperature profile across the vessel. The vessel is designed to minimize the possibility of plugging. As stated previously, once the vessel is exposed to pile radiation, maintenance is impossible due to induced radioactivity. A strainer containing forty 1/16-inch holes is located on the outlet pipe (see Figure 12). Thus, there is a good chance that the outlet line will remain open even after a number of the strainer's holes become clogged. Since the inlet is recessed into the bottom of the vessel, complete draining is possible. A reverse purge scheme, described on page 167 , is used to force any liquid out of the vessel and thus prevent coking. The vertical baffle in the upper section of the vessel (baffle "D") is necessary to prevent air pockets from forming. Without the baffle, a liquid feed entering the bottom of the vessel would only rise to the height of the exit line, which is slightly lower than the top of the vessel in order to have room for the strainer already described.

A thermowell, as shown on Figure 12, is located in the upper section of the vessel. Thermocouples, starting with TC-1 located at the "core-end" of the vessel, record temperatures every 4-1/2 inches (see Figure 13). Also, two thermocouples are located on the outer surface of the reaction vessel wall. Cooling coil "C" can remove small heat loads from the vessel. It is mainly intended to remove heat generated in a chemical reaction or to aid in quickly lowering the temperature of

the vessel to new run conditions. It should be noted that the coil is not included to control the heat addition due to radiation absorption. The latter heat input is very small and, in fact, does not cause a temperature rise in the system of more than a couple of degrees. In addition, the cooling coil might conveniently be used as a flow system in conjunction with a chemical dosimeter to obtain a continuous measure of dosimetry during a run. Extensive calibration would be necessary to do this, however.

(c) Shielding

As shown in Figure 10, the pressure vessel is located at the end of a five-foot shielding plug. The entire assembly of shielding plug and reaction vessel measure nine feet, 1-3/4 inches in length.

The shielding plug is formed from a section of 7-3/4 inch O.D. 25-aluminum pipe filled with barytes concrete. Two 3/4 inch pipes are embedded in the concrete to permit passage of utility lines through to the reaction vessel. A complete 360° spiral in these pipes prevents radiation streaming.

The end of the shielding plug is slightly recessed so that a lead gasket about 4-inches thick can be forced between the plug and beam-port wall to prevent radiation streaming, (see Figure 14). A rubber "O" ring seal can also be used around the end of the plug to form a water-tight seal, but for work such as the present experiment where the port is run dry (if desired, the port may be flooded as described on page IV-6 of Reference 64) such a seal is unnecessary.

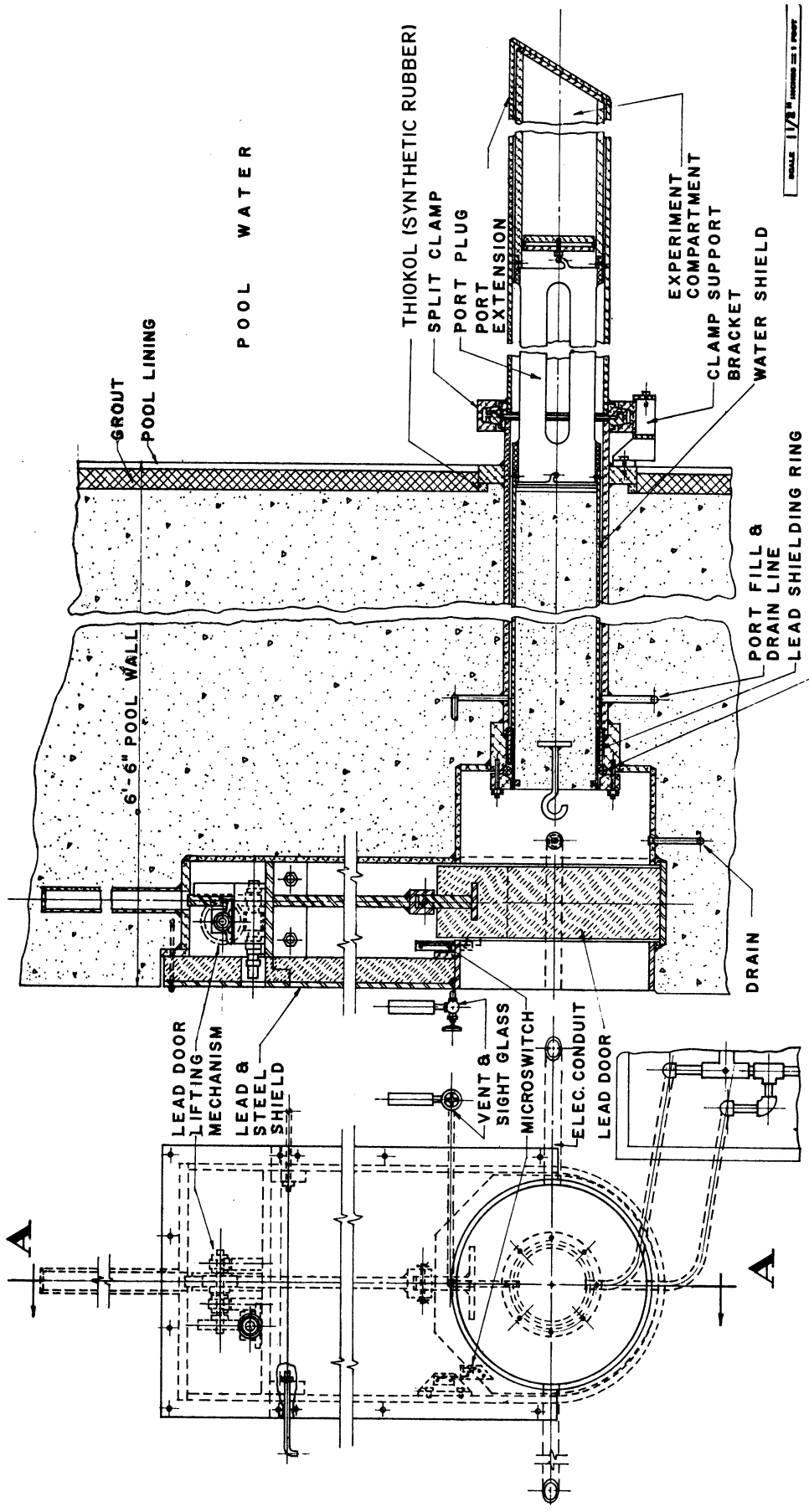

Figure 14. Section and Elevation View of a Typical Experimental Port with Plug and Door

Each beam-port is provided with a 6-inch-thick lead shielding door which is lowered into the port vestibule area once the plug is in position. It was found necessary to leave a small crack at the bottom of this door for passage of the reaction vessel tubing and wiring. Actually, special access pipes lead through the reactor wall into the port vestibule for this purpose, but could not be used because their location required an excessively sharp bend in the feed line.

No radiation streaming was observed through the cracked beam-port door; nevertheless, such operation presents a hazard. The nuclear reactor safety system is designed with an interlock which prevents reactor operation unless the port door is closed. However, this interlock is defeated to allow operation without the door being completely in place. Such operation leaves open the possibility of an accidential pile start-up while work is being performed in the beam-port. For this reason, the interlock defeat should always be removed before any work requiring an open beam-port is performed.

The shielding described above proved satisfactory for most experiments. However, fission plate experiments required additional external shielding to reduce the fast neutron flux. A four-foot-thick wax barrier backed with a boral plate was placed directly in front of the port for this work.

(d) Support of the Pressure Vessel

The support for the reaction vessel shown in Figure 15 does not require that the vessel be rigidly attached to the shielding plug. Rather the vessel sits loosely in the aluminum extension, so that it

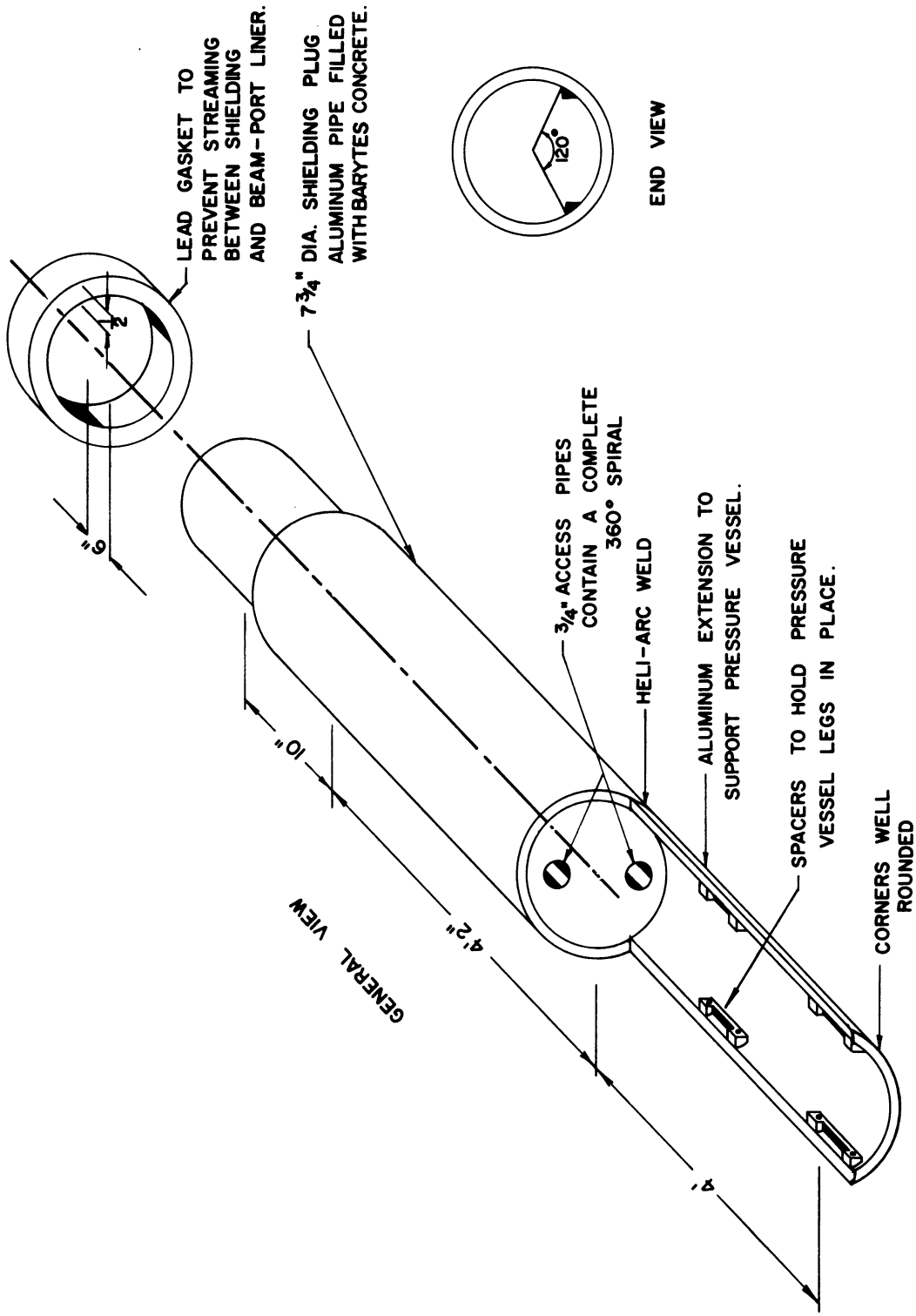

Figure 15. Sketch Showing the Shielding Plug and Reaction Vessel Support

can be easily dropped away from the shielding plug if the entire assembly is rotated 180°. This feature aids in the final disposal of the radioactive vessel as described in Appendix E. On the other hand, as long as the assembly is held in an upright position, the vessel is rigidly held in place. In addition, the extension provides a good bearing surface when sliding the assembly into a beam-port.

(4) Instrumentation

(a) Reaction Vessel Temperature Control

Figure 13 shows the general arrangement of the reaction vessel heaters. All the heaters shown are controlled by powerstats, and the input to the main calrod heater, RH-1, is also connected to a relay actuated by temperature recorder controller, TRC-2. This controller is wired to operate with any thermocouple in the system, but in practice either TC-0 or TC-1 was used. Since the power rating for RH-1 is a sizable fraction of the total heat input, automatic control with TRC-2 alone produces large temperature oscillations as RH-1 is turned off and on. However, such oscillations can be damped out by proper manual adjustment of the powerstats and temperatures are easily maintained within $\pm$ 3° of the set-point. Other temperatures throughout the system may be monitored without disturbing TRC-2 by means of temperature indicator, TR-1.

(b) Pressure Control

Proportional recording pressure controller, PRC-1, controls the unit exit pressure through a pneumatic control valve (see the flow diagram, Figure 7). PRC-2 serves a similar function in the special

radioactive separations system. Reduction from feed gas cylinder tank pressure to system pressure is accomplished by means of Hoke-Phoenix Regulators. Inlet pressures, usually maintained 10 to 15 lbs above the outlet, are monitored by pressure gauges PG-1 through PG-3. The system pressure can be controlled within ± 10 psi.

(c) Feed Rates

Gas feed rates are controlled manually by proper adjustment of the pressure regulator and needle valves throughout the system. As already described, page 38, LL-3 provides an accurate measurement of feed gas flow from T-4 and T-5. Rotameter RM-2 provides a rough visual check of this rate. Rotameter RM-1 is used to measure gas rates in conjunction with T-2 and T-3. Wet-test meters TM-1 and TM-2 measure exit gas flow-rates.

Liquid feed rates are controlled by the two variable feed rate pumps, P-1 and P-2, or by needle valve, 19, if a gas pressurized feed system is used. Inlet rates are measured by liquid level gauges LL-1 and LL-2, and exit rates by measurement of the liquid sample volume collected in flask, R-1.

(d) Radioactivity Measurement

A Keleket Radiation Meter is used to monitor gas and liquid product lives. In addition, the general area is serviced by several Jordon Area Monitors which are connected to a recorder in the reactor control room. Also, a number of various neutron and gamma survey meters were used throughout the work for spot checks of radioactivity. Film badges, and, on occasion, finger tabs and self-reading pocket dosimeters were worn by the experimenter.

(e) Nuclear Reactor Operating Data

The reactor instrumentation is described in detail in Reference 61. All data concerning the reactor power level, fuel configuration, etc., are taken from the reactor log book maintained by the operating staff. This log is on file at the Phoenix Building, North Campus, University of Michigan, Ann Arbor, Michigan.

(5) Loading and Unloading Procedures for a Beam-Port

Loading and unloading operations are extremely hazardous from a point of view of safety to personnel. Assuming that the reactor core is left in the beam-port irradiation position, radiation hazards arise from two different sources. First, a sizable gamma flux is emitted from the open beam-port even with the pile shut down. Secondly, the pressure vessel and parts of the shielding plug and support become radioactive after exposure. The magnitude of these sources varies with the past operating history of the reactor and the exposure time for the vessel. But, the order of magnitude of the radiation is illustrated by the observed values of 3 r/hr at the entrance to "G"-port when empty, and 5 r/hr at a distance of one foot from the end of the pressure vessel. These measurements were taken 24 hours after the reactor shutdown and after the reaction vessel had accumulated about 80 hours exposure time at 100 kw. All transferral operations are performed by means of the lead handling coffin pictured in Figure 16. This coffin weighs over eight tons, most of the weight being concentrated in the 6-ft 4-inch long lead sleeve which has a 10 inch wall thickness and 8 inch inside diameter.

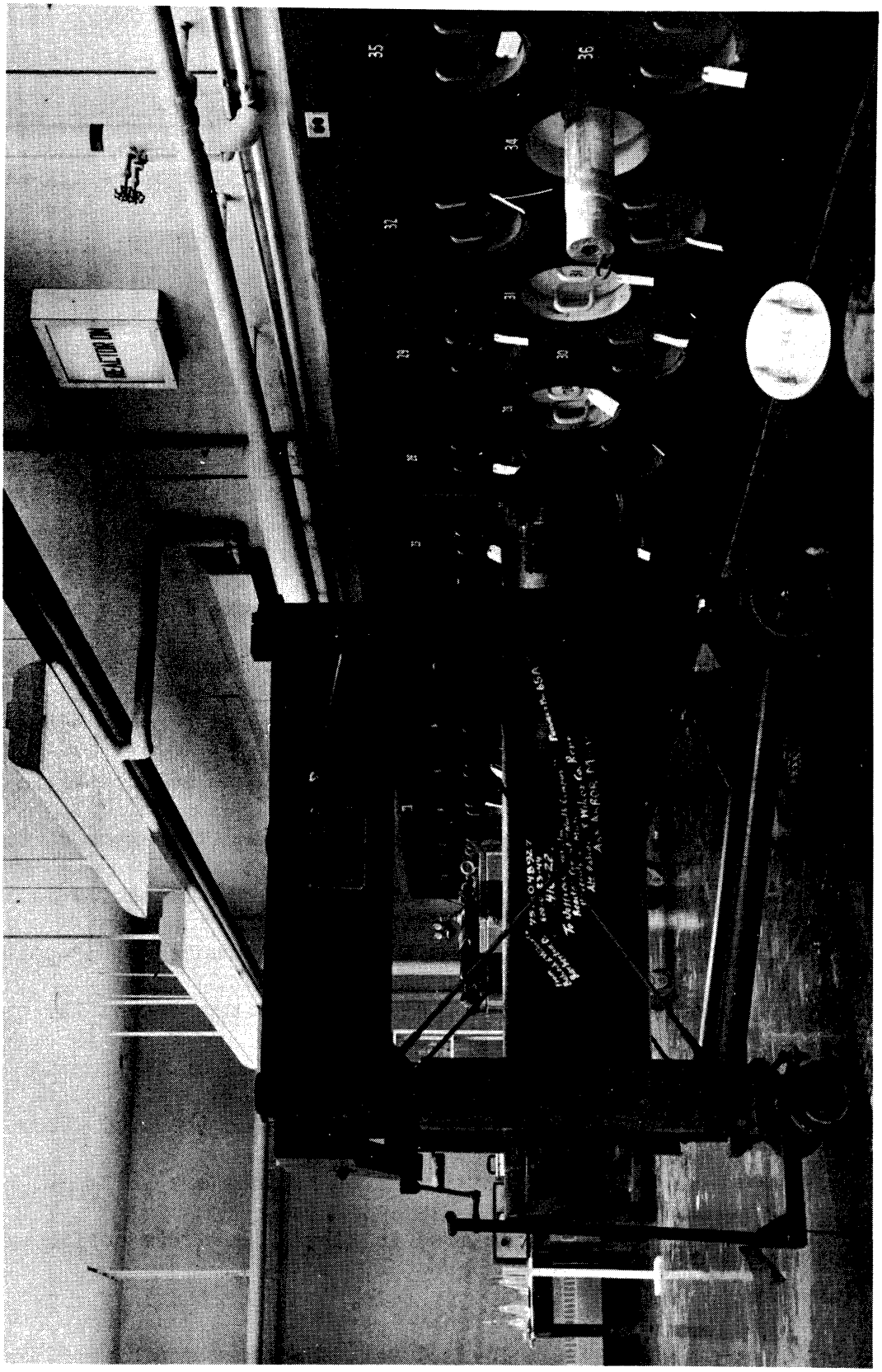

Figure 16. Beam Port Loading Coffin and Storage Area

To remove a beam-port assembly, the coffin is rolled up to the beam-port and the assembly pulled out into the lead carrying sleeve by means of a hook and grapple set-up. In most cases, the assembly is actually longer than the coffin, so that the radioactive or core end of the assembly is kept in the coffin, while the other end protrudes out of the lead sleeve. Detailed loading and unloading instructions are given in Appendix E.

The ports shown in back of the coffin in Figure 16 are actually radioactive storage ports. These ports, while the same size as the reactor beam-ports, are located on the west wall of the reactor building and extend out into the surrounding ground. Since they are approximately 15 feet below the surface, the soil provides a natural radiation shield for any radioactive assembly thus stored. Each storage port is provided with a lead door as shown.

III. BEAM-PORT FLUX CALIBRATION AND DOSIMETRY

A. General Statement of the Problem

Dosimetry measurements, i.e., measurements to determine the radiation energy actually transferred to the chemical system of interest, are extremely complicated for nuclear reactor studies due to the presence of both neutron and gamma radiation. Neutron energies range from thermal to fast, the distribution varying with location in the reactor. Likewise, the gamma flux is a mixture of fission product radiations with widely varying energies. Thus, a complete consideration of the dosimetry for a reaction system should not only show the total energy transferred but should also indicate some kind of breakdown - for example, the fraction of the dose due to gammas, slow neutrons, and fast neutrons. Unfortunately, to date, dosimetry techniques have not been developed which permit such a complete study. The present work is not an attempt to develop better dosimetry methods; rather, it is an attempt to make use of available methods to characterize the radiation used, and also to determine the total dose received. This approach is deemed sufficient for exploratory work, for enough information is provided to duplicate a given experiment and to calculate an over-all "G" value.

Two additional points concerning dosimetry work should be kept in mind. First, the dose of interest is that received inside the reaction vessel and thus is a function of the vessel wall thickness. Either the measurements must be made inside the vessel or a correction for absorption in the wall applied. Secondly, for a radiation field of specified dose

rate, the actual dose received by a flow chemical system is a function of the reactant residence time, hence, the flow pattern within the reaction vessel. The average residence time must then be assumed or measured; or alternately, a flow system dosimetry which duplicates the experimental flow conditions may be used.

B. "G" Beam-Port Calibration

(1) Experimental Measurements

(a) Gold Foil Measurements in "G" Port. Initial neutron flux calibration measurements in "G" port were made by the method of gold foil activation.[32,63] 1 mil, 24-carat gold foil cut in the form of squares, weighing approximately 100 mg each, were scotchtaped on the plywood assembly shown in Figure 17. This assembly, with foils attached, was then placed in the beam-port and irradiated for a specific time. As indicated in the drawing, foils are placed about the circumference of the three plywood discs to measure the angular flux distribution in the port, whereas foils along the pegs on the center axis provide a longitudinal measurement. The center pegs on the holder are rotated as shown in the drawing to prevent flux depression due to shielding of a foil by the preceding foil. The cadmium-covered foil was placed on the last plywood disc for the same reason.

All measurements were made with the beam-port dry and with a reactor power of 100 kilowatts. A record of the core configuration and the log N chart were obtained from the reactor operating staff after each run.

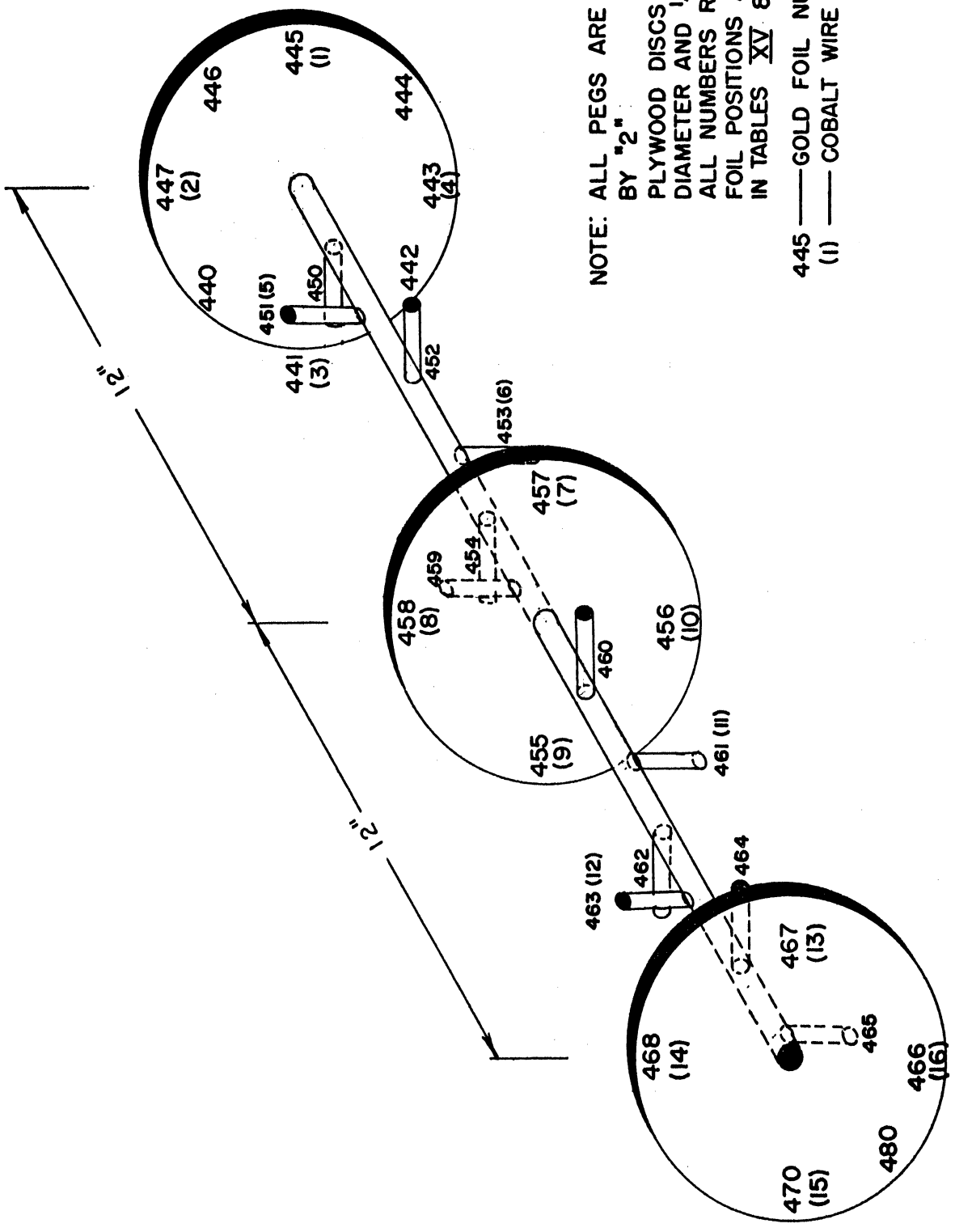

Figure 17. Plywood Holder for Beam-Port Calibration Experiments

The gamma activity from the exposed foils was measured in a well-type scintillation counter (Radiation Counter Labs Type 23-A). Activities were corrected for decay and variation in foil weight and absolute flux values were determined by comparison with foils irradiated in the standard pile at Argonne National Laboratory (see Appendix B for a sample calculation).

(b) Cobalt Wire Measurements in "G" Port. The gold foil techniques discussed in the previous sections have one serious disadvantage. Initial activities are high enough to jam the scintillation counter, so that at least a two-week decay period after irradiation is required. Not only does this cause a lengthy delay before results are available, but the possibility of error is increased because the activity level of long-lived impurities in the foil becomes more important as the 2.7 day gold activity decreases. (Fortunately, the gold foil used in these experiments proved to be relatively pure, since counts on several foils at intervals of 2, 3, and 4 weeks indicated only a small contribution to the activity due to impurities.)

A number of methods may be used to avoid this difficulty:

1) Make gold foil measurements at a low power level and extrapolate to 100 kilowatts
2) Use a short irradiation time (less than 5 min.)
3) Use foils of a smaller size, or section the 100 mg foils before counting
4) Dissolve the 100 mg foil in aqua regia and measure out a fraction of the solution for counting
5) Use some substance which has a smaller activation cross-section than gold.

Any one of the above methods appears feasible, but there are advantages and disadvantages to each. For the present work, the fifth method was chosen because it appeared reliable and rapid, and because other workers at the Phoenix Memorial Lab were interested in gaining high power level calibration experience with some material other than gold foil. Method "1" was also used for later work with the fission plate (see Section III, C). High purity cobalt wire was selected to replace gold foil because of its availability, low absorption cross-section (39 barns as compared to 98.8 for gold), and long half-life (5.2 years for Cobalt-60). Small pieces weighing about 40 mg each were cut from a spool of .04 inch diameter high purity wire. The cobalt was then scotch-taped onto the same plywood assembly used for gold foil measurements, and several gold foils were included for calibration purposes.

Cobalt wire, it was found, can be counted immediately after exposure for periods up to 10 minutes at 100 kw in the beam-port. However, a decay period of one day was allowed in order to eliminate short-lived activities. Counting was performed with the same well-type scintillation counters used for gold foils; however, the operating voltage was adjusted for the gamma ray plateau from Cobalt-60.

(c) Benzene - Water Chemical Dosimetry Measurements for "G" Port. Experimental work performed by Johnson[34] indicates that the benzene-water system can be used as a reliable chemical dosimeter for reactor radiation. This system was chosen for flow measurements in the reaction vessel located in "G" port because of the simplicity of preparation and analysis, and the low probability of corrosion or plugging in the apparatus. Also, it

was thought that some high temperature work, in addition to the dosimetry runs, might prove interesting.

Double distilled water saturated with reagent grade benzene was pumped through the reaction vessel according to operating instructions for the unit given in Case I, Appendix D. However, the reaction was carried out at room temperature and with only a slight back pressure (50 psi) to aid pumping. The product was analyzed for phenol with a Beckman Quartz Spectrophotometer, Model DU, fitted with a hydrogen lamp. Silica absorption cells were used, and the spectrophotometer set at a wavelength of 290 mμ and at a slit width of 0.50 mm. The analysis depends on the change in optical density caused by the addition of sodium hydroxide to a sample containing phenol. This analytic procedure is described in detail in Reference 34, and it is shown that the phenol concentration can be determined from the relation:

$$\frac{\text{micro moles phenol}}{\text{liter}} = 786\,[(AS-US) - (AB-UB)] \qquad (13)$$

where:

AS is the optical density for 5 ml of the product diluted with 5 ml of 0.06 N Na OH

US, AB, and UB are optical densities for 5 ml of product plus 5 ml of distilled water, 5 ml of feed stock plus 5 ml of 0.06 N NaOH, and 5 ml of feed stock plus 5 ml of distilled water, respectively.

Figure 18, also from Reference 34, shows the correlation between phenol concentration and dose. All experiments were run with high flow rates in order to keep dosages below 50 kiloreps, where the break in the pile irradiation calibration curve occurs.

(2) Results and Discussion

The basic core configuration used for all studies in "G"-port is shown in Figure 19. It is referred to as configuration "1a" throughout the reactor log book.(10)

Data from the gold foil and cobalt wire measurements are summarized in Tables XV and XVI, Appendix A, and the method of calculation used to obtain the thermal neutron flux from this data is illustrated in Appendix B. A plot of the flux along the longitudinal axis of the beam-port appears on page 69 , along with a plot of the angular distribution on page 70 . In each case, the cobalt results are consistantly higher than the gold foil. This variation is possibly due to actual differences in reactor power level -- the two experiments were run one month apart, and, during this time, some adjustments were made on the nuclear reactor instrumentation.

The discontinuity in the longitudinal flux plot is explained by radiation absorption due to the center plywood disc of the foil holder. Assuming that absorption in the leading disc is of the same magnitude (the flux is decreased by a factor of 1.54), the actual flux at the core end of the beam-port is calculated to be 8.6×10^{10} r/cm^2 sec from gold foil data, and 1.2×10^{11} n/cm^2 sec from cobalt data. These values are for a power level of 100 kilowatts. Both measurements show an exponential fall-off rate of $e^{(-0.0826D)}$ where D is the longitudinal distance in inches.

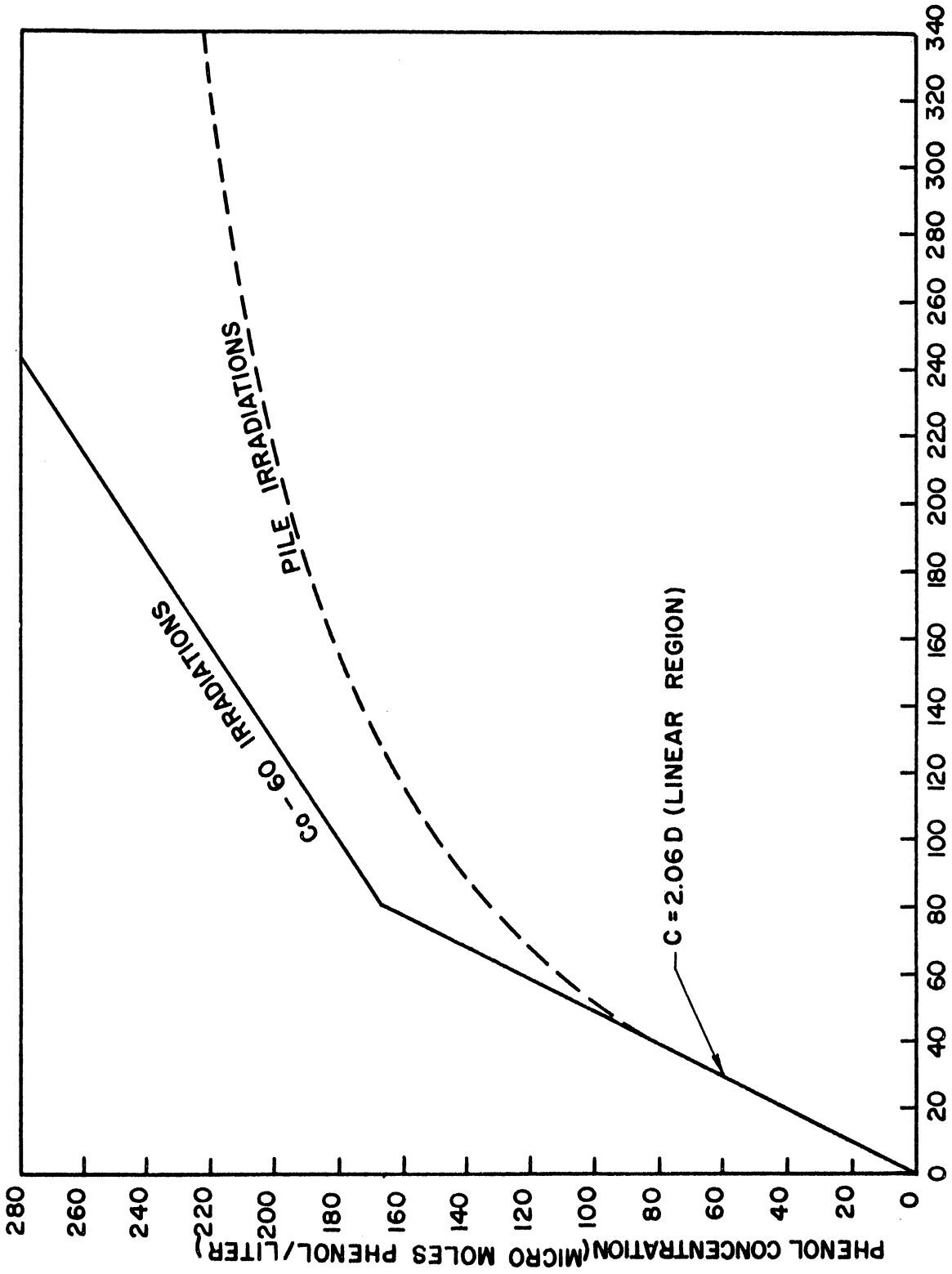

Figure 18. Correlation of Phenol Concentration and Dose for the Irradiation of Water Saturated with Benzene (Taken from data by Johnson, Reference 34)

A, B, C: Safety-Shim Rods (5 Plate Elements)
CR: Control Rod (5 Plate Element)
S: Po-Be Source
F.C: Fission Chamber

Fuel Element No. 18 in Core Position 48

Graphite Reflector Element No. 4 in Core Position 50

Loading: 2539 gms
Critical Mass: 2497 ± 5 gms

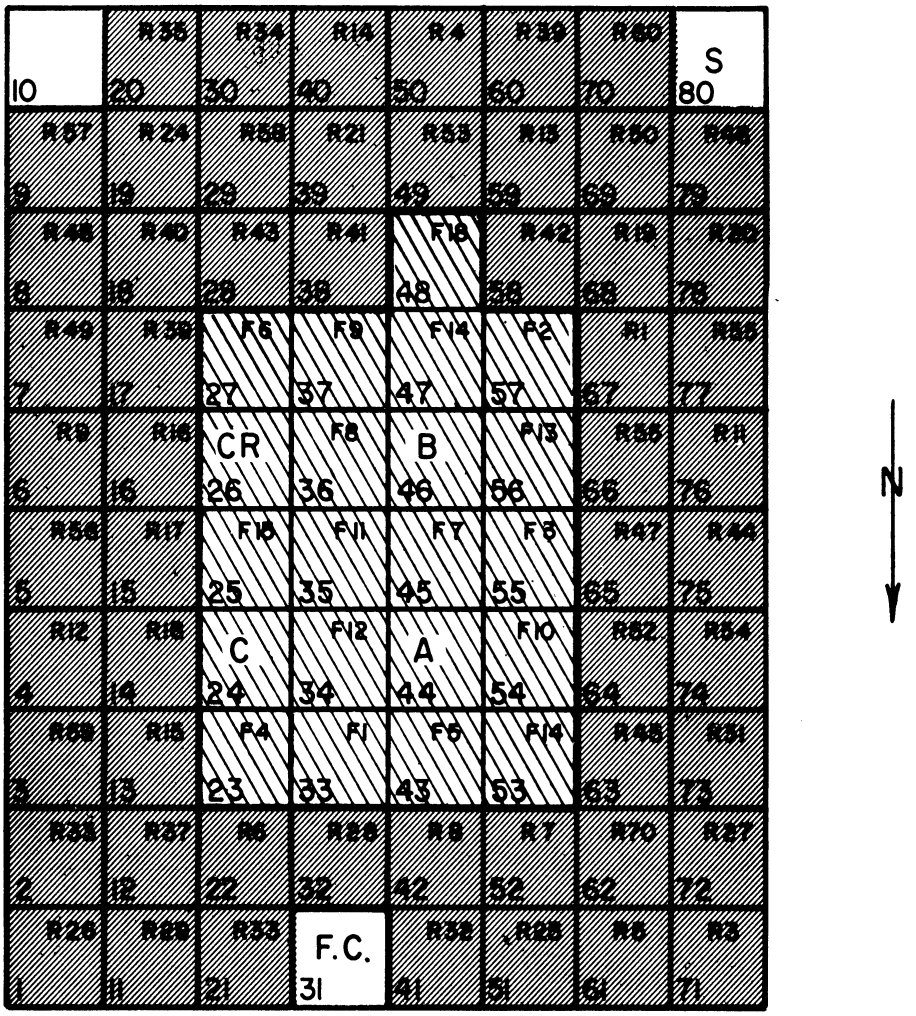

Figure 19. Core Loading "1a" Used for All "G"-Port Experiments

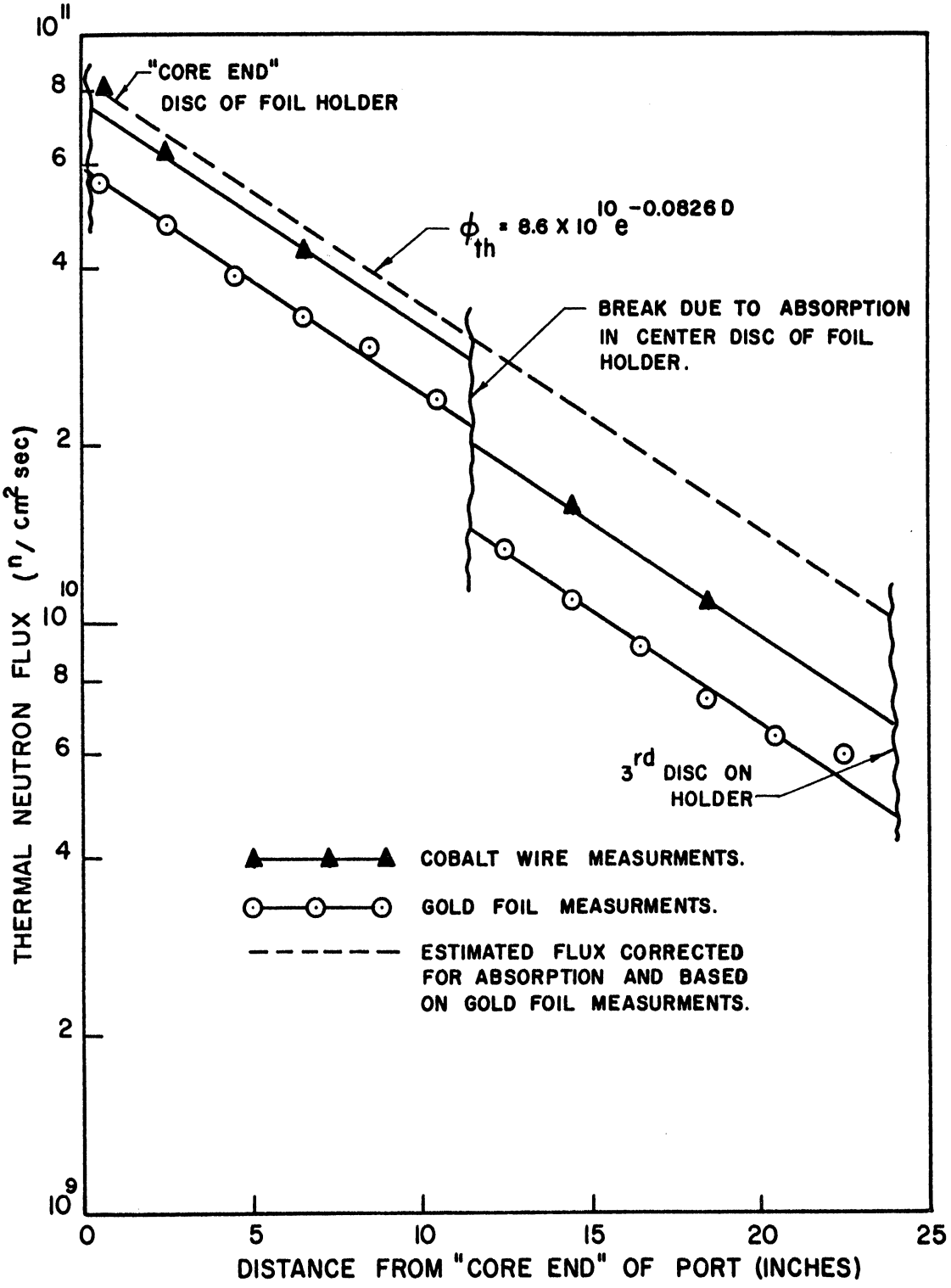

Figure 20. Thermal Flux Along the Center Axis of "G"-Port Operating Dry at 100 KW with Fuel Configuration "1a"

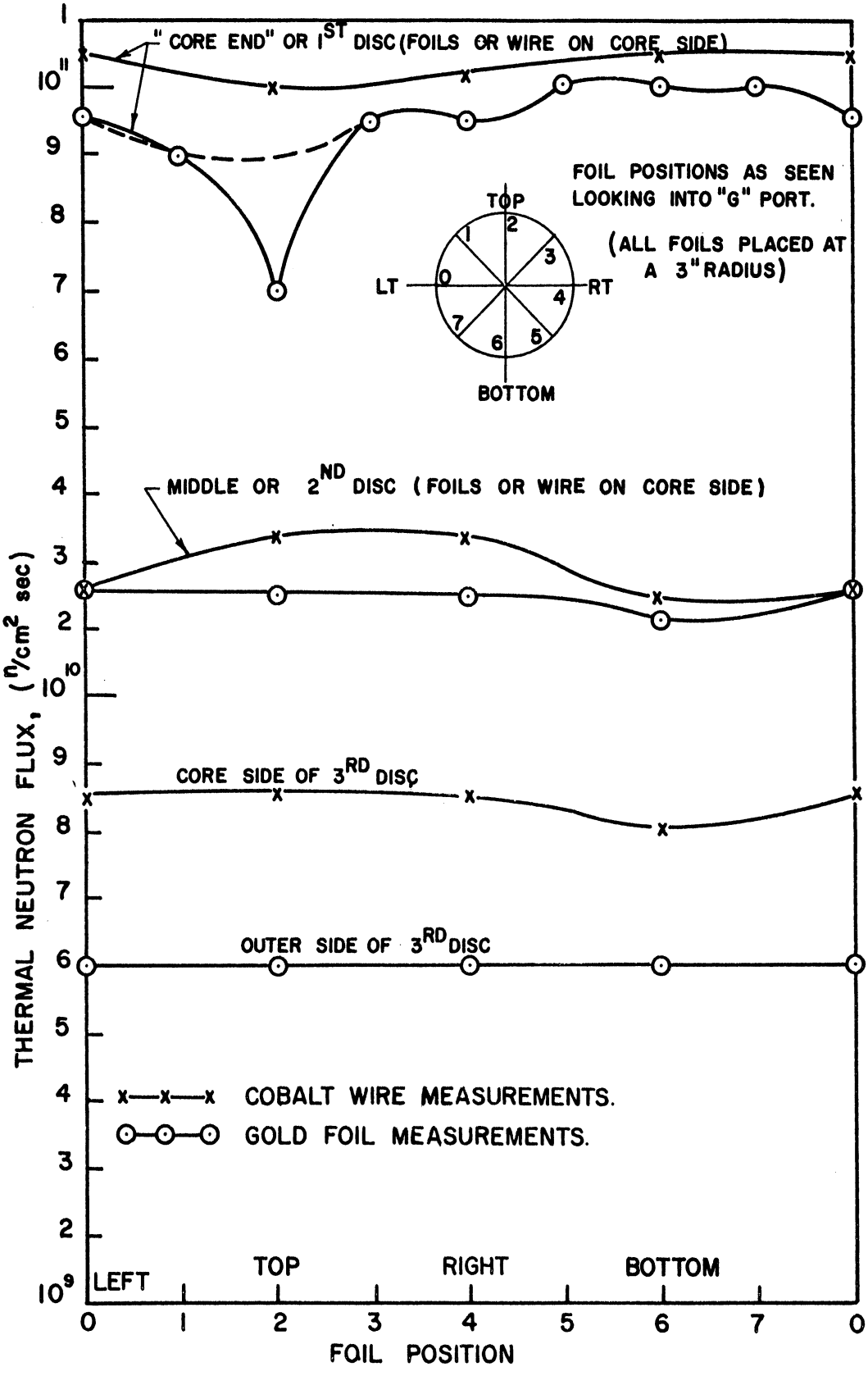

Figure 21. Angular Flux Distribution for "G"-Port Operating Dry at 100 KW

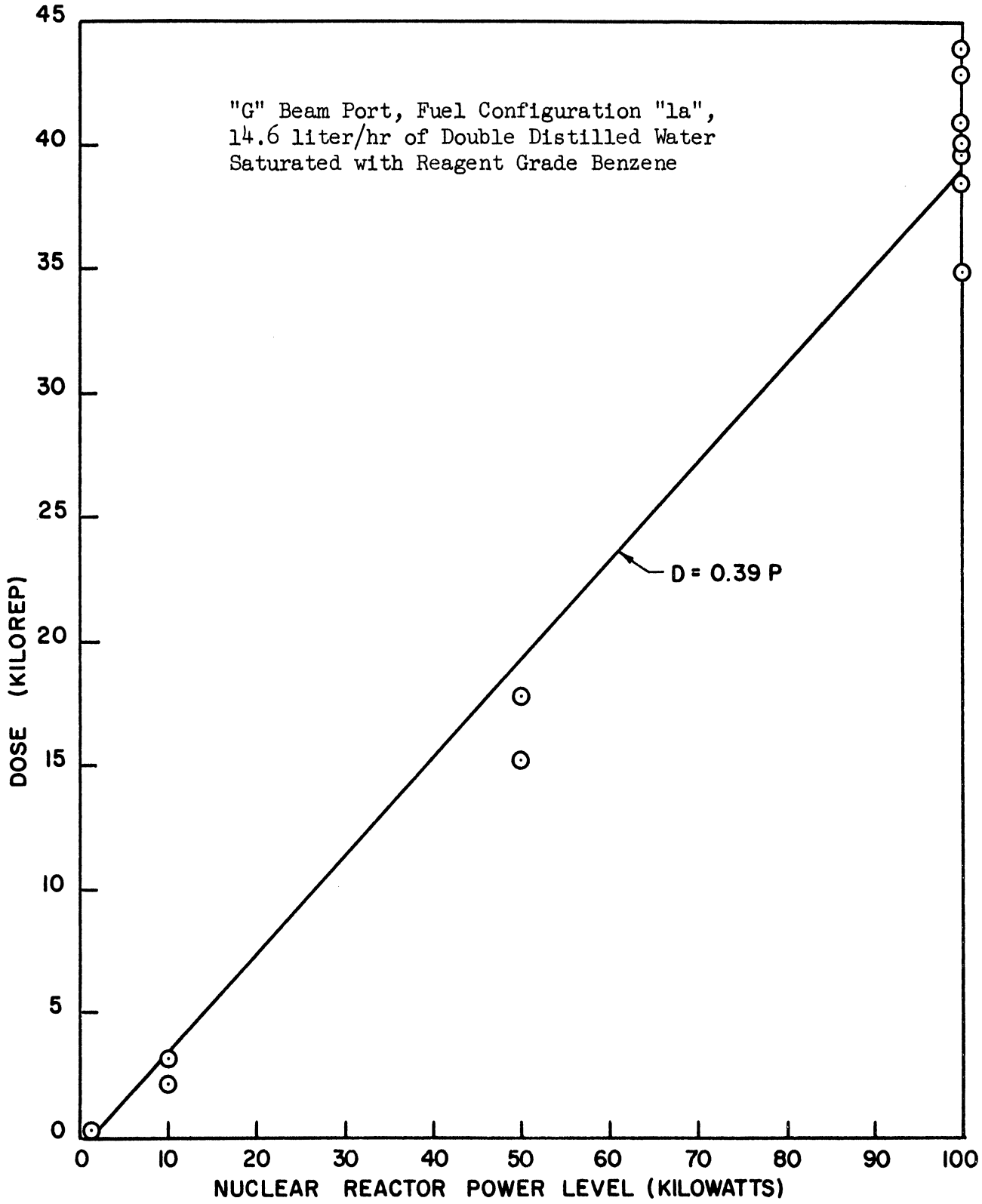

Figure 22. Dose Received in the Chemical Reaction Vessel as a Function of the Nuclear Reactor Power Level

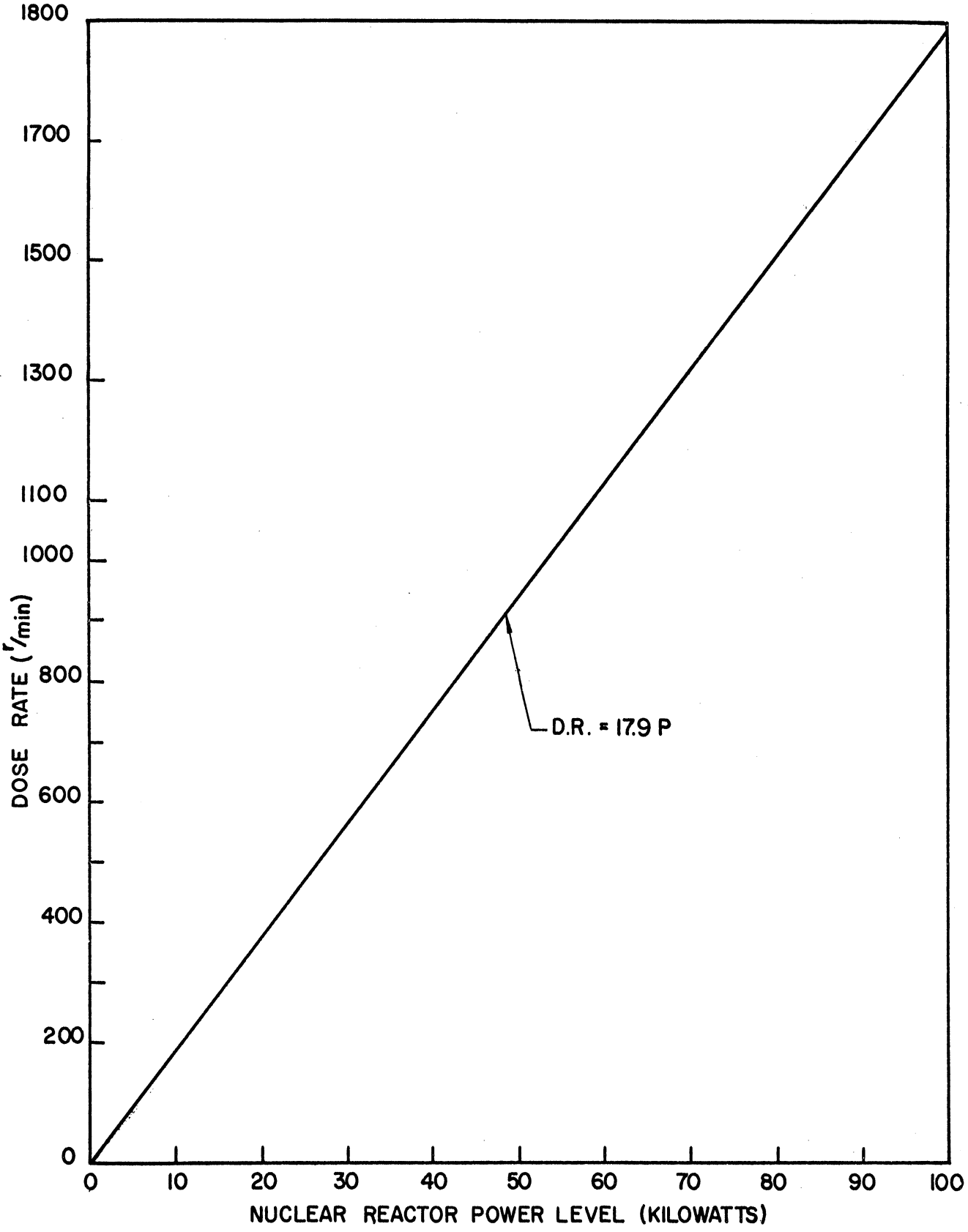

Figure 23. Calculated Dose Rate Based on an Average Residence Time (Eqn. 15) Vs. Reactor Power Level
(Chemical Reaction Vessel in "G" Port with Fuel Configuration 1a)

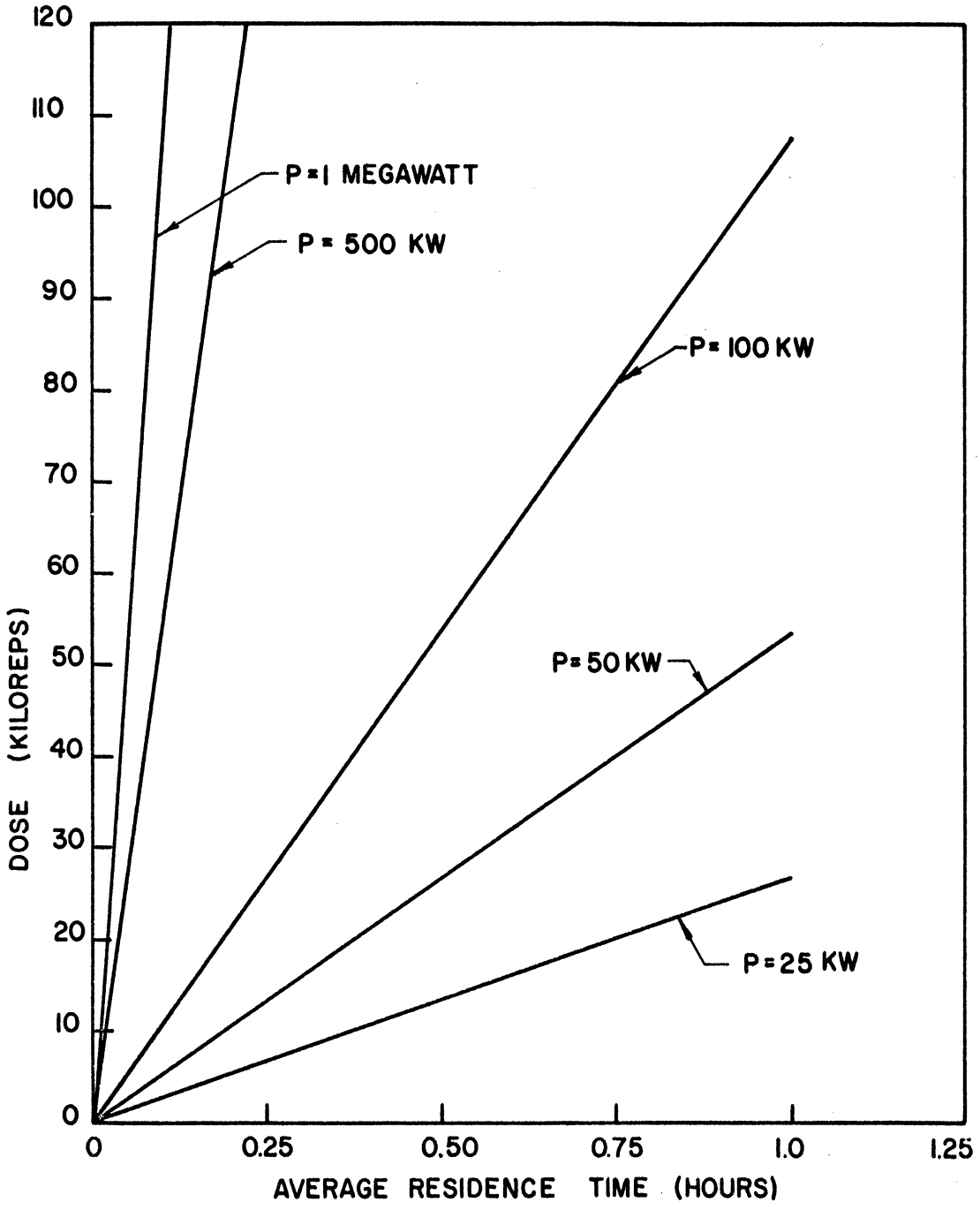

Figure 24. Dose Received Inside the Chemical Reaction Vessel as a Function of Power Level and Average Residence Time (Values are for "G" Port and Fuel Configuration "1a")

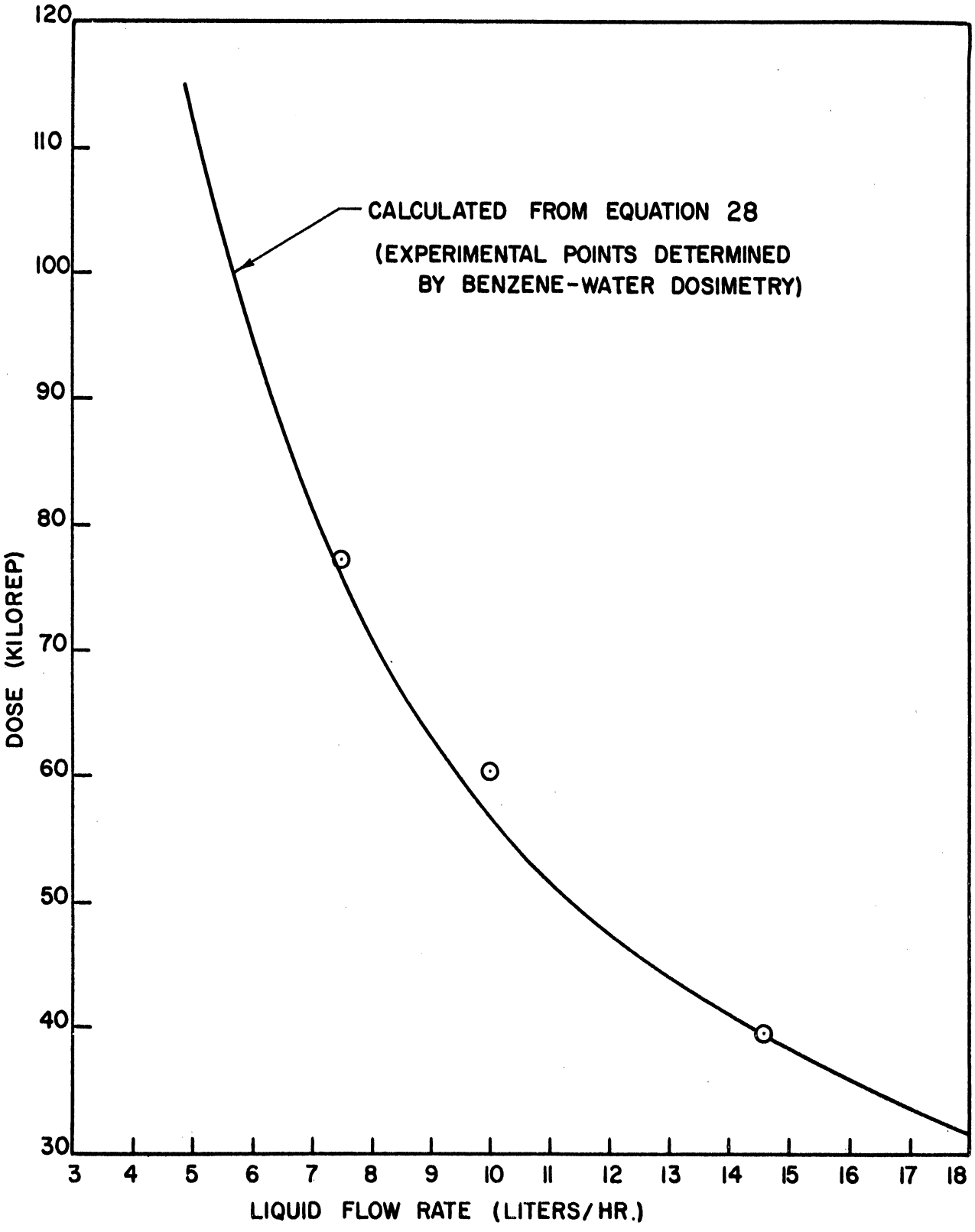

Figure 25. Variation of Dose with Flow Rate for the Reaction Vessel in "G" Port, Fuel Configuration "1a", and 100 Kilowatt Operation

Cadmium ratio values of 15.9 and 13.8 were measured for the gold and cobalt irradiations respectively. Measurements were made at a position 24-inches back from the core end of the beam-port. The cadmium ratio is defined as the ratio of activities for a bare and a cadmium covered gold foil.(32,63)

The cadmium "cut-off point" is about 0.4 ev, but care must be given to interpretation of the meaning of a cadmium ratio -- it is actually a ratio of the detector response to thermal plus resonance flux and the response to resonance flux alone.(32) Thus, it is not a direct measure of the ratio of fast to slow flux but can be used for comparative purposes. A feeling for this cadmium ratio may be gained by noting that the ratios measured inside the Ford Reactor core range from 2.0 to 6.0(63), and that the highest value measured in the thermal column at Brookhaven is 3000.(32)

It is interesting to note in Figure 21 that the angular flux distribution does not vary greatly in "G" port, despite the fact that the port and core face meet at a 75 rather than a 90 degree angle. The flux at position 2 on the core-end plywood disc obtained from gold foil measurements is extremely low, and, as indicated by the equivalent cobalt value, is probably in error.

Results from the benzene-water runs are presented in Table XI, Appendix A, and a sample calculation illustrating the method used to determine the dose from phenol yield is given in Appendix B.

Figure 22 shows the total dose received (due to both gamma radiation and neutrons) by the benzene-water system as a function of reactor power level with a constant flow rate of 14.6 liters/hour. Although the

data show some scatter, a reasonably linear relationship, as expected, is obtained. The scatter may be due to changes in reactor power level, as well as experimental and analytic errors. (For a complete discussion of various factors which may affect the accuracy of the benzene-water dosimetry, see Reference 34).

The dose received is a function of reactant residence time in the radiation field and field strength, i.e., flow rate and reactor power level. Hence, Figure 22 is only valid for a constant flow rate of 14.6 liters/hour and cannot be used directly to determine the dose received by a system operating at a different flow rate.

One method of getting around this difficulty is to convert the dose to a dose rate which then is only a function of power level. But, since dose, D, and dose rate, D.R., are related by the equation

$$D.R. = \frac{D}{\tau} \; 1000 \qquad (14)$$

it is evident that the residence time, τ, must be averaged over the actual residence time distribution for the flow reactor in order to obtain an absolute value for the dose rate. On the other hand, it can be shown that if some average residence time is calculated by a consistent method, dose rates calculated from Equation (14), although they are not absolute dose rates, may still be used for comparative purposes.

Assume that a benzene-water dosimetry system shows a yield of z micromoles/liter of phenol (equivalent to a dose D_1, in kiloreps) when exposed for a time τ_1 based on the actual residence time distribution. Let some average residence time $\tau_{1,\text{avg.}}$ be calculated by simply dividing the reaction vessel volume V by the flow rate F_1, so that

$$\tau_{1,Avg} = 60V/F_1 \tag{15}$$

Then

$$\frac{\tau_{1,Avg}}{\tau_1} = \frac{60V/F_1}{\tau_1} \equiv a \tag{16}$$

Where a is simply a constant. Next, a chemical reaction is studied in the same vessel but at a new flow rate F_2, with a corresponding residence time τ_2 based on the actual distribution. If the flow pattern in this case is the same as that for the dosimetry work, the ratio of residence times will not change, that is,

$$\frac{\tau_{2,Avg}}{\tau_2} = \frac{60V/F_2}{\tau_2} \equiv a \tag{17}$$

Then, combining (15) and (16),

$$\frac{V/F_2}{\tau_2} = \frac{V/F_1}{\tau_1} \tag{18}$$

or

$$\frac{\tau_2}{\tau_1} = \frac{V/F_2}{V/F_1} \tag{19}$$

Rigorously, D_2 the dose received by the second system is the dose, D_1, received in the first case multiplied by the ratio of the actual residence times, or

$$D_2 = \frac{\tau_2}{\tau_1} D_1 \tag{20}$$

or from (19),

$$D_2 = \frac{V/F_2}{V/F_1} D_1 \tag{21}$$

and, since

$$\frac{D_1}{60V/F_1} = \frac{D.R.}{1000} \tag{22}$$

Equation (21) becomes

$$D_2 = \frac{60V}{F_2}\left(\frac{D.R.}{1000}\right) \tag{23}$$

Hence, the dose for the chemical system of interest may be calculated from a dose rate based on an arbitrary average residence time, even though the dose rate thus obtained is not a true absolute value.

Figure 23 shows a plot of dose rate, D.R., versus power level, P, where the dose rate has been calculated by assuming an average residence time as in Equation (15). In specific, the dose rate was calculated by noting that,

$$D.R. = \frac{1000D}{\tau_{Avg}} = \frac{1000D}{60V/F} \tag{24}$$

and that from Figure 21,

$$D = 0.39P \tag{25}$$

hence,

$$D.R. = \frac{390P}{(60V/F)} \tag{26}$$

and, for the present work, V is 5.3 liters and F is 14.6 liters/hr so that,

$$D.R. = 17.9P \tag{27}$$

where the dose rate is in R/min and the power level is in kilowatts.

A general expression for the dose received inside the pressure vessel may now be derived by combining Equations (23) and (27).

$$D_2 = 1.07\left(\frac{V}{F_2}\right)P \tag{28}$$

For convenience, this relation is shown graphically in Figure 24.

Throughout this discussion, it has tactfully been assumed that the flow pattern (channeling, etc.) does not markedly change over the flow rates of interest. In order to check this assumption, three runs were made at different flow rates, and the results are compared with Equation (28) in Figure 25. Reasonably good agreement is indicated.

The values of dose rate obtained from the benzene-water runs may be used as a rough check of the neutron flux in the port. A reasonably accurate correlation of neutron flux and dose rate for regions outside of the reactor core has been developed.(34)

$$D.R. = 1.64\ \Phi_S^{0.337} \qquad (29)$$

Assuming that this relation is also valid inside the pressure vessel, a neutron flux of about 9×10^8 n/sec cm^2 is calculated from dose rate data at 100 kw. As expected, due to absorption in the vessel wall, this value is several factors of 10 lower than the measured flux for a dry beam-port.

In addition to the work already discussed, the gamma flux in the pool water along the side of "G" port was measured. Details of this measurement are given in Section III, C, and the results in Figure 28.

(3) Summarized Conclusion

a) Gold foil and cobalt wire measurements show that the thermal neutron flux in "G"-port is given by $\Phi_{th} = 8.6 \times 10^{10}\ e^{-0.0826\,L}$ where L is the distance from the core end of the port in inches. This is for 100 kw operation with the port dry.

b) The angular thermal neutron distribution is fairly constant.

c) The cadmium ratio for "G" port running dry at 100 kw is about 15 at a point 24 inches from the core end.

d) As determined by benzene-water dosimetry, the total dose (gamma plus neutron) received in the reaction vessel located in "G" port is given by

$$D_2 = 1.07 \left(\frac{V}{F_2}\right) P \qquad (28)$$

where $\left(\frac{V}{F_2}\right)$ is the average residence time in hours for the system under consideration, and P is the reactor power level in kilowatts. This expression is based on the assumption that the flow pattern for the system of interest is not markedly different from that obtained with the benzene-H_2O system.

e) Assuming that the relation D.R. = $1.64 \Phi_S^{0.337}$ which was derived from measurements in the pool water is valid inside the reaction vessel, the average neutron flux in the vessel is calculated to be 9×10^8 n/sec cm^2 .

f) Gamma flux measurements in the pool water along the side of "G" port are summarized in Figure 28.

C. Fission Plate - "J"-Port Calibration

(1) Experimental Measurements

(a) Gold Foil Measurements. A reproducible method for positioning gold foils at the face of the fission plate which utilizes a 13-inch-square of 1/4" thick sheet polyethylene was devised. As in previous work, 100 mg gold foils were scotch-taped to this holder in positions indicated on page 62 . Then a lead strip was attached to the bottom of the plastic sheet for weight, and the entire assembly was connected to strings and

dropped down through the pool water next to the fission plate. Two small hooks on the top of the plastic sheet are designed to fit over the top of the fission plate and aid in accurate positioning of the foil holder.

Four ten-minute irradiations at 10 watts were performed. The first two measurements, one with bare gold foils and one with cadmium covered foils, were run on the east face of the core with the standard configuration "1a" (see Figure 19). Then the measurements were repeated with the fission plate in place on the east face (see Figure 26 for a diagram of this fuel configuration).

Since precise power adjustments are difficult at 10 watts, a gold foil was attached to a reflector element on the south face for each run. This foil served as a power level monitor and was used to normalize the runs to 10 watts.

Counting and calculation techniques used are the same as those already described for "G"-port measurements.

(b) Gamma Measurements Along "J" Port. A Victoreen Roentgen Rate Meter was used to make gamma flux measurements in the pool along the side of "J" port. The Rate Meter probe was sealed in a plastic tube to prevent damage from the water, and several strings were tied to it to aid in the under-water positioning. Distances along the beam port were measured by using a long aluminum pipe to manipulate a meter stick into position along the port.

Three sets of measurements were run. Readings were taken along "J" port at 100 kilowatts with and without the fission plate in

position. Then, for comparison, a similar measurement was taken along "G" port with the standard "1a" fuel configuration, i.e., without the fission plate.

(c) Threshold Measurements. Several threshold measurements[60] were made using aluminum and magnesium foils. Five such foils, located at six-inch intervals, were taped on a narrow strip of polyethylene, lowered down through the pool water to a position directly on top of "J" port, and placed parallel to the major axis of the port. The closest foil was then two inches from the surface of the fission plate. Also, some foils taped to thin plastic sheets were placed directly between the plates in several of the core fuel elements. One to two hour irradiations at 100 kilowatts were required for all runs. The following reactions were considered:

TABLE V

THRESHOLD REACTIONS FOR Al AND Mg (REFERENCE 60)

Foil	Reaction	Threshold (Mev)	Half Life	Cross Section (mb)
Al	$Al^{27}(n,p)Mg^{27}$	5.3	9.7 min	80
	$Al^{27}(n,\alpha)Na^{24}$	8.6	15.0 hr	110
Mg	$Mg^{24}(n,p)Na^{24}$	6.3	15.0 hr	48

Mg^{27} was counted with a 3" x 3" NaI crystal and absolute counting technique[28] and checked with a 4π counting set-up. Due to the very short

half-life and low activation, some difficulty was encountered in measuring this activity for foils irradiated at a distance from the fission plate.

The Na^{24} was originally counted in the same manner, but to speed the work a well-type scintillation counter (RCL Type 23-A) was calibrated for this purpose.

(2) Results and Discussion

Original data from foil measurements and gamma measurements taken with the fission plate in place are presented in Tables XIV, XVII, and XVIII in Appendix A.

Figure 27 indicates the thermal neutron flux and cadmium ratios measured by gold foil techniques across the face of the fission plate. Values are also shown for the core face without the fission plate, i.e. with fuel configuration "1a". Due to the positioning of the plastic foil holder, the later measurements are for locations approximately 2 inches higher than the equivalent fission plate values.

Examination of the three upper foil positions indicates that insertion of the fission plate causes the thermal neutron flux to decrease by a factor of 1.1 - 1.2. Also the cadmium ratios are decreased by a factor of 1.4 - 1.5. The measurements taken at the two lower foil positions are not consistent, since they indicate a marked decrease in thermal flux but no decrease in the cadmium ratio. This discrepancy is probably the result of placing the foils too low on the fission plate so that the base plate of the fission plate holder actually interferred with the flux.

A, B, C: Safety-Shim Rods (5 Plate Elements)
CR: Control Rod (5 Plate Element)
S: Po-Be Source
F.P: Fission Plate
F.C: Fission Chamber

F18 / 23 — Fuel Element No. 18 in Core Position 23

R41 / 50 — Graphite Reflector Element No. 41 in Core Position 50

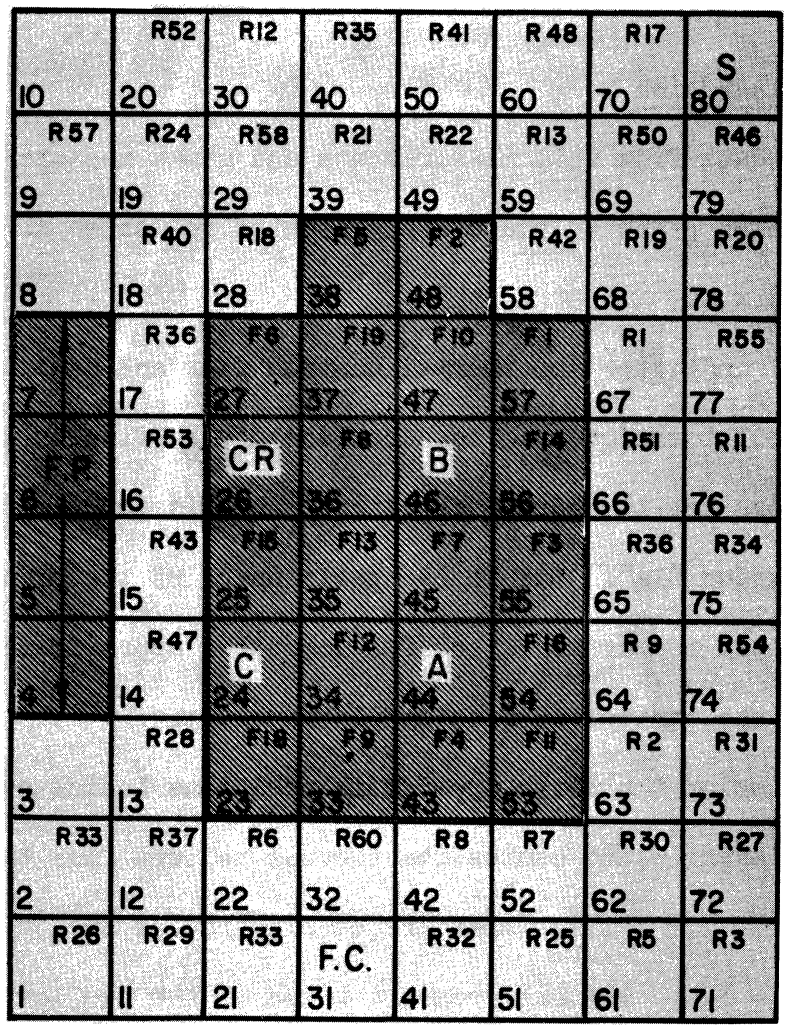

Figure 26. Core Loading "lfp" Used for All Fission Plate Experiments

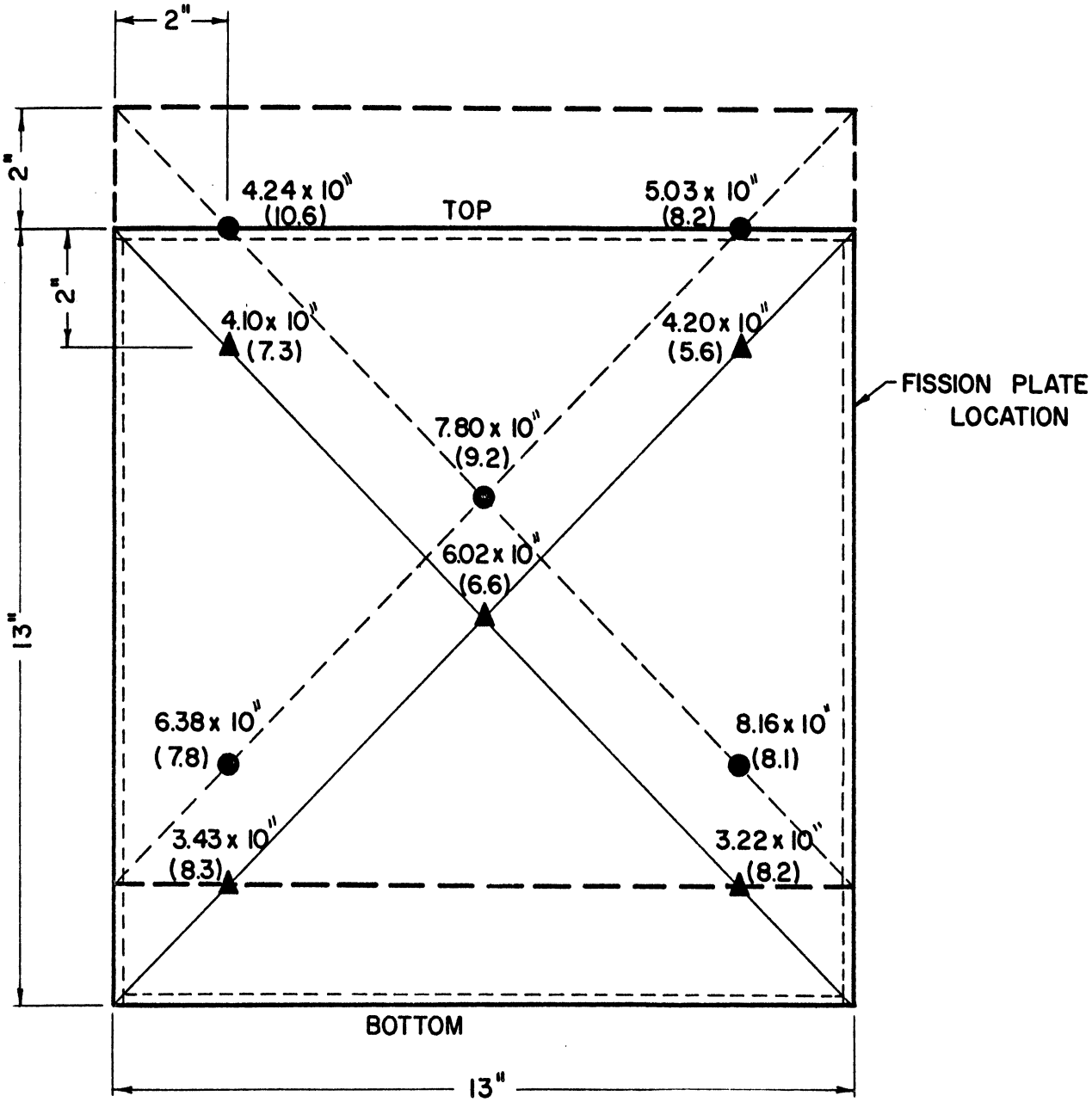

SYMBOLS:

● Measurements on East Face of Core with Fuel Configuration "1a"

▲ Measurements on East Face with Fission Plate in Position

4.24 x 10" ← Thermal Neutron Flux, n/cm^2sec

(10.6) ← Cadmium Ratio

Figure 27. Effect of the Fission Plate on the Thermal Neutron Flux and Cadmium Ratio

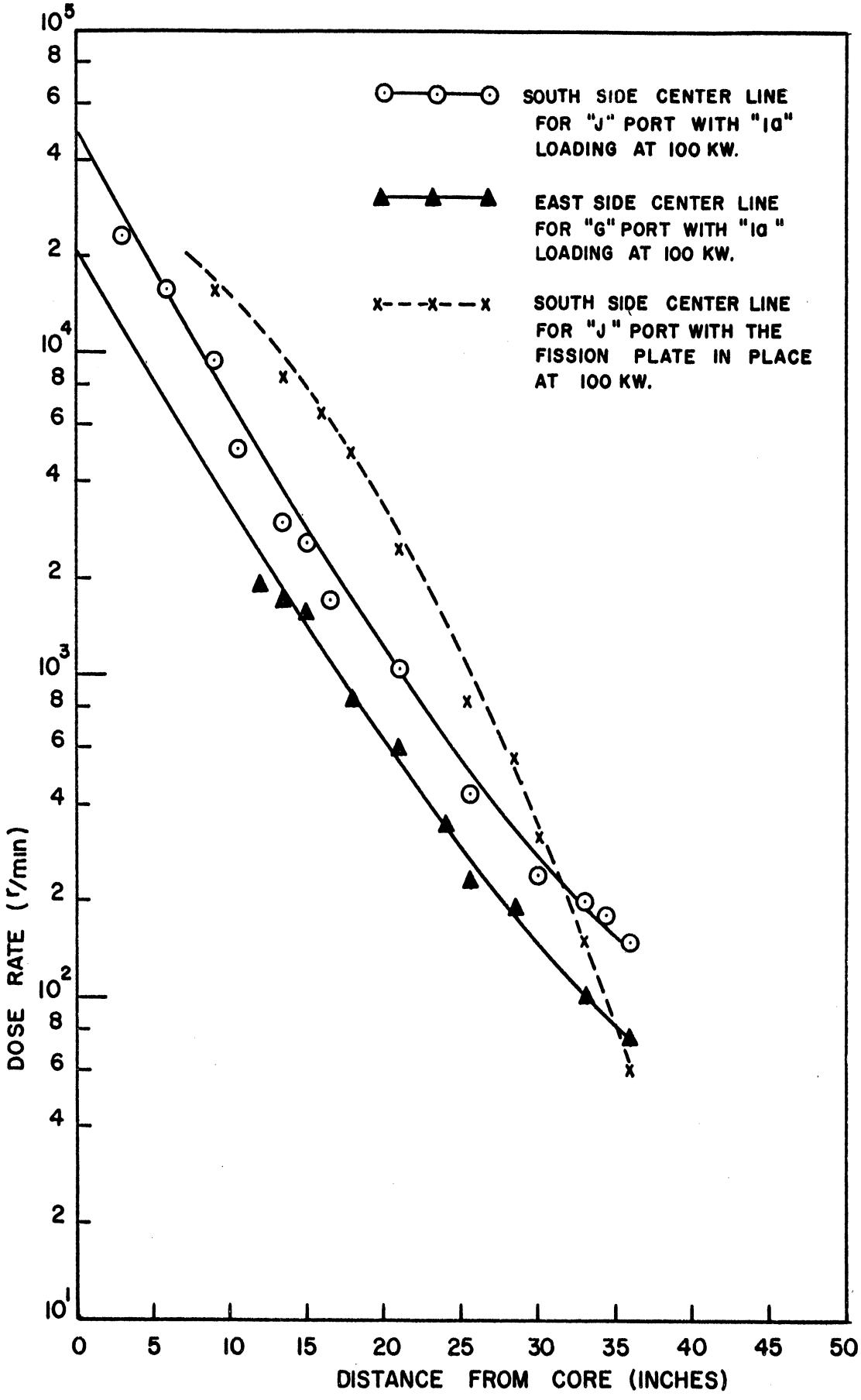

Figure 28. Comparison of Gamma Dose Rates Measured in the Reactor Pool Along "G" and "J" Ports

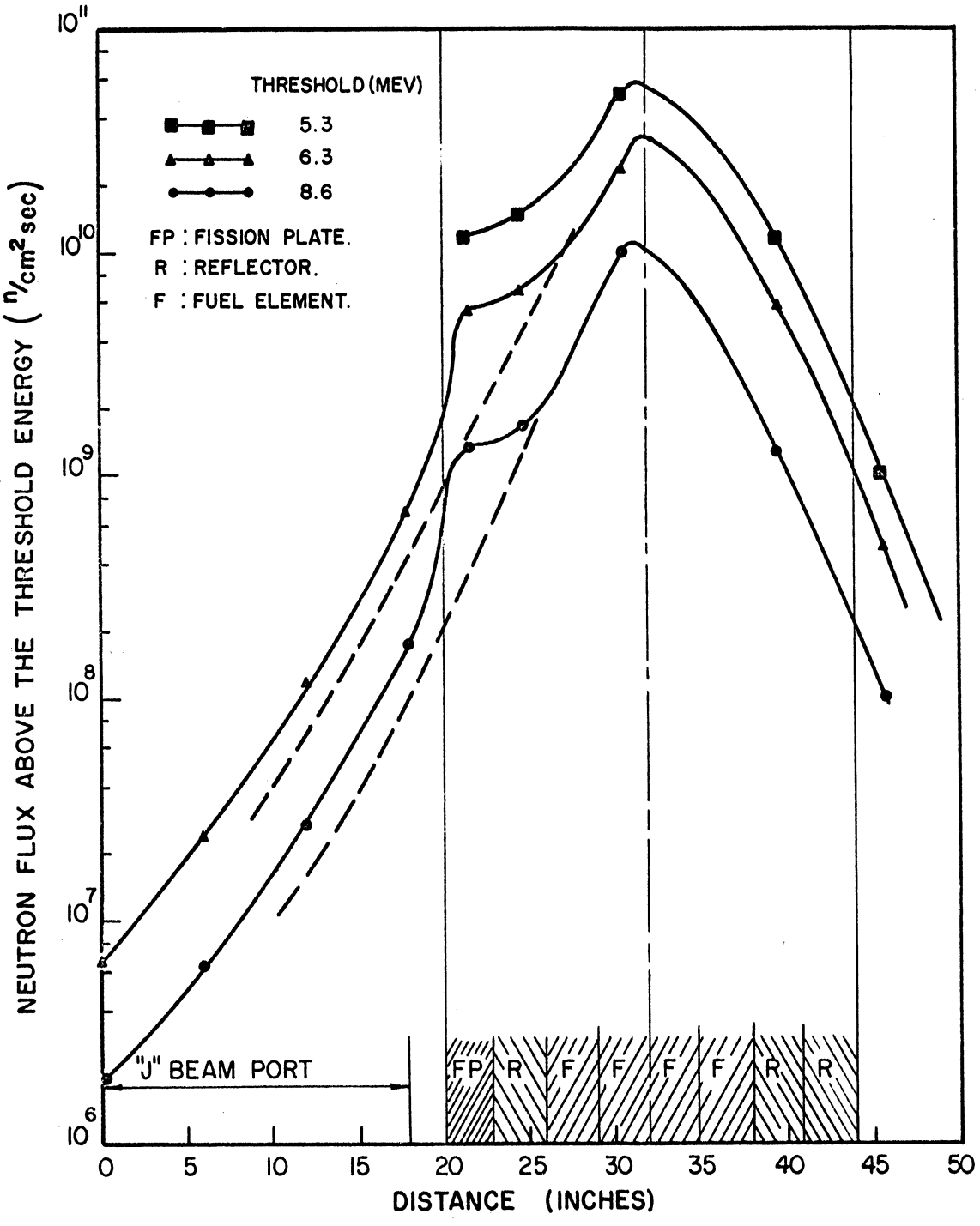

Figure 29. Threshold Flux Measurements with the Fission Plate Located on the East Face of the Core and the Reactor at 100 Kilowatts

Figure 28 summarizes gamma flux data obtained with the Victoreen Meter. Comparison of the curves for "G" and "J" ports indicates that even with the standard "1a" fuel configuration, the gamma flux along "J" is approximately twice that along "G". This is probably due to the fact that "J" port is closer to the core center line than is "G" (see Figure 6). The slight curvature of both plots is due to the fact that measurements are along the beam port, i.e. at a 75° angle to the core, rather than perpendicular to the core.

The gamma flux curve for "J" port with the fission plate in place is definitely higher than the standard "J" port curve and has an entirely different shape. In order to insert the fission plate, it is necessary to remove reflector elements on both sides of the plate (see Figure 26). Also, since the plate itself is only about 1/2 the height of a fuel element, it only covers a part of the core face. Thus, the surface of the core with the fission plate in position is very irregular and can no longer be considered a plane source of radiation. This, along with some spurious readings resulting from the high fast neutron flux, may have caused the irregular shape of the gamma rate curve.

Neutron flux measurements obtained from threshold techniques are shown in Figure 29. The curves represent the total neutron flux composed of neutrons having energies above the appropriate threshold valves indicated. The fission plate causes a sharp jump in all of the curves. If it is assumed that the flux profile is normally symmetrical and that the profile is extended as shown by the dashed line in the figure, there appears to be approximately a two-fold increase in the neutron flux above the various thresholds. The low energy curve was not extended into the pool because of counting difficulties due to the short half-life of Mg^{27}.

(3) Summarized Conclusion

a) The fast neutron flux is increased by the fission plate as indicated by an average decrease in cadmium ratios by a factor of 1.5, and two-fold increase of high energy threshold flux values as shown in Figure 29, page 87 .

b) The thermal neutron flux is slightly decreased (factors range from 1.1 to 1.2) by use of the fission plate.

c) The gamma flux is increased along "J" port by use of the fission plate. The magnitude of this increase varies with position as shown in Figure 28, page 86 .

d) For fuel configuration "1a", the gamma flux along "J" port is approximately twice that for "G" port.

IV. EXPERIMENTAL WORK AND RESULTS

A. The Heptane - Hydrogen System

(1) Experimental Procedure

Operating and sampling procedures described in Chapter III and Appendix D were followed for all normal heptane-hydrogen runs. In general, the nitrogen purge and heat-up were begun two hours before the start of a run. In each case, variables such as temperatures, pressures, and feed rates were lined out at run conditions and held at a steady state for at least 15 minutes before the run. Runs lasted from 20 to 50 minutes, followed by a 20 minute nitrogen shut-down purge.

Runs were considered valid if the maximum variation in temperature at any fixed point was less than $\pm$ 5°F and pressure variations were less than $\pm$ 10 psi. In most cases, variations were well within these limits.

Gas and liquid samples were collected as indicated in Appendix D. Gas samples were immediately sealed and removed to the analytic lab. The collection flasks for liquid samples were maintained at a constant temperature by means of a cooling bath. The liquid was quickly sealed upon removal from the system and placed in a refrigerator freezing compartment until analysis. Liquid recovered in the cold traps was handled in a similar manner.

Initially, three or four samples were taken during each run, and all samples were analyzed. In all instances, results agreed within $\pm$ 10%, indicating that reasonably steady-state operation was obtained. In later work, two liquid samples were analyzed for each run and the results were averaged. Gas samples were taken once during these runs.

For some runs, the off-gas composition was not of interest, and only the liquid samples were analyzed.

All runs were made in "G" port with the exception of fission plate irradiations where it was necessary to use "J" port. Radiation runs were considered valid if the reactor power level was maintained within $\pm$ 5% of the set point. Details concerning the operation of the nuclear reactor (such as rod positions, time of start-up and shutdown, etc.) are permanently recorded in the reactor log book maintained in the Phoenix Building of the University of Michigan. Page references to this book are listed for each run so that the nuclear reactor operation data may be checked for any given run (Table VIII).

Blank runs were also performed with the pressure vessel in place in the beam port, but with the nuclear reactor shut down. At least 24 hours was allowed between the pile shutdown and a given blank run. Thus, the residual gamma radiation from the reactor core was at a low level. However, some radiation due to induced radioactivity in the pressure vessel was present during these runs. Even so, the total gamma field in the vessel was only 10-20 R/hr and can be considered negligible in comparison to the dose rates ($\sim 10^5$ R/hr) used for radiation runs.

Over 70 runs were made with the hydrogen-heptane system covering the following range of variables:

Temperature	500 - 750°F
Liquid Flow Rate	1 - 4 ℓ/hr
Moles H_2/Mole heptane	0 - 5
Dose	3 - 30 kilorep
Dose Rate	either 0 or 1790 R/min (0 or 100 KW)
Pressure	All runs at 250 psi

Phillips Petroleum pure grade normal heptane was used for all runs. Hydrogen gas was from Liquid Carbonic Corporation cylinders, and as pointed out in Chapter II, oxygen and water were removed from this gas before it entered the reaction vessel.

Some similar runs were made in which nitrogen, helium, or argon were used in place of hydrogen. These gases were purchased from the Baird Gas Corporation, Airco, and the Matheson Company respectively.

Special note should be made of the check-out procedure used when the pressure vessel was first inserted into the beam port (Appendix F).

(2) Methods of Analysis

Liquid samples were analyzed with a partition chromatography unit, and gas samples were analyzed by means of a mass spectrometer. Details of the procedures used are given in Appendix G.

(3) Results

Data obtained from n-heptane runs are summarized in Tables VIII and IX, Appendix A.

The liquid conversion, the radiation conversion, the percent of the total conversion, and G values are shown as a function of temperature in Figures 30 through 34. These figures all refer to runs with a mole ratio of hydrogen to heptane in the feed of about 0.7 and residence times of about 9 minutes ($\sim 1.5 \times 10^4$ Rep.).

Figures 35 through 39 show the effect of changing the feed rate, and hence residence time, and total radiation dose.

The effects of gas ratio and type of gas used in the feed are illustrated by Figures 40 through 42.

Figure 43 compares G values from the present work with data from Reference 40 for high temperature radiation cracking but for different systems.

Gas product compositions are plotted in Figure 44, and a comparison with some published data is given in Table VII.

(4) Discussion of Results

(a) Definition and Significance of Liquid Conversion.--The terms "liquid phase conversion" and "liquid conversion" are used throughout this report to represent the mole percent cracked hydrocarbon in the liquid product as determined by partition chromatography techniques (see Appendix G for details). This was found to be an easy, cheap, and reasonably accurate measurement, and, as discussed in the Appendix, the liquid conversion was found to be numerically equal to the normal heptane decomposition for the sampling conditions and low conversions used in this work.

(b) The Effect of Process Variables on Overall Yields

(i) Temperature.-As shown in Figure 30, the total liquid conversion is a rapidly varying function of temperature. The two curves representing radiation runs are of the same general shape as the blank run; however, since they are slightly displaced toward lower temperatures the yield for a given temperature is increased. The total liquid conversion is plotted on semi-log paper in Figure 32, and it is seen that the conversion deviates from an exponential function of (1/T) at low temperature.

The differences in yields between the blank runs and radiation runs are plotted as a function of temperature in Figure 33. These

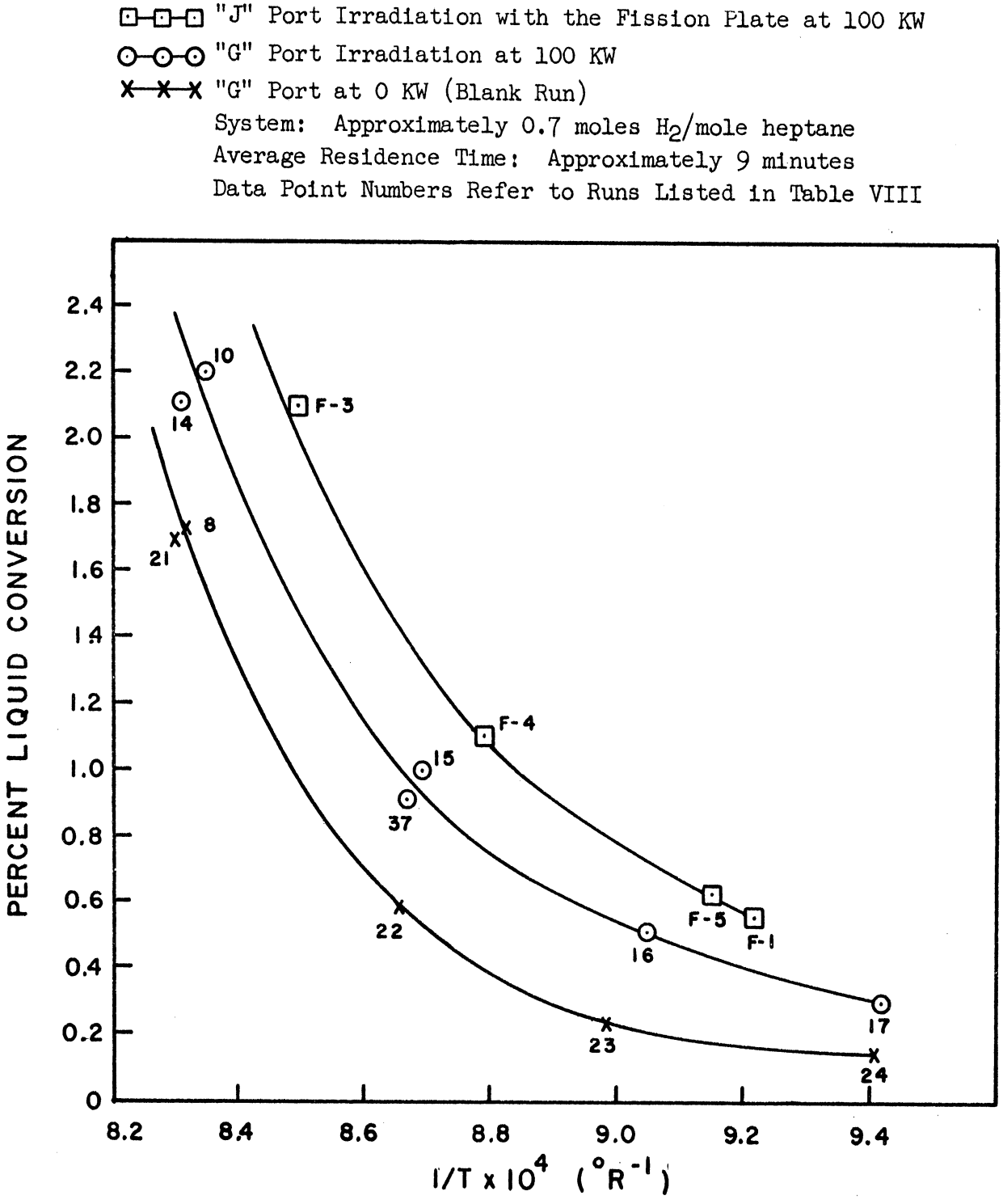

Figure 30. Liquid Conversion Vs. Temperature

TABLE VI

A Summary of Runs Below 600°F

Run	Temperature (°F)	Reactor Power Level (kw)
28	548	0
29	548	0
54	515	0
57	513	100
F-2	546	100 plus the fission plate

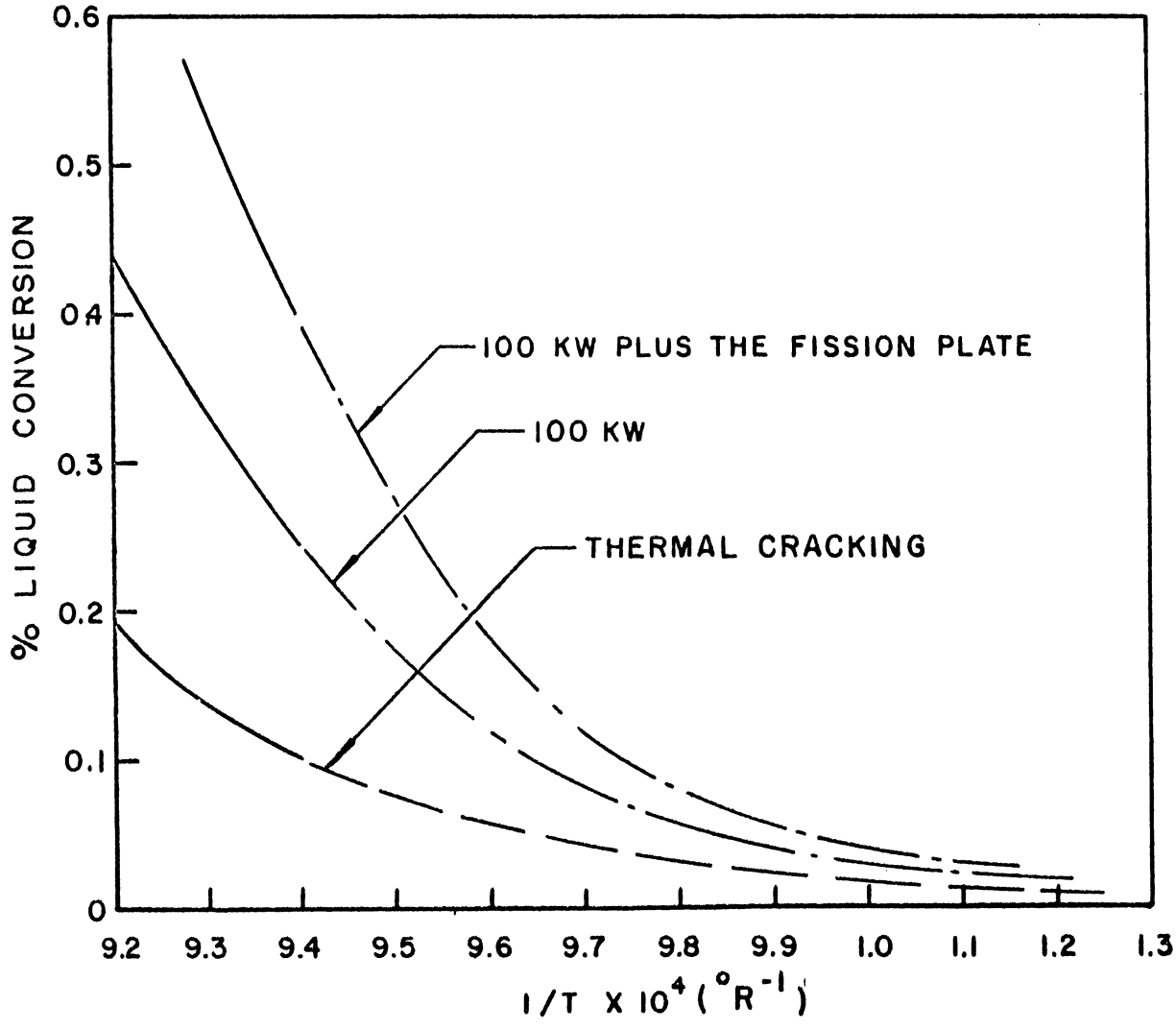

Figure 31. Postulated Initial Cracking Curves

⊡-⊡-⊡ "J" Port Irradiation at 100 KW with the Fission Plate

⊙-⊙-⊙ "G" Port Irradiation at 100 KW

X-X-X "G" Port at 0 KW (Blank Run)

System: Approximately 0.7 moles H_2/mole heptane

Average Residence Time: Approximately 9 minutes

Data Point Numbers Refer to Runs Listed in Table VIII

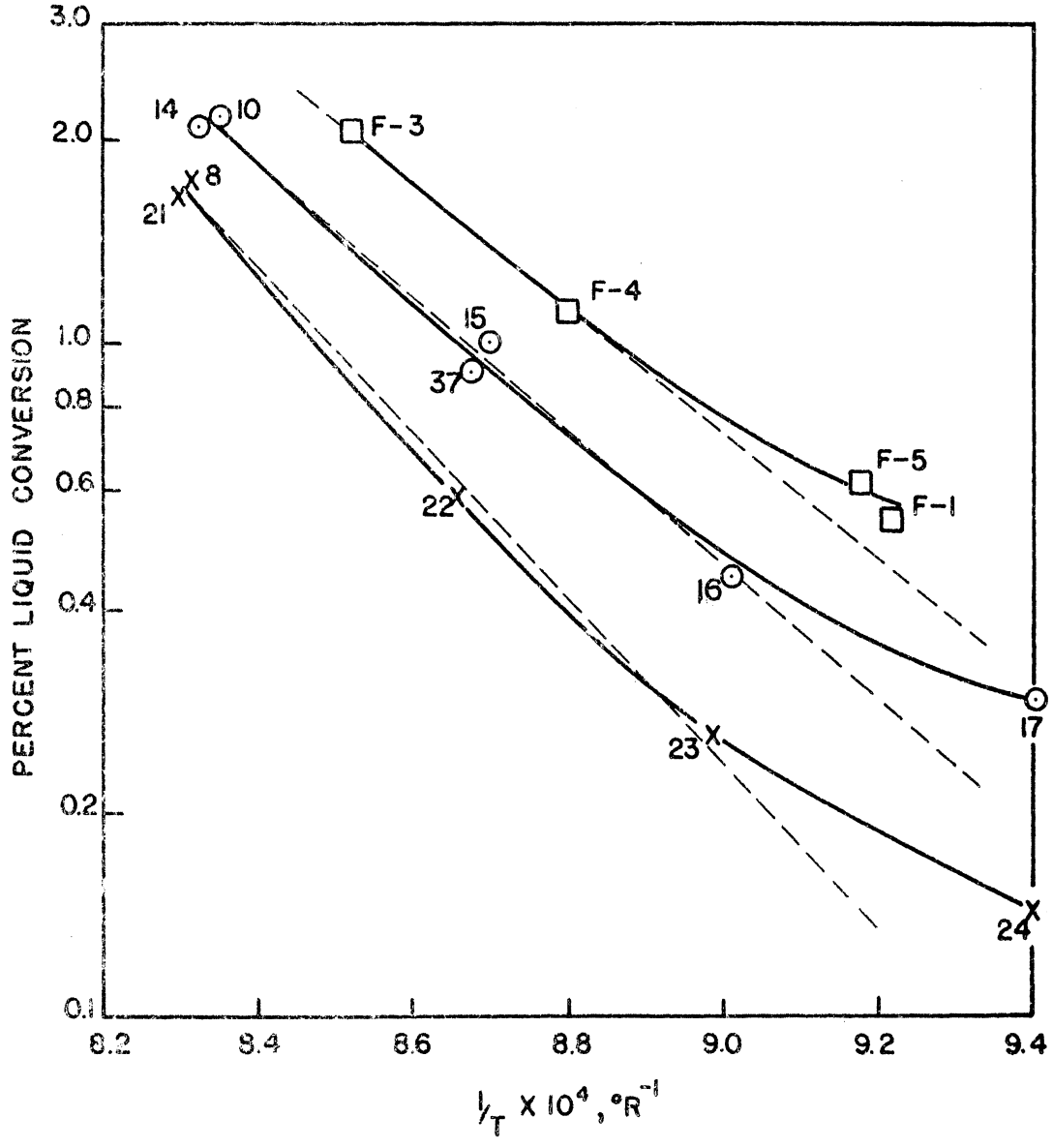

Figure 32. Log Liquid Conversion Vs. Temperature

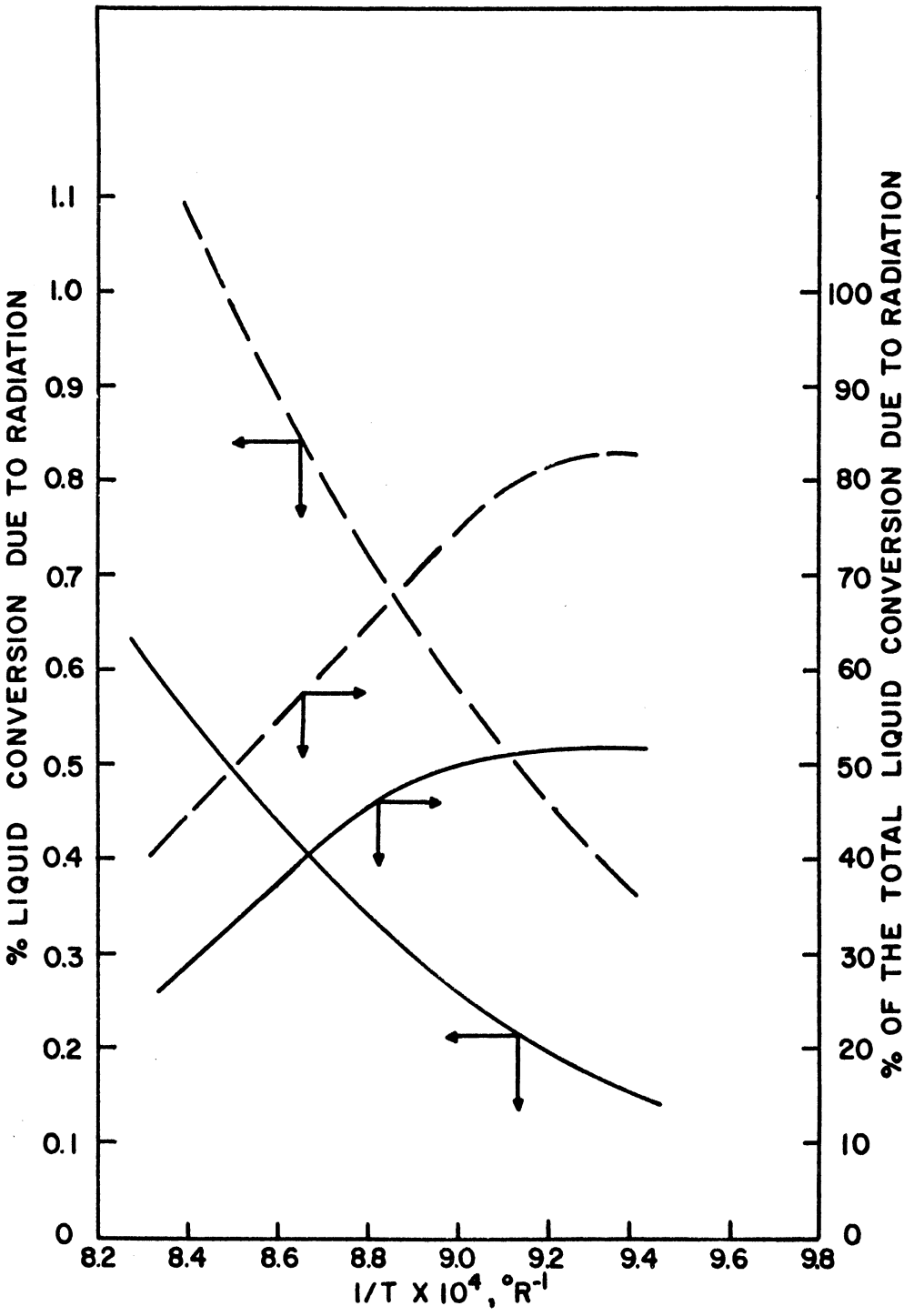

– – – Calculated Difference of % Liquid Conversion from Smoothed Curves in Figure 30 for "J" Port Irradiations and the Blank Runs

——— Calculated Difference of Liquid Conversion for "G" Port Irradiations and Blank Runs

Figure 33. Radiation Conversion (Total Liquid Conversion Minus Thermal Conversion) and the Percent of the Total Conversion Due to Radiation Vs. Temperature

System: 0.7 Moles H_2/Mole n-C_7 at 250 psig
Irradiations in "G" Port with Fuel Configuration "1a"

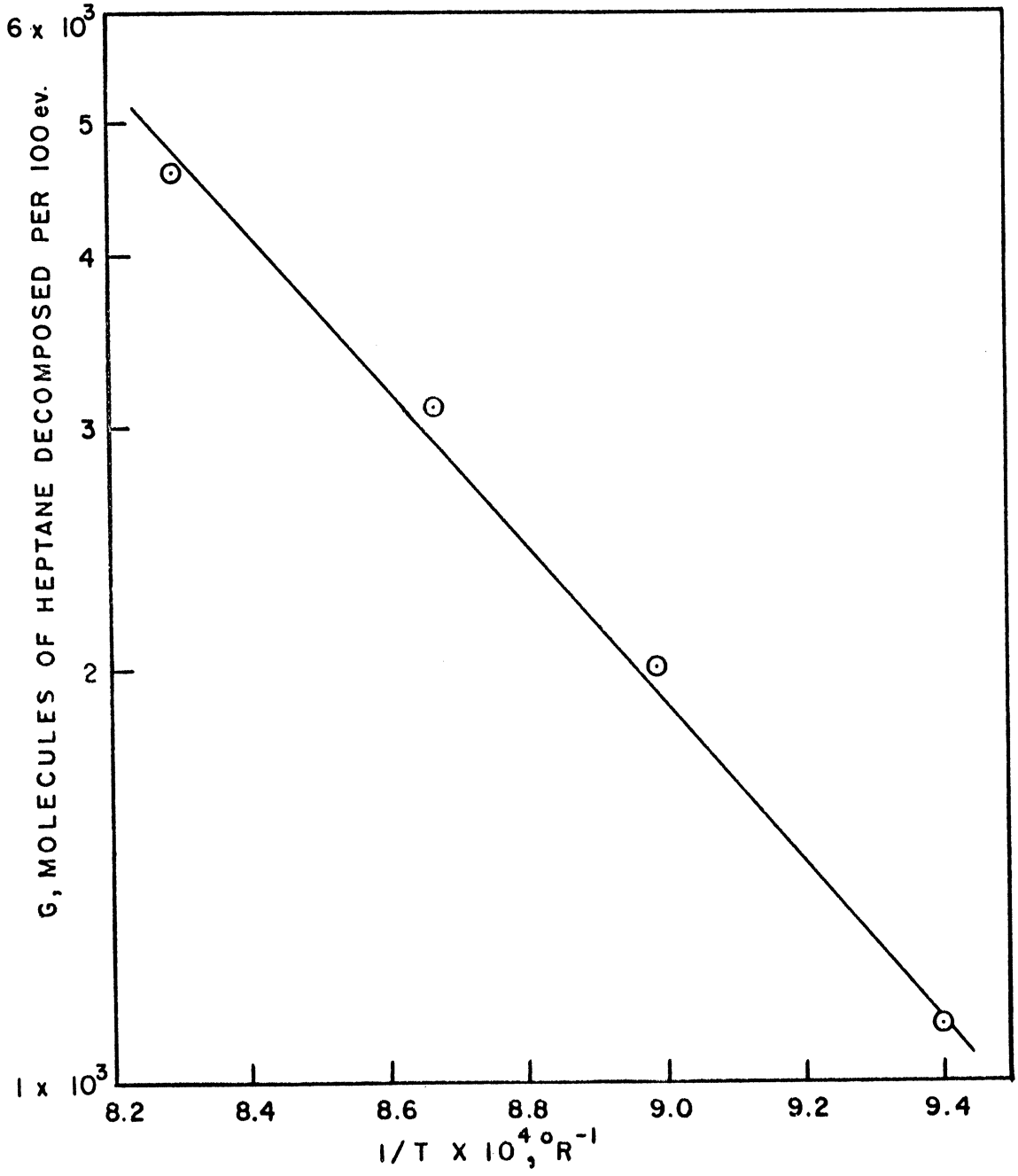

Figure 34. Radiation Yield Vs. Temperature

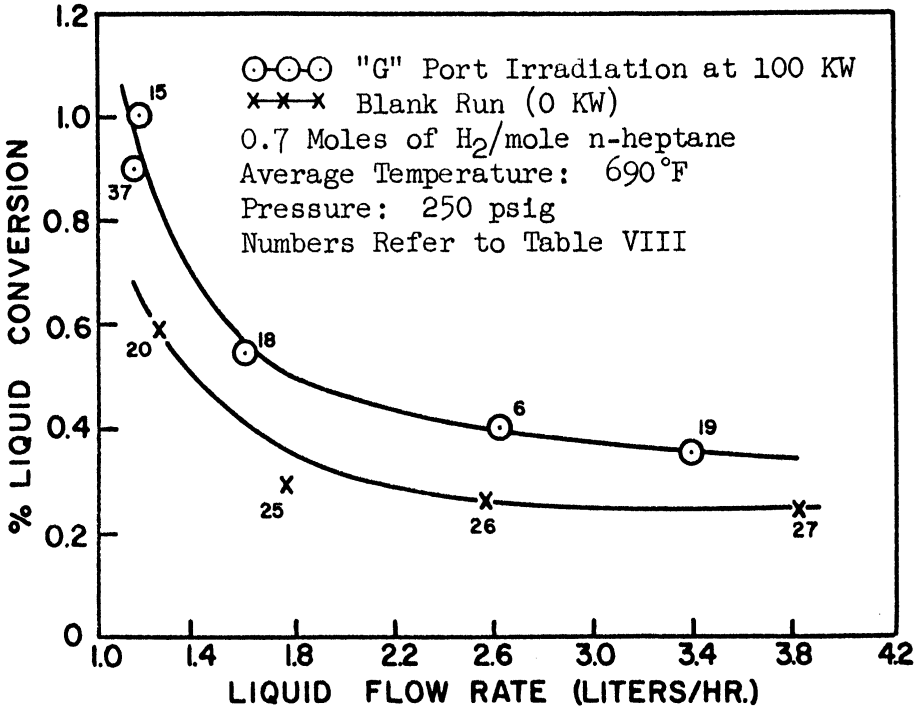

Figure 35. Liquid Conversion Vs. Liquid Flow Rate

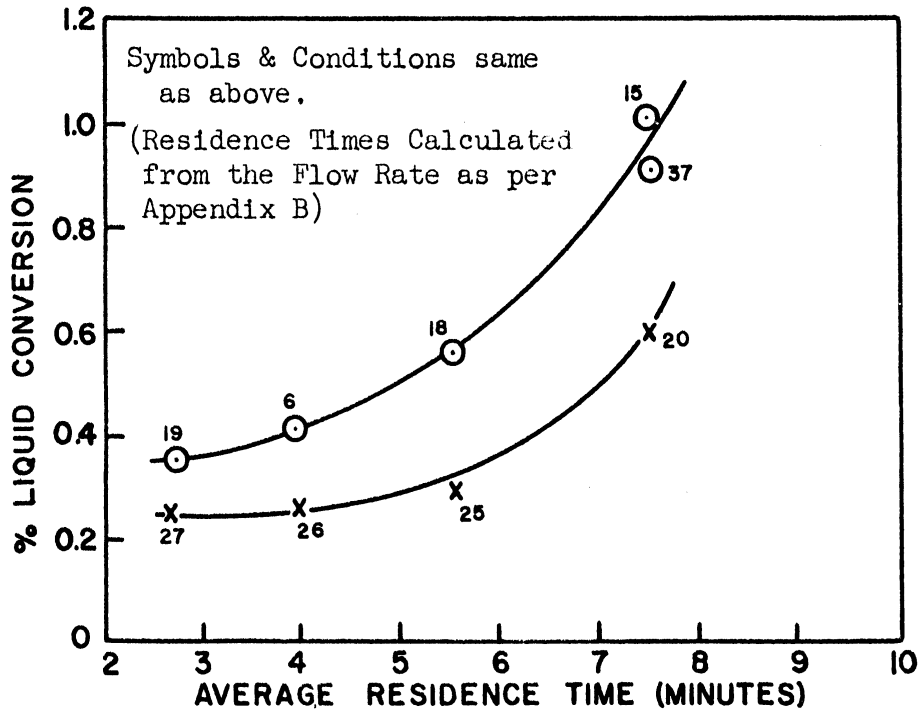

Figure 36. Liquid Conversion Vs. Average Residence Time

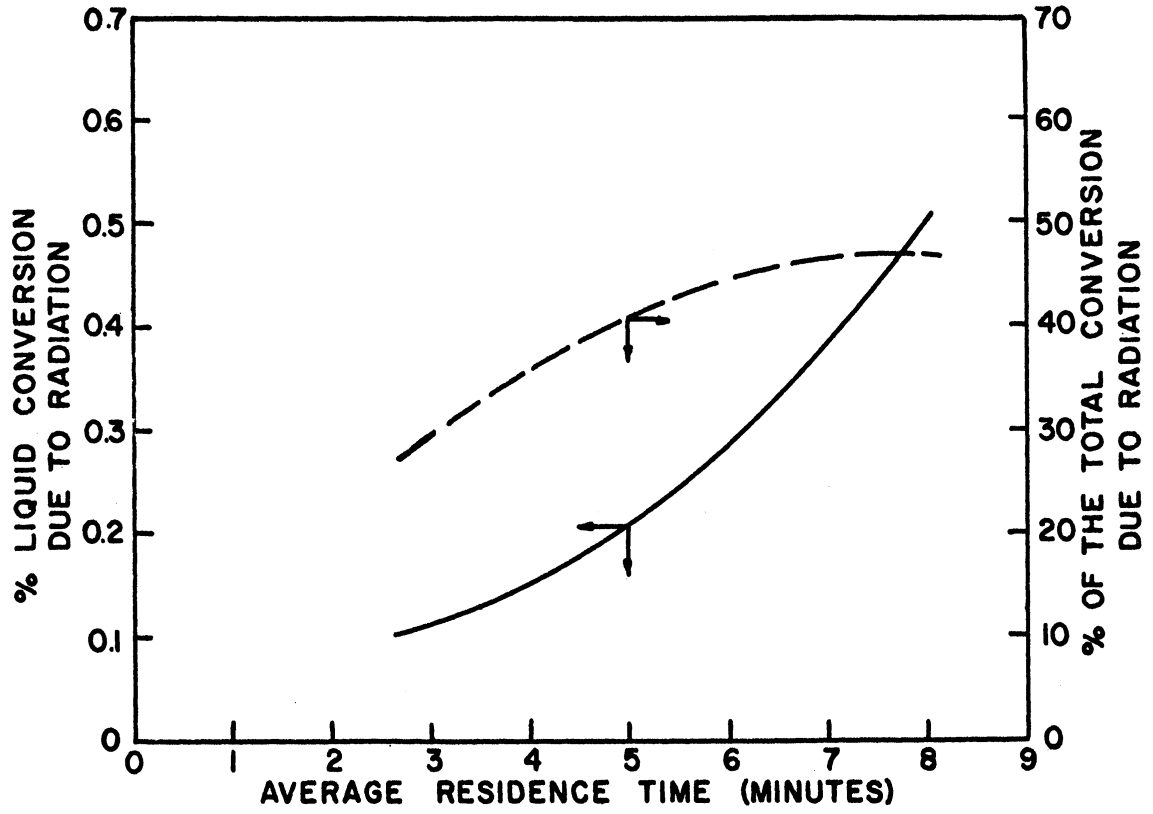

0.7 Moles H_2/mole n-heptane
"G" Port Irradiation at 100 KW
Differences Calculated from Smoothed Curves in Figure 36

Figure 37. Radiation Conversion (Total Minus Thermal) and the Percent of the Total Conversion Due to Radiation Vs. Residence Time

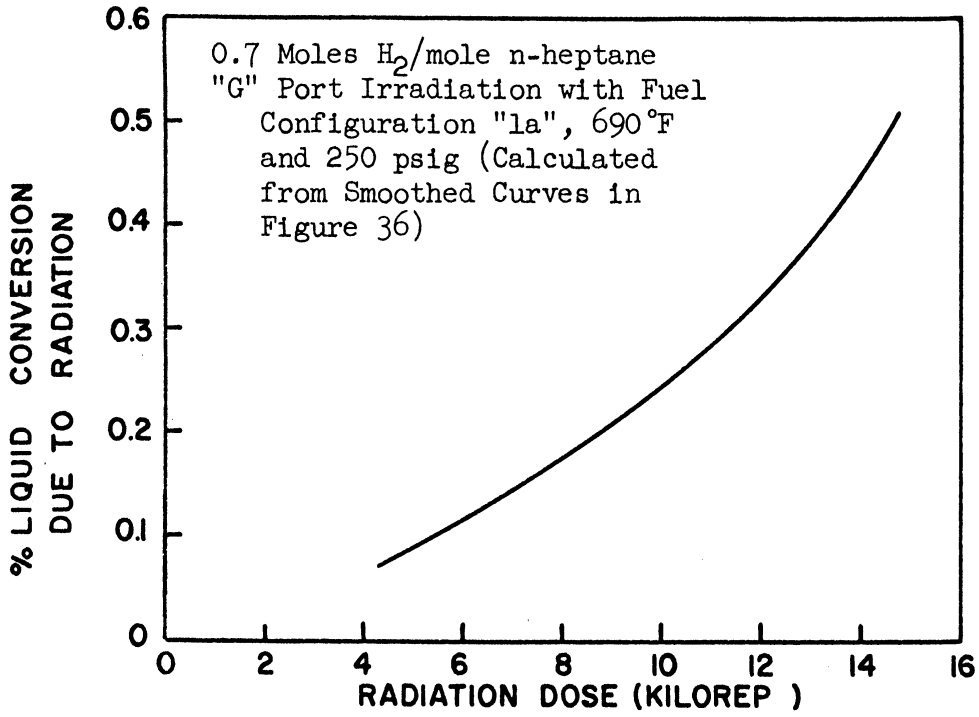

Figure 38. Radiation Conversion (Total Liquid Conversion Minus Thermal) Vs. Dose

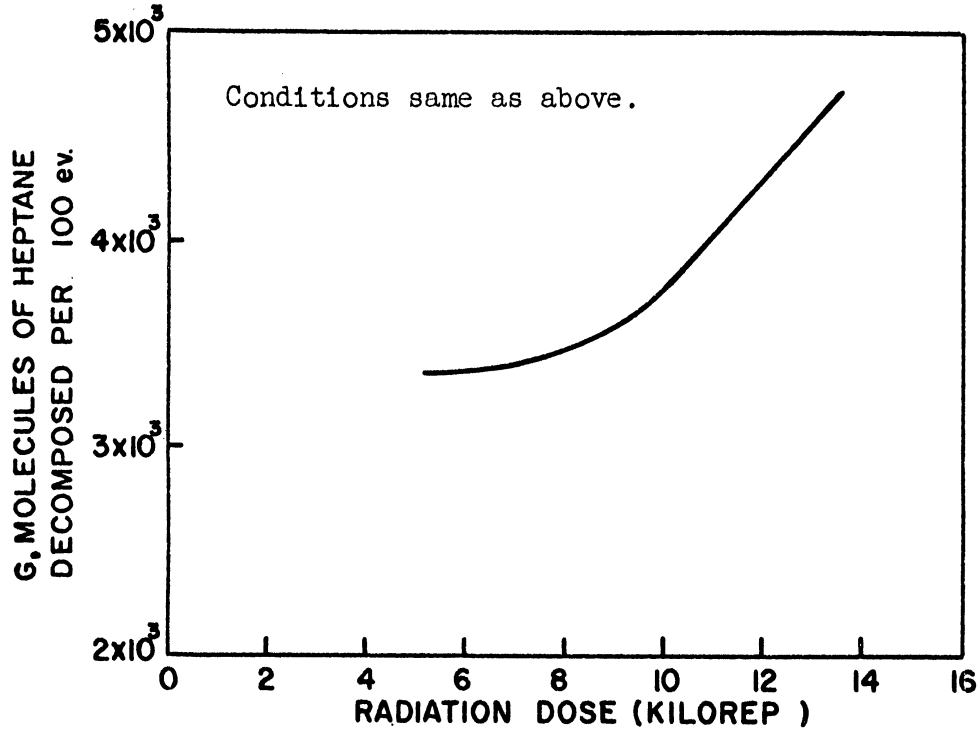

Figure 39. Radiation Yield Vs. Dose

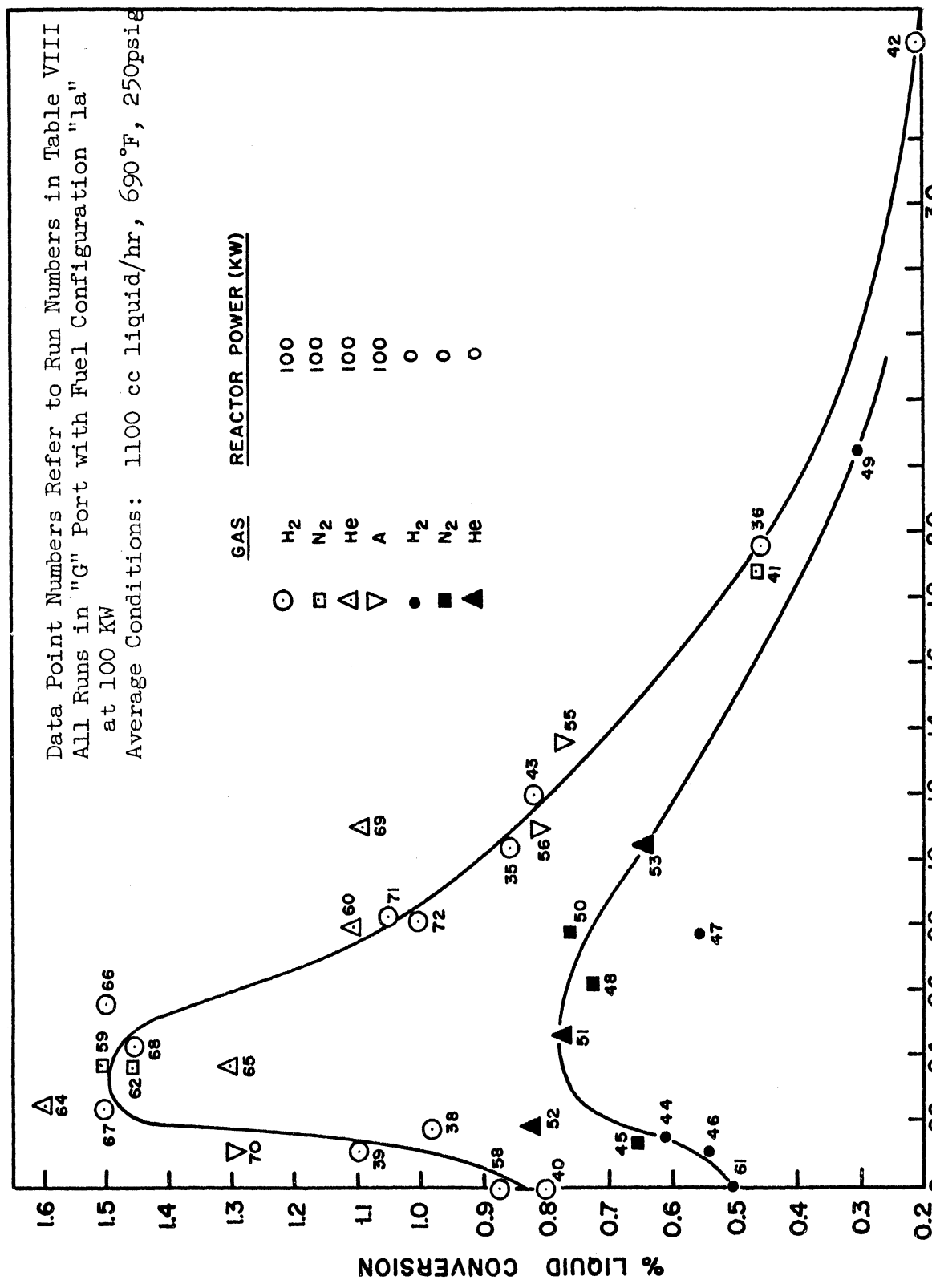

Figure 40. Liquid Conversion Vs. Molal Gas to Liquid Ratio

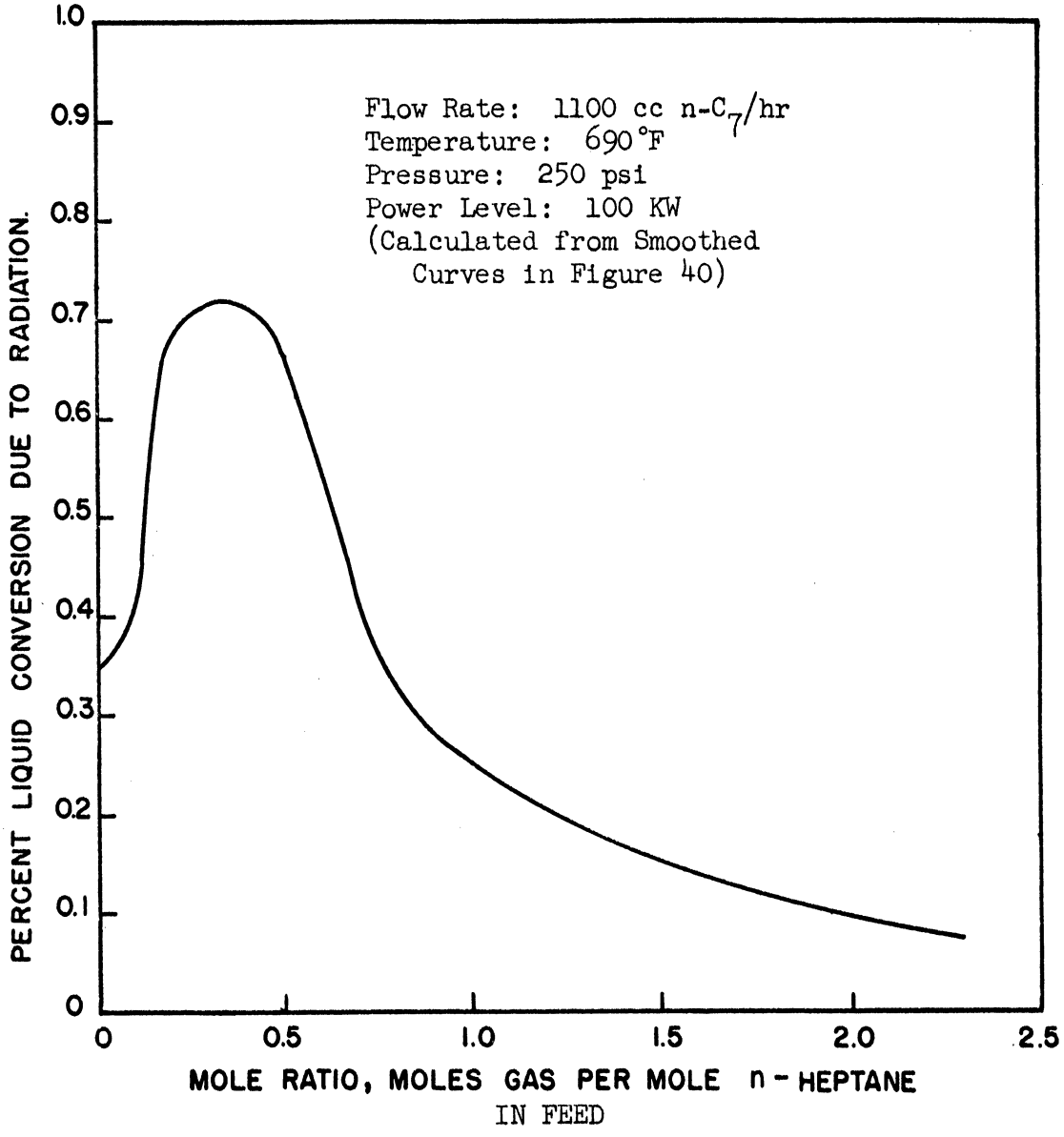

Figure 41. Radiation Conversion (Total Minus Thermal) Vs. Gas Ratio

——— "G" Port Irradiation, 1.1 liter n-C_7/hr, 690°F, 250 psig
(Conversions used in calculations from smoothed curve in Figure 40)

– – – Corrected for Variation of Total Dose

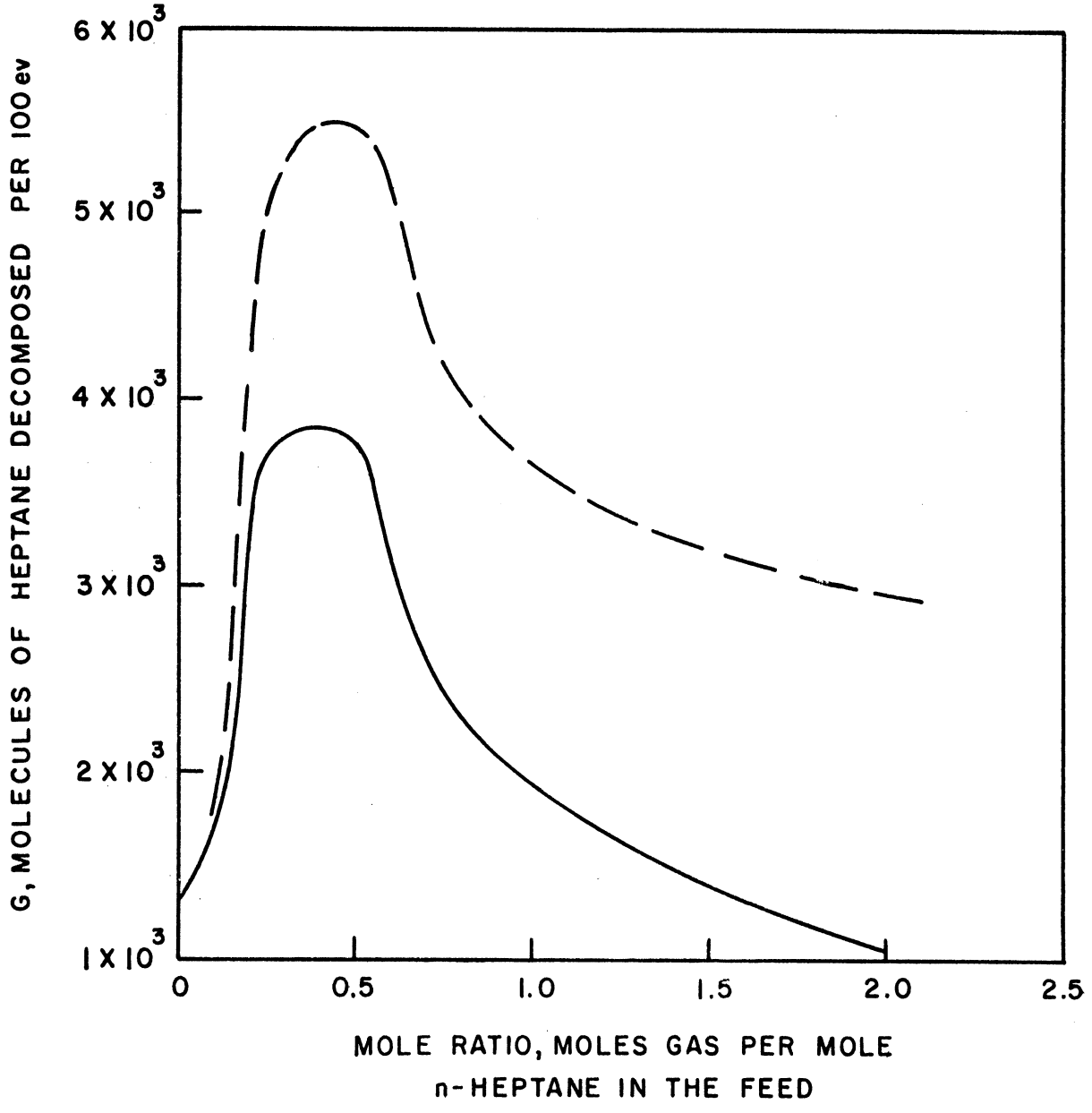

Figure 42. Radiation Yield Vs. Gas Ratio

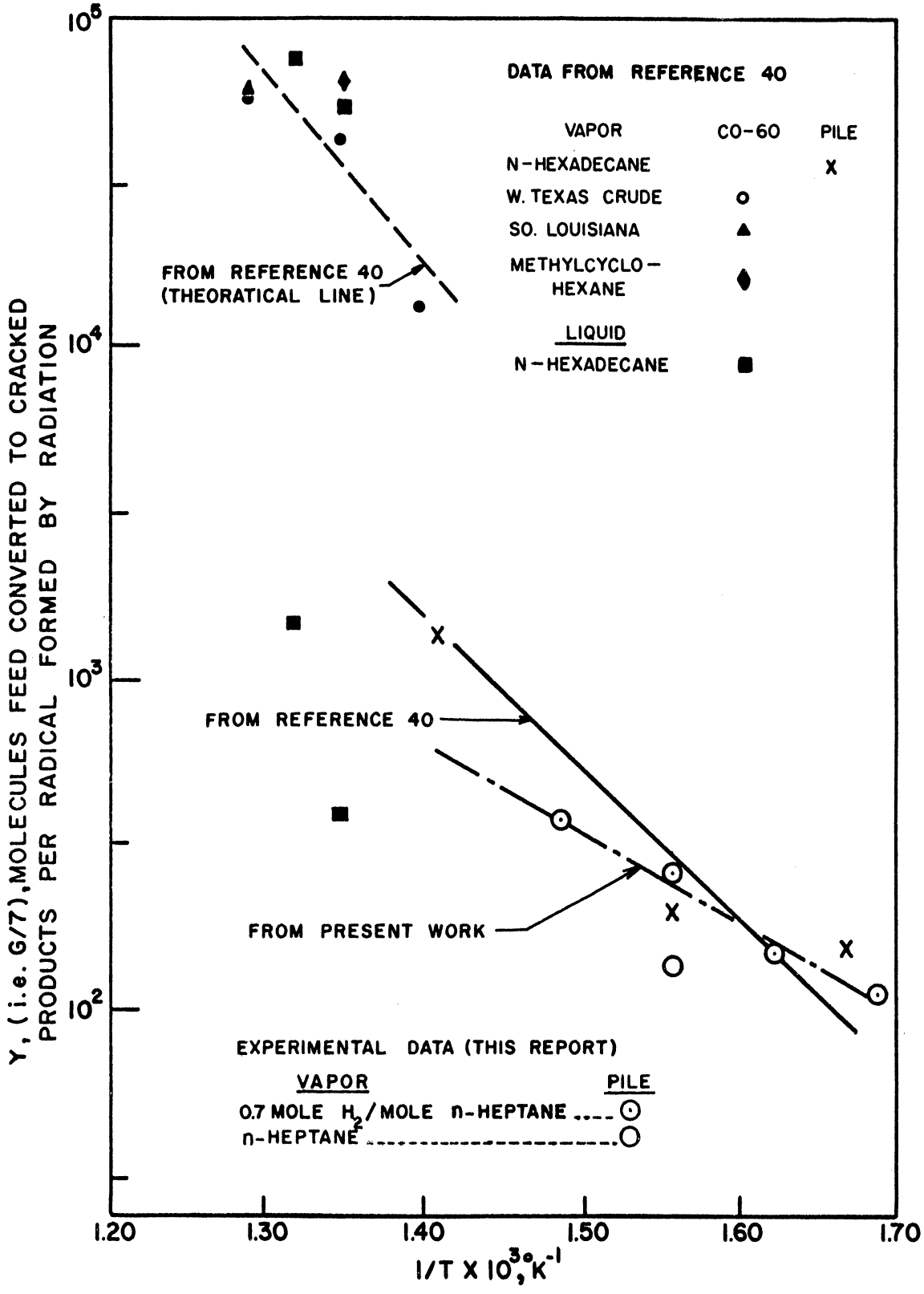

Figure 43. Comparison of Radiation Yields with Data from the Literature

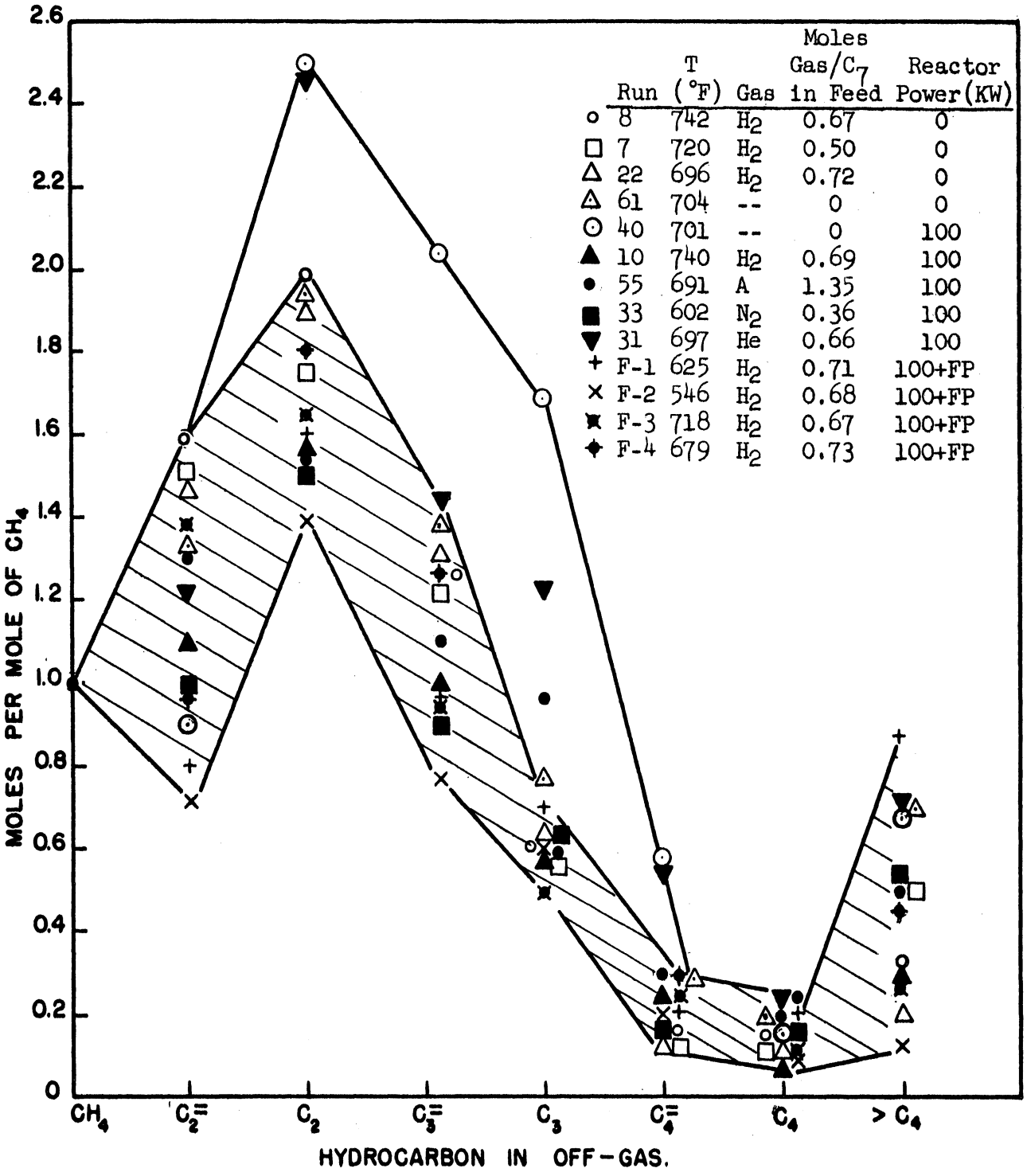

Figure 44. A Comparison of Product Gas Compositions

TABLE VII

A COMPARISON OF RADIATION AND BLANK RUN GASEOUS PRODUCT COMPOSITIONS WITH OTHER PUBLISHED DATA

		Composition, Mole Percent							
		(a) Run #8	(b) Run #10	(c) Run #61	(d) Run #40	(e) Reference 1	(f) Reference 25	(g) Reference 40	(h) Reference 40
H_2		(i)	(i)	(i)	(i)	2	5.1	(j)	(j)
CH_4		14.3	17.1	12.9	10.1	18	6.9	19.2	31.1
C_2	(Total)	48.5	46.3	43.0	38.9	46	33.6	47.2	55.1
	C_2H_4	21.2	19.7	17.2	9.1	30	21.0	(j)	(j)
	C_2H_6	27.3	26.6	25.8	29.8	16	12.6	(j)	(j)
C_3	(Total)	29.6	27.1	29.2	39.2	17	34.3	21.8	12.2
	C_3H_6	19.5	16.3	18.7	22.2	16	28.0	(j)	(j)
	C_3H_8	10.1	10.8	10.5	17.0	1	6.3	(j)	(j)
C_4	(Total)	4.4	4.8	6.3	4.8	14	11.6	8.3	1.2
	C_4H_8	2.4	3.4	4.1	4.1	11	5.5	(j)	(j)
	C_4H_{10}	2.0	1.4	2.2	0.7	3	6.1	(j)	(j)
$>C_4$		3.3	4.6	8.5	7.1	4	(j)	3.2	0

NOTES:

(a) 0.67 moles H_2/mole C_7, 742°F, 250 psig, no radiation.

(b) 0.69 moles H_2/mole C_7, 740°F, 250 psig, "G" port @ 100 kw.

(c) n-C_7, no hydrogen, 704°F, 250 psig, no radiation.

(d) n-C_7, no hydrogen, 701°F, 250 psig, "G" port @ 100 kw.

(e) n-C_7, no hydrogen, 1076°F, 1 atm, no radiation.

(f) n-C_7, no hydrogen, 1112°F, 1 atm, catalyst, no radiation.

(g) n-C_{16}, no hydrogen, 932°F, 1 atm, no radiation.

(h) n-C_{16}, no hydrogen, 700°F, 1 atm, "Pile Radiocracking".

(i) Not analyzed for H_2.

(j) Values not reported.

differences are attributed to radiocracking and, as shown, this radiation conversion increases rapidly with temperature. However, the fraction of the total conversion due to radiation cracking actually decreases at higher temperatures because the increase in the thermal cracking rate is even more rapid and tends to mask the radiation contribution.

G values, as shown in Figure 34, are an exponential function of the reciprocal of the absolute temperature with a slope corresponding to an activation energy of about 18 K cal/mole.

(ii) Residence Time (or Dose).-As seen from Figures 36 and 37, the conversion due to radiation increases with increasing residence time. However, the percent of the total conversion due to radiation cracking reaches a maximum at a residence time of about 7 minutes. Beyond this point, the thermal cracking rate apparently increases more rapidly than does the radiation cracking rate. This is analogous to the results obtained by increasing the temperature.

The radiation dose received is proportional to the residence time, and, as shown in Figure 38, the radiation conversion is not a linear function of the dose. The significance of this deviation from linearity is best illustrated by Figure 39, which shows the corresponding G values as a function of dose. The G value increases by a factor of 1.5 from 5 to 14 kilorep.

This increase of G value with total dose is unusual. For example, as discussed in I-D, Colichman et al.[17] have reported that the G value for polyphenyl is a decreasing function of dose. The cause of

the increase observed in the present work is not clear. Other workers have observed reconversion reactions with prolonged irradiation (see the discussion of work by Honig in Section I-D). Perhaps, in the region of initial cracking studied in the present work, there is an interaction between decomposition products and the heptane which sensitizes the latter.

Another possibility is that the flow pattern within the reaction vessel changed from low to high feed rate runs. The low G values were obtained at high feed rates and might be the result of increased channeling. Thus, the reactants would receive a smaller dose than calculated from average residence time techniques.

It should be noted, however, that changes in flow pattern were not observed during flow system dosimetry runs where the feed rate was changed (Chapter III and Figure 25). However, the flow rates and viscosities for the latter work are not identical to those for the heptane system.

(iii) Gas Ratio and Type of Gas.-Figures 40 through 42 show a sharp peak in conversions and G values for a mole ratio of 0.4. It is also seen that conversions are not significantly different for runs with hydrogen, nitrogen, argon, and helium.

The peak at a mole ratio of 0.4 is unusual and ordinarily would not be expected. Since the n-heptane concentration and residence time are decreased by increasing the mole ratio, the runs with pure n-heptane (gas ratio = 0) would be expected to show the largest yields. One possible explanation for the marked decrease in yields actually obtained is that the initial decomposition products may undergo reconversion reactions which are quenched by the addition of a gas such as hydrogen to the feed. Reconversion of products has been observed in some experiments, but under

different circumstances (see a discussion of Honig's work with methane in Section I-D and Figures 1 and 2).

It is pointed out in the discussion of product gas compositions, page 114, that the composition from pure n-heptane runs is slightly different from that obtained from runs with a mole ratio greater than 0.4, and it is shown that these differences are consistent with the assumption of certain reconversion reactions. One of these reactions involves the polymerization of unsaturated products, and any reaction of this type would result in coking the reactor walls or the formation of high molecular weight products which could not be detected with the present analytic procedures. Thus, if this reaction occurs, the apparent yields determined by measurement of lighter products will be decreased, and hence, this is a possible explanation of the peaking phenomenon which is shown in Figure 40.

The fact that comparable yields were obtained from runs with the four different gases used is interesting for two reasons. First, this indicates that hydrogen does not enter directly into the reaction mechanism. Secondly, this indicates that the neutron contribution to energy transfer is small.

If hydrogen entered into the mechanism, it would be expected that the use of an inert gas would decrease the yield.

Helium has a first ionization potential almost twice that for hydrogen or the other gases, and it might be expected that this would increase the efficiency of energy transfer. The yields from helium runs, Runs 64, 60 and 69, are slightly higher than yields from runs with other gases. However, since Run 65 is lower, no definite conclusion is possible.

Each of the four gases has a different neutron absorption cross-section, scatter cross-section, and neutron reaction. For example, nitrogen undergoes a (n,p) reaction with a cross-section of 1.75 barns, and hydrogen undergoes a (n,α) reaction with a cross-section of 0.33 barns. Hence, the energy transferred to the chemical system through the interaction of neutrons with the feed gas is different for each type of gas, and as a result, the chemical yields might be expected to be different. However, as pointed out in Chapter I, according to theoretical considerations, the energy transfer due to neutron interactions should only account for a small fraction of the total transfer, and hence, even large changes in magnitude of the neutron contribution will not cause a significant change in the total transfer or yields. This is consistent with the results obtained.

(iv) Neutron Energy Spectrum.-Five runs, F-1 through F-5, were made in "J" port with the fission plate in place. Radiation conversions obtained from these runs were roughly doubled as shown in Figures 30 through 33.

The purpose of these runs was to investigate the effect of fast neutrons on reaction yields and product distribution.

However, as discussed in Section III-C, not only was the fast neutron spectrum increased by use of the fission plate, but the gamma flux was also approximately doubled. For this reason, the fast neutron effects are difficult to sort out, and the results of the experiment are not conclusive.

(c) Comparison of G Values with Published Data.--The results from the present work are compared in Figure 43 with high temperature radiocracking

data from work reported by Baeder et al.[40] Y values are shown in this plot instead of G values, but as explained in Reference 40, the Y value is equal to G/7 since approximately 7 radicals are formed per 100 ev absorbed for the hydrocarbons under consideration.

As is seen, the Y values from the present n-heptane and n-heptane—hydrogen runs agree in order of magnitude with data from the pile irradiation of n-hexadecane. However, the slope of the line drawn through the data points from the present work is slightly different from the slope obtained by Baeder et al. The activation energy calculated from the latter slope is 25 K cal/mole as compared to 18 K cal/mole for the n-heptane system.

Until present, Reference 40 has been the only article in the literature dealing with high temperature radiocracking. The surprisingly high G values reported in this reference lead the authors to conclude that, as opposed to room temperature radiolysis, high temperature radiocracking is a radical chain reaction of moderately long chain length, which can be explained by the Rice-Herzfeld radical mechanism.

The present work adds support to these results and, in fact, may be explained by assuming the same type of mechanism as proposed by Baeder et al., in Reference 40.

(d) Comments about Initial Cracking.--Liquid conversion curves shown in Figure 30 are not extended below 600°F because of a lack of accuracy in analysis for lower conversions. However, a series of runs were made at lower temperatures in an effort to find some temperature at which the entire yield would be due to radiation cracking. These runs are listed in Table VI.

Analysis of the liquid product from the lowest temperature blank run (No. 54 at 515°F) showed that even at this temperature a minute thermal conversion occurred. Some conversion was also obtained from the corresponding radiation run (No. 57), but the peaks from both this and the blank run were so small that an accurate quantitative comparison of the yields was impossible. The peak heights appeared to be of the same order of magnitude, however. The yield from Run F-2 did not appear to be significantly larger than the yield from Run 29.

These results are consistent if it is assumed that under the conditions used in the present work, initial cracking points for both thermal and radiation cracking occur at approximately the same temperature. This is illustrated graphically by the hypothetical extension of Figure 31.

The existence of thermal cracking has not previously been reported in this low temperature region. Indeed, the yields are so low that, for practical purposes, they may be neglected. However, strictly speaking, it was impossible to obtain radiation yields completely free of thermal cracking with the present set-up and residence times. Apparently, much longer residence times and even lower temperatures are necessary to achieve this.

(e) Liquid Phase Product Distribution.--Because of the extremely small yields obtained, a complete identification of the various liquid phase products was not feasible. As shown in Figure 47, five peaks in addition to the air-methane peak were observed from chromatographic analysis. Retention times for these peaks correspond to times for C_2 through C_6

hydrocarbons. Since the resolution obtained was poor, in all probability isomers, saturates and unsaturates appear in the same peak.

Although individual components were not identified, the relative peak heights obtained for each sample were measured. Reasonable agreement was obtained for all runs, blank and radiation. Thus, there was not a drastic change in the liquid phase product distribution for any of the runs. Admittedly, however, minor changes could have passed undetected due to the difficulty of accurate analysis for individual components.

(f) Gas Phase Product Distribution.--As seen from Figure 44, the gas product compositions for all runs fall in the same general pattern. A fairly wide scatter of data occurred, and there is a question of whether or not the scatter is caused by sampling and analytic errors or by actual variation in the product composition. Runs 7, 8 and 22, which were without radiation but at different temperatures, show very good agreement, thus indicating that some of the wider variations observed for the other runs may be the result of actual changes in composition rather than experimental error. If this is assumed to be the case, some trends are noted.

The majority of data points for $C_2^=$, C_2 and $C_3^=$ for radiation runs are lower than for blank runs, regardless of temperature, gas ratio, or type of gas in the feed. This indicates that in radiation cracking, as opposed to thermal cracking, CH_4 is a slightly more favored product than are two and three carbon hydrocarbons. It is interesting to note that Baeder et al.[40] also noted an increase in CH_4 production for the high-temperature radiation cracking of n-hexadecane (Table VII).

However, since any increase in the ratio of $CH_4/C_2^=$, etc., due to radiation is very slight, the gas product from high temperature

radiocracking of n-heptane is almost identical to that from thermal cracking. This is in sharp contrast to low temperature radiocracking (Section I-D), which results in a product consisting mostly of hydrogen and methane. Baeder et al.[40], report a similar effect for other hydrocarbon systems and explain it in terms of a change in mechanism from a non-chain process to a long-chain reaction in passing from low to high temperatures.

Run 40, a radiation run using n-heptane but no hydrogen, shows the biggest deviation from the general composition pattern and, in particular, from the corresponding blank run, No. 61. It is also interesting to note that the liquid conversion and G values measured for the runs without hydrogen are unexpectedly lower than for runs with a reasonable mole ratio of hydrogen to heptane in the feed (Figures 40 through 42). These facts indicate that a difference, probably in reaction mechanisms, exists between runs with and without hydrogen.

A clue to the reason for these differences may be obtained from noting the marked decrease in C_2H_4 and increase in C_3H_8 content, along with smaller decreases in CH_4 and C_4H_{10} percentages for radiation Run 40 as opposed to blank Run 61 (see Table VII).

One possible explanation for this shift in composition is to assume that the following reactions are catalyzed by radiation

$$C_2H_4 + CH_4 \rightarrow C_3H_8 \qquad (30)$$

$$C_2H_4 + C_2H_4 + \ldots \rightarrow nC_2H_4 \qquad (31)$$

$$C_4H_{10} \rightarrow CH_4 + C_3H_6 \qquad (32)$$

In fact, if Reactions (30) and (32) are assumed to proceed until C_2H_4 and C_4H_{10} percentages for Run 61 are reduced to the exact values found in the radiation run, Run 40, the gas composition would be:

	% by Volume
CH_4	6.2
C_2H_4	9.1
H_2H_6	27.9
C_3H_6	21.7
C_3H_8	19.9
C_4H_8	4.5
C_4H_{10}	0.7
C_7	9.2

As seen, the CH_4 percentage is too low, and C_3H_8 too high in comparison to actual values from Run 40. Hence, the assumption that all of the C_2H_4 reduction is caused by Reaction (30) is probably in error. A reasonable explanation is that some of the C_2H_4 reduction occurs as the result of polymerization as illustrated by Reaction (31). The polymer would show up as coke in the reactor or simply as heavy hydrocarbon in the liquid phase.

The reaction vessel was cleaned with a solvent after Run 72, and small amounts of coke or gum were removed. Hydrocarbons higher than C_7 were not detected in the liquid by gas-phase chromatography, but very small amounts could easily have passed undetected.

This theory fits in well with the observed decrease in G value for runs at a low hydrogen ratio or with pure heptane. Due to polymerization and coking as in Reaction (31), some of the decomposed heptane

may not have been measured as product from these runs, and hence, the calculated G values would not be expected to be as high as for coke-free runs.

Even if postulated Reactions (30), (31) and (32) are accepted, there is no clear explanation for the absence of similar results for runs with hydrogen in the feed. Apparently, hydrogen quenches the reactions. Whether hydrogen enters into the mechanism or simply dilutes the reactants is not clear. Under the conditions of the present experiment there is no apparent saturation of unsaturated products for hydrogen runs; however, there is always the possibility that a high hydrogen concentration will prevent a chain polymerization by simply adding onto the end of a free radical.

Runs 31, 33 and 55, made with gases other than hydrogen in the feed, give some insight into the role played by hydrogen. Runs 33 and 55 using nitrogen and argon, respectively, fall within the general composition pattern for all radiation runs. This similarity of results rules out the possibility that hydrogen enters directly into the decomposition mechanism.

Run 31 with helium, on the other hand, comes the closest of all runs to duplicating the pure heptane run, Run 40. The first ionization potential for helium is almost twice that for hydrogen or the other inert gases used. Thus, the energy transfer resulting from ionization or excitation of the diluent gas may be an important factor in explaining the effect of adding a gas to the feed. However, since other factors such as the neutron absorption cross-section are different for the various gases, evidence that the differences are related to ionization potential is not conclusive.

It is also noted from Figure 44 that compositions from fission plate runs (F-1 through F-4) fall within the general pattern indicated for other radiation runs. This is not, however, proof that fast neutron irradiation results in the same product distribution as does gamma radiation. The gamma flux, as well as the fast neutron flux, was increased by using the fission plate. Hence, any differences due to the fast neutrons may have been masked by the increased yield due to the high gamma flux.

It is interesting to compare the off-gas composition from Run 61 with data from Reference 1, also shown in Table VII. In general, the total amounts of C_1's, C_2's, etc., are comparable for the two runs, but the ratio of saturates to unsaturates is much higher for Run 61. Both runs are for the thermal cracking (no radiation) of normal-heptane. However, Run 61 is for 704°F, 250 psi and a yield of about 1/2%, as opposed to 1076°F, 1 atm. and a yield of over 10% for the run from Reference 1. These differences in reaction conditions are probably the cause for the discrepancy in the saturate to unsaturate ratios for the two runs.

To insure the accuracy of the results for the present work, the saturate to unsaturate ratio obtained from the mass spectrometer was checked by gas-phase chromatography techniques for several runs (see Appendix G).

(g) Estimated Accuracy and Possible Experimental Errors.--Since the present work is based on the measurement of very small differences in conversion for blank and radiation runs, any experimental errors will be magnified. Experience has shown, however, that reasonable reproducibility can be obtained with the experimental and analytic techniques

used in the present work (see Appendix H for a discussion of the reproducibility of reaction conditions such as temperature and pressure for blank and radiation runs). For example, three runs were duplicated in the series studying the effect of temperature on conversion (Runs 21 and 8, 14 and 10, and 15 and 37). Figure 30 shows that exceptionally good agreement was obtained for these runs. The runs involving a change in gas ratio show a little more scatter, but again reasonable agreement was obtained (see Figure 40).

Another conceivable experimental error is the possibility that the stainless steel reaction vessel walls served as a catalyst throughout the study. However, as already pointed out, a small carbon or polymer layer was gradually deposited on the vessel wall during this series of runs. If the vessel walls were acting to catalyze the reaction, it might be expected that a decrease in activity and,hence, yields would occur with this coking. Such a decrease was not observed.

The reported G values not only contain an uncertainty due to the accuracy of conversion measurements, but are also dependent upon the accuracy of dosimetry measurements. While conversion measurements may be valid within $\pm$ 20%, reactor dosimetry measurements are commonly considered to be reliable only within a factor of two.[40]

Even allowing for maximum errors, the G values obtained are significantly higher than those for room temperature radiocracking. Results obtained from the present work are comparable with data from the literature[40] for high temperature radiocracking. A two-fold uncertainty was also placed on the latter work; however, the fact that similar results are obtained from independent experiments using completely different techniques is significant and strengthens the confidence level of the results.

(5) Summarized Conclusions

The following conclusions strictly apply to the initial cracking region (750°F max.) for the pile irradiation of the normal heptane-hydrogen system.

a. Liquid phase conversion measurements using partition chromatography were found to be a good technique for low yield measurements ($< 2\%$) in the incipient cracking region for the hydrogen-heptane system.

b. Radiation cracking increases with temperature, but not as rapidly as thermal cracking. For example, at a total conversion of 0.3% at 620°F, radiation cracking amounted to about 50% of the total. At 740°F, where a total conversion of 2.2% was recorded, slightly less than 30% was due to radiation (both runs with a hydrogen ratio of 0.7 and a dose of about 1.5×10^4 R (see Figures 30 and 33).

c. The G value is a function of temperature, radiation dose, and gas ratio. G values were found to be an increasing function of temperature with an activation energy of approximately 18 K cal/mole. An apparent increase of G value with dose was observed as shown in Figure 39, and an unusual peaking effect was measured at a gas ratio of about 0.4 moles of hydrogen per mole of heptane in the feed (see Figure 42). This peaking may be the result of product "reconversion" reactions (see Section f as follows).

d. The high G Values ($> 10^3$) found in this work agree with results obtained from high temperature radiocracking studies by Baeder et al.[40], using other hydrocarbon systems. This agreement adds support to Baeder's conclusion that radiocracking is a chain reaction with moderately long chain length at high temperatures.

e. Evidence indicates that hydrogen does not enter directly into the radiocracking mechanism, despite the effect of hydrogen ratio on the G value as noted in Section c above. (Experiments in which hydrogen was replaced with helium, argon, and nitrogen did not significantly change the product distribution or the G value.)

f. In general, the cracked product distribution is not significantly altered in radiocracking as compared to thermal cracking.

No major differences were noted by partition chromatography analysis of liquid products, but some small changes could have occurred undetected.

With the exception of a slight trend towards methane production in radiation runs, the gas product composition was found to be comparable for blank and radiation runs with the heptane-hydrogen system. However, some differences were observed for the pure heptane system. C_2H_4, CH_4 and C_4H_{10} yields were slightly

lower and the C_3H_8 and C_3H_6 yields increased for radiation runs. These changes can be rationalized by assuming that radiation catalyzes the following "reconversion" reactions in the gas product:

$$C_2H_4 + CH_4 \rightarrow C_3H_8 \quad (30)$$

$$C_2H_4 + C_2H_4 + \ldots \rightarrow n\ C_2H_4 \quad (31)$$

$$C_4H_{10} \rightarrow CH_4 + C_3H_6 \quad (32)$$

The addition of hydrogen or an inert gas to the system apparently quenches these reactions.

g. Results from fission plate runs do not indicate a difference in effect due to fast neutrons, but since the plate caused an increase in gamma as well as fast flux, the results are not conclusive and do not preclude such an effect.

B. Other Systems Studied

(1) Benzene-Water

(a) Experimental Procedure and Method of Analysis.--The experimental and analytic procedures used to study the production of phenol from the irradiation of benzene-water have already been described in Chapter III, Section B.

In all cases, the system was prepared by saturating double or triple distilled water with reagent grade benzene.

(b) Results and Discussion.--Table XI, Appendix A, summarizes the data obtained from all benzene-water runs.

Runs B-6 through B-11 were used for dosimetry measurements in the reaction vessel and are discussed in detail in Chapter III.

Runs B-1 through B-5 were not intended for dosimetry work, but were used to study the effect of temperature on the G value for the reaction. Yields of 85 ± 4 μ moles of phenol per liter were obtained from these runs at 82, 119, 152, 181 and 186°F. Since the yield was not affected by temperature, the G value for phenol is evidently not a function of temperature. This adds to the attractiveness of this system for use as a chemical dosimeter as suggested in Reference 34.

(c) Summarized Conclusion.--G(phenol) for the irradiation of water saturated with benzene is independent of temperature in the range 70-190°F.

(2) Nitrogen-Hydrogen

(a) Experimental Procedure and Method of Analyses.--Operating procedures for simultaneously feeding two gases described in Chapter II were followed for all runs.

Liquid Carbonic Corporation hydrogen cylinders and Baird Gas Corporation nitrogen cylinders were used. The hydrogen, but not the nitrogen, was passed through the silica-gel drier in the pilot unit.

Product gases were analyzed by bubbling the off-gas through a dilute sulfuric acid solution during a run. The acid was titrated before and after each run to determine the ammonia production. As a check, several samples were also analyzed with a mass spectrometer (Mass Spec. Log Book No. 4640).

(b) Results and Discussion.--Data from these runs are presented in Table XII, Appendix A.

As indicated, no detectable amounts of ammonia were obtained from any of the runs in the range 600-750°F and 250-300 psi with residence times ranging up to 57 minutes ($\sim 10^5$ Rep.).

Thus, unless other techniques are developed, radiation cannot be used to initiate the nitrogen-hydrogen reaction. This is surprising since the reaction conditions used in the present experiments, except for the absence of a catalyst, are similar to those necessary for ammonia production. Ammonia is produced commercially by the Haber process which uses high pressures (up to 1000 atm.), fairly high temperatures (750-1100°F), and a catalyst such as iron and potassium aluminate.(55) At the same temperatures, but with lower pressures, moderate ammonia production is feasible. For example, a 2-to-1 mole mixture of hydrogen and nitrogen will react at 750°F, 250 psi, and with a catalyst to form a mixture containing about 4% ammonia at equilibrium. (This was calculated assuming an equilibrium constant $K_p = 1.69 \times 10^{-4}$ at 750°F(55)). Equilibrium should be reached in a matter of minutes under these conditions.(55)

(c) Summarized Conclusion.--No ammonia yield was obtained from nitrogen-hydrogen irradiations with temperatures up to 750°F, pressures up to 300 psi, and doses up to 10^5 rep.

(3) Nitrogen-Oxygen

(a) Experimental Procedure and Method of Analysis.--Air from a compressed air cylinder was fed into the reaction vessel according to operating procedures outlined in Chapter II and Appendix D. The air was metered through tanks T-4 and T-5 in the same manner as described for hydrogen

in the operating procedures. All product gas samples were analyzed with a mass spectrometer.

(b) Results and Discussion.--Data from all air irradiation runs are presented in Table XIII, Appendix A. Although traces of the products, NO_2 and N_2O, were noted for the conditions studied, i.e., 575-750°F, 300 psi, and doses from 5×10^4 to 2×10^5 Rep, the yields obtained were negligible ($< 0.1\%$). Apparently, residence times attainable with the present flow system are too low to obtain reasonable yields. This might be expected since Dondes and Harteck[27] report very low G values unless UO_2 is added to the reaction vessel to obtain fission fragments. Dondes and Harteck obtained reasonable yields without using fission fragments by going to long irradiation periods (1 to 10 days).

(c) Summarized Conclusion.--Only trace yields of N_2O and NO_2 were detected from nitrogen-oxygen irradiations under maximum conditions of 750°F, 300 psi, and 2×10^5 Rep.

APPENDIX A

TABLES CONTAINING ORIGINAL DATA

TABLE VIII

SUMMARY OF DATA FROM NORMAL HEPTANE RUNS

Run No.	1	2	3	4	5	6	7	8	9	10	11	12	14	15	16	17	18	19	20	21	22	23	24	25	26	27	28	29	30	31	32	33	34	35	36	37	38	39
Thermocouple T2-1 (F°)	659	695	692	799	485	670	705	730	05	725	6[illegible]	717	724	679	634	590	6[illegible]	674	699	730	6[illegible]	644	59[illegible]	683	675	673	57[illegible]	542	681	685	678	670	668	679	665	683	699	704
T2-3	650	690	[illegible]96	796	480	670	705	726	703	722	6[illegible]	716	725	675	631	588	683	672	6[illegible]	72[illegible]	6[illegible]7	641	591	681	675	673	572	53[illegible]	681	683	675	669	668	678	664	680	693	696
T2-2	651	684	695	[illegible]00	494	700	730	750	720	749	732	736	750	701	65[illegible]	609	705	700	702	751	702	656	606	704	702	700	5[illegible]6	551	707	704	702	701	679	702	700	702	708	708
T2-0	65[illegible]	692	692	[illegible]00	500	710	740	760	730	[illegible]1	746	750	760	711	663	620	715	709	712	763	713	665	614	711	710	705	595	560	716	715	715	710	711	715	720	712	714	715
T2-4	451	462	550	521	325	440	460	441	450	445	447	4[illegible]1	440	420	395	372	440	452	425	452	427	403	382	443	440	45[illegible]	379	354	434	434	428	422	428	437	439	431	440	448
T2-5	630	670	926	830	375	520	51[illegible]	695	660	690	[illegible]0	69[illegible]	[illegible]92	625	572	530	549	599	581	676	5[illegible]0	560	511	545	546	510	462	480	643	628	637	646	678	630	622	611	599	603
T2-6	560	535	695	593	447	625	660	672	640	671	645	6[illegible]4	671	631	5[illegible]5	444	639	634	633	675	633	620	549	635	637	620	529	503	625	632	621	609	605	632	624	633	641	648
Liquid Feed Rate cc/hr	2200	2220	2020	2220	2550	2620	2660	1150	1000	1130	1710	1230	1195	1170	1120	1130	1690	3350	1260	1120	1126	1175	1140	1700	2570	3020	1060	1050	1320	1090	1260	1190	980	1292	1180	1170	1370	1230
(1) Moles Gas/Mole C_7	N_2 0.28	0.43	0.50	1.5	0.74	0.69	0.50	0.67	0	0.69	1.8	N_2 0.36	0.76	0.74	0.72	0.70	0.71	0.68	0.72	0.6[illegible]	0.72	0.6[illegible]	0.70	0.66	0.6[illegible]	0.70	0.6[illegible]	0.63	He 0.54	He 0.66	He 1.0	N_2 0.36	N_2 1.26	1.01	1.95	0.74	0.18	0.11
(2) Power Level, KW	0	0	0	0	100	100	0	0	0	100	100	100	100	100	100	100	100	100	0	0	0	0	0	0	0	0	0	0	0	100	100	100	100	100	100	100	100	100
Pressure, psig	200	200	800	800	250	250	250	250	250	250	250	250	250	250	250	250	250	250	250	250	250	250	250	250	250	250	250	250	250	250	250	250	250	250	250	250	250	250
(3) Aver. Temp., °F	694	691	[illegible]09	799	490	648	720	742	715	740	714	730	742	691	646	602	696	690	696	744	696	653	602	695	691	688	594	548	697	697	693	69[illegible]	698	694	688	694	704	706
°C	346	366	476	426	254	364	382	394	379	393	376	3[illegible]5	394	366	341	317	369	366	369	396	369	345	317	36[illegible]	366	364	307	287	369	369	367	364	361	368	364	368	373	374
(4) Percent Liquid Conversion	0	0.2	[illegible].73	2.0	0	0.40	0.57	1.76	1.05	2.20	1.01	2.0[illegible]	2.10	1.0	0.45	0.30	0.[illegible]	0.35	0.59	1.73	0.5[illegible]	0.27	0.14	0.2[illegible]	0.27	0.25	<0.1	<0.1	0.51	0.65	0.46	0.53	0.79	0.83	0.45	1.0	0.98	1.1
(5) Reactor Log Book Page and Experiment No.	-	-	-	-	210-151	210-151	-	-	-	213-153	213-153	213-153	217-155	217-155	217-155	217-155	217-155	217-155	-	-	-	-	-	-	-	-	-	-	-	224-159	224-159	224-159	224-159	226-160	226-160	226-160	226-160	226-160

Run No.	40	41	42	43	44	45	46	47	48	49	50	51	52	53	54	55	56	57	58	59	60	61	62	63	64	65	66	67	68	69	70	71	72	F-1	F-2	F-3	F-4	F-5
Thermocouple T2-1 (F°)	699	665	615	690	690	687	700	673	686	651	670	663	679	650	506	[illegible]3	5[illegible]1	505	702	69[illegible]	680	703	694	690	704	696	699	696	998	675	697	678	683	629	555	702	663	626
T2-3	694	665	623	675	688	683	692	670	685	6[illegible]7	672	661	695	679	503	6[illegible]0	6[illegible]1	506	695	691	6[illegible]	696	698	688	699	699	695	691	692	675	693	676	680	633	550	728	689	641
T2-2	702	702	669	706	709	701	704	704	701	695	703	701	703	704	525	696	709	51[illegible]	706	705	711	704	704	712	715	717	715	711	712	709	711	701	708	635	556	740	699	650
T2-0	710	707	711	720	717	712	711	715	712	710	717	719	714	715	527	709	721	524	70[illegible]	710	70[illegible]	712	704	711	704	705	701	699	699	695	699	711	712	601	524	703	663	616
T2-4	461	442	463	440	449	454	459	429	42[illegible]	430	435	434	435	426	339	434	420	340	467	450	429	465	422	407	414	400	405	405	400	398	402	420	431	216	196	247	237	227
T2-5	621	637	634	649	627	652	621	649	65[illegible]	637	642	660	611	639	45[illegible]	642	6[illegible]3	460	4[illegible]5	445	556	705	456	470	46[illegible]	451	455	447	46[illegible]	455	448	625	611	536	471	601	560	525
T2-6	646	600	592	634	633	633	643	620	627	613	618	618	640	629	465	615	616	469	648	635	625	645	629	61[illegible]	645	637	640	637	642	618	635	631	633	547	482	619	582	542
Liquid Feed Rate cc/hr	1180	1270	1230	1060	1300	1290	1100	1170	1170	1180	1120	1330	1000	965	1240	1030	974	1360	1100	1010	1240	1120	1110	1100	1100	1030	1120	1210	1100	1140	1100	1170	1170	1170	2450	1130	1070	1160
(1) Moles Gas/Mole C_7	0	1.7	3.6	1.2	0.16	N_2 0.13	0.11	1.7[illegible]	N_2 0.61	2.25	N_2 0.79	Be 0.45	He 0.1[illegible]	He 1.12	0.66	A 1.35	A 1.06	0.54	0	N_2 0.38	He 0.79	0	N_2 0.39	N_2 0.57	He 0.26	He 0.3	0.57	0.24	0.42	He 1.1	A 0.07	0.82	0.80	0.71	0.68	0.67	0.73	0.67
(2) Power Level, KW	100	100	100	100	0	0	0	0	0	0	0	0	0	0	0	100	100	100	100	100	100	0	100	100	100	100	100	100	100	100	100	100	100	100 +FP	100 +FP	100 +FP	100 +FP	100 +FP
Pressure, psig	250	250	250	250	250	250	250	250	250	250	250	250	250	250	250	250	250	250	250	250	250	250	250	250	250	250	250	250	250	250	250	250	250	250	250	250	250	250
(3) Aver. Temp., °F	701	6[illegible]5	655	699	701	698	702	691	695	678	691	6[illegible]8	702	695	515	691	69[illegible]	513	728	699	695	704	700	700	6[illegible]1	705	703	699	700	6[illegible]9	700	691	694	625	546	718	679	634
°C	372	363	346	371	372	370	372	366	371	359	366	364	372	368	268	366	370	267	387	371	36[illegible]	373	371	371	361	374	373	371	371	365	371	366	36[illegible]	330	285	381	359	334
(4) Percent Liquid Conversion	0.80	0.45	0.2	0.42	0.62	0.66	0.54	0.55	0.73	0.29	0.77	0.77	0.83	0.65	Trace	0.77	0.83	Trace	0.87	1.5	1.1*	0.5	1.45	2.4	1.6	1.3	1.5	1.5	1.45	1.1	1.3	.105	1.0	0.54	<0.1	2.16	1.1	0.62
(5) Reactor Log Book Page and Experiment No.	226-160	227-161	227-161	227-161	-	-	-	-	-	-	-	-	-	-	-	232-163	232-163	232-163	235-165	235-165	235-165	-	237-166	237-166	237-166	23[illegible]-167	23[illegible]-167	233-167	238-167	240-171	240-171	240-171	240-171	286-190	288-190	290-192	290-192	290-192

NOTES:

(1) Unless marked otherwise, the mole ratio represents moles of hydrogen per mole of normal-heptane

(2) All runs except F-1 thru F-5 were in "Q" port with fuel configuration "1a". F-1 thru F-5 were run in "J" port with the fission plate in place, i.e. the power level is marked 100 + F.P.

(3) Averaged over T2-1, T2-3, T2-2, and T2-0 only.

(4) As measured by a Fisher-Gulf Partitioner, Type 11-130.

(5) Page numbers and experiment numbers refer to the Ford Nuclear Reactor Log Book kept on file in the Phoenix Lab, University of Michigan. This log gives full details on reactor operation for a particular experiment.

TABLE IX

SUMMARY OF DATA FROM MASS SPECTROMETER ANALYSES
OF GAS SAMPLES FROM NORMAL HEPTANE RUNS

Mass Spec. Run No.	4472	4471	4528	4526	4531	4527	4532	4530	4529	4534	4524	4535	4523	4533	4567	4575	4568	4569	4573	4570	4574	4571	4592	4572	4576
Sample No.	3-1	3-2	6-1	7-1	7-2	8-1	8-2	9-2	10-1	10-2	11-1	11-2	12-1	12-2	14-1	14-2	15-1	16-1	16-2	17-1	17-2	21-1	21-2	22-1	22-2
Mole % C_1	1.559	0.6297	0.0989	0.2845	.5328	0.4913	0.5679	0.549	0.4447	0.7373	0.139	0.0083	1.65	2.173	0.4242	1.21	0.1183	0.0490	0.0653	0.0398	0	0.1796	1.146	0.5090	0.451
C_2	2.989	0.2846	0.1350	0.4273	2.849	0.6648	4.470	2.006	0.5749	5.661	0.216	0.1663	1.53	8.768	0.5413	8.89	0.2326	0.1158	1.044	0.0639	0.5718	0.2614	6.575	0.7787	2.392
$C_2^=$	0.5698	0.1006	0.0184	0.3737	2.104	0.5909	2.976	1.31	0.4498	3.510	0.161	0.9945	1.86	8.59	0.3552	5.49	0.0625	0.0219	0.1643	0.0398	0.484	0.1317	3.635	0.6756	1.22
C_3	1.6411	0.1328	0.0861	0.1862	1.206	0.2353	1.974	0.9176	0.2118	2.685	0.121	0.0931	0.320	2.701	0.2244	4.329	0.176	0.1350	0.9301	0.0975	0.4613	0.1454	2.621	0.2575	1.108
$C_3^=$	1.6436	0.1498	0.1025	0.2825	2.245	0.3860	3.377	1.575	0.3152	4.902	0.179	0.1751	0.773	7.020	0.3150	6.828	0.2393	0.0912	1.061	0.0545	0	0.1362	4.598	0.5421	1.63
C_4	0.3247	0.0295	0.0149	0.0304	0.2404	0.0464	0.4881	0.1544	0.0267	0.7961	0.0183	0.0156	0.085	0.6487	0.0449	0.933	0.0305	0.0107	0.3045	0.0097	0.1350	0.0300	0.4268	0.0632	0.263
$C_4^=$	0.1561	0.0659	0.0175	0.0484	0.5054	0.0671	0.7058	0.363	0.0665	1.187	0.043	0.0441	0.132	1.037	0.0620	15.97	0.0169	0.0105	0.2495	0.0107	0.4518	0.0335	0.9341	0.0514	0.351
C_7	0.0189	0.0067	0.0984	0.2619	0.3782	0.1674	0.4324	0.461	0.1082	0.6090	0.215	0.0444	0.193	0.7008	0.1112	0.266	0.143	0.0993	0.2112	0.1424	0.2508	0.1247	0.2720	0.0956	0.257
Air	0.6008	0.0839	0.117	4.251	35.68	4.320	61.79	47.15	0.1107	60.26	0.227	50.45	0	14.75	0.1397	52.40	2.427	1.423	30.74	0.1610	36.73	0.3644	35.86	0.4311	
Wet Test Meter #1 (Std. ft^3/hr.)	9.73		12.4	7.65		3.82			4.22		17.6		2.64		5.34		5.74	6.0		5.95		4.36		4.05	
Wet Test Meter #2 (Std. ft^3/hr.)		1.33			0.30		0.14	0.16		0.11		0.13		0.22		0.15			0.10		0.08		0.12		0.40

Mass Spec. Run No.	4601	4593	4600	4596	4603	4606	4604	4595	4598	4594	4599	4607	4602	4605	4636	4608	4637	4638	4677	4679	4678	4680	4683	4684	4685	4686
Sample No.	31-1	31-2	33-1	33-2	38-1	38-2	4 -1	40-2	46-1	46-2	52-1	52-2	55-1	55-2	65-1	65-2	69-1	69-2	f-1-1	f-1-2	f-2-1	f-2-2	f-3-1	f-3-2	f-4-1	f-4-2
Mole % C_1	0.1807	0.0897	0.4030	0.362	0.334	1.004	0.4167	0.730	0.354	1.260	0.2235	0.368	0.2468	0.389	1.104	1.748	3.1647	2.4374	0.097	0.419	0.274	0.793	0.689	1.54	0.194	0.442
C_2	0.2822	2.026	0.5188	2.840	0.4086	4.18	0.3972	4.037	0.1391	3.119	0.2122	0.961	0.3366	2.22	1.1245	6.968	1.8398	6.479	0.097	2.56	0.321	2.46	0.863	7.26	0.301	2.87
$C_2^=$	0.1336	0.9934	0.3402	1.73	0.1469	1.65	0.1239	1.206	0.0664	1.635	0.1457	0.329	0.2802	1.396	1.0927	6.179	2.296	6.2116	0.044	1.50	0.157	1.60	0.823	5.25	0.162	1.47
C_3	0.1391	1.232	0.230	1.410	0.234	2.022	0.2106	0.2524	0.1063	1.652	0.1045	0.658	0.148	1.255	0.4821	2.228	0.3454	1.727	0.047	1.14	0.134	0.968	0.261	2.82	0.181	1.57
$C_3^=$	0.1217	1.584	0.2954	2.093	0.2392	2.465	0.1965	3.017	0.0714	1.910	0.1092	0.840	0.2218	2.111	0.5756	4.724	0.7659	3.693	0.045	1.91	0.164	1.65	0.431	5.48	0.211	2.43
C_4	0.0089	0.0005	0.0376	0.1440	0.0240	0.432	0.0145	0.0868	0.0044	0.6373	0.0083	0.049	0.0220	0.3015	0.0891	0.696	0.0529	.3083	0.013	0.262	0.027	0.267	0.041	0.663	0.046	0.434
$C_4^=$	0.0445	0.3828	0.0429	0.4773	0.0183	0.463	0.0252	0.6233	0.0060	0.094	0.0195	0.139	0.0588	0.584	0.0794	1.073	0.1080	0.7353	0.0068	0.279	0.030	0.269	0.091	1.23	0.039	0.500
C_7	0.1112	0.2128	0.2170	0.2709	0.1144	0.154	0.1365	0.8559	0.0704	0.8587	0.1010	0.158	0.1267	0.309	0.3347	0.728	0.2202	0.2639	0.055	1.65	0.018	0.409	0.172	0.381	0.148	0.367
Air	0.1379	65.62	0.1746	61.07	0.1467	34.06	4.061	61.21	1.134	27.13	0.1209	55.81	0.1507	3.853	2.504	56.43	0.5637	59.072	0.154	32.2	0.739	9.03	1.56	29.4	0.238	29.4
Wet Test Meter #1 (Std. ft^3/hr.)	4.15		2.48		1.44		0.348		0.73		1.06		8.06		2.25		7.40		8.40		8.10		3.82		3.92	
Wet Test Meter #2 (Std. ft^3/hr.)		0.32		0.11		0.23		0.16		0.17		0.07		0.25		0.06		0.08		0.24		0.30		0.17		0.11

NOTE: The above percentages do not add up to 100%. The difference is due to H_2, A, N_2, or He which were added to the feed. In the case of pure n-heptane runs (no gas added) the difference is due to N_2 which was forced through the high pressure trap to maintain the system pressure (see Appendix D, Section 1).

TABLE X

A TYPICAL DATA SHEET (RUN 14)

Run No. 14
Date June 20, 1958
Purpose Radiation Run
Feed H_2 and n-C_7
Liquid Feed Rate 1195 cc/hr
Hydrogen Feed Rate 5.5 ft^3/hr at 70°F and 1 atm
Hydrogen Ratio 0.76 moles H_2/mole C_7

Pressure 250 psig
Temperature 742°F
Run Time 31.9 min
Reactor Power 100 kw
Off-Gas Volumes
WTM #1 5.34 ft^3/hr
WTM #2 0.15 ft^3/hr

START-UP DATA

Barometric Pressure 29.64 inches
Room Temperature 89°F
WTM #1 Temperature 80°F
WTM #2 Temperature 80°F
Radioactivity: 60 C/M @ product receiver
100 C/M @ beam port
Pressures:
PG-1 0 psig H_2 Tank 520 psig
PG-2 0 psig N_2 Tank - psig
PG-3 300 psig PRC-1 235 psig
PRC-2 0 psig
Time Feed Pump is Started 11:00 A.M.
L-1 Reading at the Above Time 4.0"
ΔP for Wet Test Meter #1 0.1", #2 0.1" H_2O

Powerstat Settings:
RH-1 115 H-4 30
RH-2 115 H-5 0
RH-3 115 H-6 0

Temperatures when Leveled Out (Time 11:10)
TC-0 760°F 5 695
1 772 6 671
2 744 7 82
3 723 8 82
4 452

RUN DATA

Time (sec)	WTM #1 (ft^3)	WTM #2 (ft^3)	L-1 (inches)	L-2 (inches)	L-3 (inches)	Radioactivity (C/M)	Gas Samples No.-Volume (ml)	Liquid Samples No.-Volume (ml)	Thermocouples (°F) 0	1	2	3	4	5	6	7	8
0(11:30a.m.)	02.387	08.494	19.4	NOT USED	38.3 ↓	60			761	728	749	723	450	695	671	82	82
300						60			761	728	750	724	449	693	671	82	82
356	02.960																
600			24.3						760	728	750	725	448	691	671	82	82
617					31.1 ↓	60											
900									760	728	750	725	448	690	671	82	82
910	03.789							1-302									
930							1-250										
980						60											
1090					25.6 ↓												
1200			29.2						760	728	751	724	447	691	671	82	82
1250	04.307					60											
1300						70											
1500						80			759	728	751	723	447	690	671	82	82
1530					20.8 ↑	70											
1770	05.103						2-250										
1800			33.2						759	728	749	725	448	691	671	82	82
1810					24.0 ↑	70											
1914	05.327	08.575	35.1		25.2 ↑	70		2-333	760	728	748	725	448	692	670	82	82

SHUTDOWN DATA

Sample Record:

Liquid Samples No.	Volume (ml)	Gas Samples No.	Volume (ml)
1	302	1	250
2	250	2	250

Time pump stopped 12:02 p.m., L-1 reading 35.1 inches.
Barometric Pressure 29.64".
Room Temperature 88°F.
WTM #1 Temperature 80°F.
WTM #2 Temperature 80°F.
Comments Powerstat settings changed to 110 at 11:40 a.m.
Beam-port Used G , Fuel Configuration 1a.
Reactor Log Book Exp. No. 155, page 217.
Reactor Operator Sangpetch.
Log N 98-100, Power Level 99 kw.
(Include Log N chart if possible).
Linear Level 100.
Rod Positions: A 94% B 94% C 94% CR 63-79%.

TABLE XI

SUMMARY OF DATA FROM THE IRRADIATION OF THE BENZENE-WATER SYSTEM

RUN	B-1	B-2	B-3	B-4	B-5	B-6	B-7	B-8	B-9	B-10	B-11
Temp. (°F)											
TC-1	81	119	154	182	185	81	82	81	81	80	80
TC-3	82	119	152	181	185	80	81	80	80	79	79
TC-2	83	118	153	182	186	81	82	81	82	81	80
TC-0	83	119	155	186	199	81	81	81	80	80	80
TC-4	85	108	135	159	161	82	81	81	81	81	81
TC-5	82	85	90	93	95	81	81	81	81	81	81
TC-6	88	115	158	192	196	83	85	86	85	85	84
Feed Rate(cc/hr)	14,600	14,100	14,600	14,600	14,600	14,600	14,600	14,600	14,600	14,600	14,600
Reactor Power Level (KW)	100	100	100	100	100	1	10	50	100	100	100
Pressure (psig)	50	50	50	50	50	50	50	50	50	50	50
Reactor Log Book (Page and Exp. No.)	241-169	241-169	241-169	241-169	241-169	242-170	242-170	242-170	242-170	242-170	242-170
Sample No. and Time (min.) after start of run.	1(28.7) 2(37.8) 3(42.8) 4(47.9) 5(53.3) 6(57.5)	1(84.3) 2(91.0) 3(103) 4(110)	1(142) 2(148) 3(153) 4(160)	1(202) 2(208) 3(215) 4(220)	1(232) 2(235)	1(20.3) 2(28.8) 3(34.2) 4(38.0)	1(61) 2(64.5) 3(69.8) 4(76)	1(101) 2(107) 3(112) 4(116)	1(135) 2(139) 3(143) 4(146)	1(172) 2(176)	1(208) 2(212)
μ Moles phenol per liter											
For Sample 1	71.5	89.5	88.1	85.6	87.6	0.78	a	a	a	119	128
2	78.6	88.0	87.5	83.1	87.2	0.79	a	a	a	117	128
3	83.3	84.0	88.0	84.0	88.7	0.79	7.08	37.0	81.9		
4	84.2	88.8	89.2	84.1	88.8	0.79	4.72	31.5	81.5		
5	87.3										
6	90.5										

NOTES: a) Not analyzed since equilibrium not obtained.

b) All runs made with double or triple distilled water saturated with reagent grade benzene.

TABLE XII

SUMMARY OF DATA FROM N_2-H_2 RUNS

RUN	N-1	N-2	N-3	N-4	N-5
TC-1	607	644	672	587	695
TC-3	639	686	712	610	730
TC-2	691	743	773	662	794
TC-0	719	775	802	675	785
TC-4	390	419	430	379	430
TC-5	738	797	829	694	758
TC-6	575	610	636	535	643
Pressure Psig	280	250	300	250	300
Power Level KW	100	100	100	100	100
H_2 Rate Std. ft^3/hr	2.3	2.3	2.3	2.3	0.67
N_2 Rate Std. ft^3/hr	0.74	0.74	0.74	0.74	1.3
Moles (H_2/N_2)	2.1	2.1	2.1	2.1	0.52
Conversion	~ 0	~ 0	~ 0	~ 0	~ 0
Average Residence Time (min)	37	33	39	33	57
Reactor Log Book, page-Experiment No.	234-164	234-164	235-165	235-165	235-165
Mass Spec. Log Book No.		4640	4639		4641

TABLE XIII

DATA FROM AIR (OXYGEN-NITROGEN) IRRADIATIONS

RUN	A-1	A-2	A-3	A-4	A-5	A-6	A-7	A-8	A-9
TC-1	665	639	595	648	659	668	615	569	525
TC-3	692	664	610	686	692	704	639	590	538
TC-2	750	719	648	755	755	774	792	640	578
TC-0	741	710	640	748	748	764	688	635	575
TC-4	375	369	350	378	389	372	354	328	305
TC-5	710	680	610	725	721	749	660	608	541
TC-6	594	570	439	580	590	595	549	505	465
Pressure (psig)	300	320	300	320	310	310	310	280	280
Power Level (KW)	100	100	100-150	100	100	100	100	100	100
Flow Rate (Std. ft^3/min)	0.012	0.025	0.025	0.038	0.088	0.024	0.037	0.029	0.031
Reactor Log Book, page Exp. No.	243-171	243-171	243-171	244-172	244-172	244-172	244-172	244-172	244-172
Mass Spec. Log Book Nos.	4682		4683			4681			4684

TABLE XIV

A SUMMARY OF DATA FROM VICTOREEN RATE METER MEASUREMENTS TAKEN ALONG THE EDGE OF "G" AND "J" PORTS

Inches from Core Face	Configuration 1a		Fission Plate
	"G" Port (R/min.)	"J" Port (R/min.)	"J" Port (R/min.)
3		23,000	
6		16,000	
9		9,500	16,000
10.5		5,000	
12	1,900		8,500
13.5	1,700	3,000	
15	1,600	2,600	6,500
16.5		1,700	
18	850		5,000
21	600	1,050	2,500
24	350		
25.5	230	430	830
28.5	190		550
30		240	320
33	100	200	150
34.5		180	
36	75	150	50

TABLE XV

DATA FROM GOLD FOIL MEASUREMENTS IN "G" PORT

Gold Foil Number	Foil Weight (mg)	Date Counted	Time (PM)	Counts	Counting Time (Seconds)	Counts per Second	Counts per Second Corrected for Background	Activity Corrected for Decay Counts/Second	Activity Corrected for Foil Weight C/Sec/100 mg.	Thermal Flux
439	92.1	2/21/58	2:34	12,123	120	101.0	96.0	2.683×10^4	2.9131×10^4	4.07×10^8
440		3/6/58	1:24	46,613	60	769.2	764.1	6.12×10^6		
441	96.2	3/6/58	1:12	50,475	60	834.7	829.6	6.6548×10^6	6.918×10^6	9.68×10^{10}
442	90.5	3/6/58	1:12	50,885	60	850.1	845.0	6.7783×10^6	7.3899×10^6	1.05×10^{11}
443	20.5	2/21/58	2:46	311,182	60	5186.0	5181.0	1.4479×10^6	7.063×10^6	9.88×10^{10}
443	85.6	3/6/58	1:20	48,017	60	809.4	804.3	6.4518×10^6	7.5371×10^6	1.05×10^{11}
444	91.9	3/6/58	1:07	51,433	60	863.6	857.5	6.8786×10^6	7.5514×10^6	1.06×10^{11}
445	34.3	3/6/58	1:55	17,955	60	297.2	292.1	2.3431×10^6	6.8311×10^6	9.56×10^{10}
446	96.8	3/6/58	1:45	49,499	60	817.7	812.6	6.5184×10^6	6.7339×10^6	9.42×10^{10}
447	76.0	3/6/58	1:40	35,589	60	491.2	586.1	4.7015×10^6	4.9386×10^6	6.91×10^{10}
450	108.3	3/6/58	1:49	33,057	60	551.5	546.4	4.3830×10^6	4.0471×10^6	5.66×10^{10}
451	105.2	3/6/58	1:35	26,704	60	449.1	444.0	3.5616×10^6	3.3856×10^6	4.74×10^{10}
452	27.3	2/21/58	2.57	163,525	60	2725.0	2720.0	0.76016×10^6	2.7845×10^6	3.89×10^{10}
452	84.4	3/6/58	1:44	17,867	60	299.0	293.9	2.3576×10^6	2.7934×10^6	3.91×10^{10}
453	110.9	3/6/58	1:30	20,171	60	334.4	329.3	2.6415×10^6	2.3819×10^6	3.33×10^{10}
454	112.2	3/6/58	1:26	18,059	60	300.2	295.1	2.3672×10^6	2.1098×10^6	2.95×10^{10}
455	113.7	3/6/58	1:16	16,587	60	276.5	271.4	2.1771×10^6	1.9147×10^6	2.68×10^{10}
456	105.7	3/6/58	2:18	337,503	60	5618.0	5613.0	1.5687×10^6	1.4841×10^6	2.08×10^{10}
457	107.4	3/6/58	2:54	396,603	60	6610.0	6605.0	1.8459×10^6	1.7182×10^6	2.40×10^{10}
458	107.5	2/21/58	2:14	398,275	60	6638.0	6633.0	1.8537×10^6	1.7244×10^6	2.41×10^{10}
459	105.5	2/21/58	2:44	385,897	60	6432.0	6427.0	1.7962×10^6	1.7026×10^6	2.38×10^{10}
460	107.2	2/21/58	2:41	214,493	60	3575.0	3570.0	9.977×10^5	9.3069×10^5	1.30×10^{10}
461	120.4	2/21/58	2:21	200,401	60	3340.0	3335.0	9.320×10^5	7.7409×10^5	1.08×10^9
462	109.4	2/21/58	2:16	151,513	60	2525.0	2520.0	7.043×10^5	6.4378×10^5	9.01×10^9
463	117.4	2/21/58	2:39	135,620	60	2260.0	2255.0	6.302×10^5	5.3680×10^5	7.51×10^9
464	110.8	2/21/58	2:23	114,013	60	1900.0	1895.0	5.296×10^5	4.7798×10^5	6.69×10^9
465	106.7	2/21/58	2:12	101,263	60	1688.0	1683.0	4.704×10^5	4.4086×10^5	6.17×10^9
466	106.0	2/21/58	2:37	100,619	60	1677.0	1672.0	4.673×10^5	4.4084×10^5	6.17×10^9
467	112.1	2/21/58	2:26	105,253	60	1754.0	1749.0	4.888×10^5	4.3604×10^5	6.10×10^9
468	114.5	2/21/58	2:05	218,505	120	1821.0	1816.0	5.075×10^5	4.4323×10^5	6.20×10^9
470	110.5	2/21/58	2:28	106,141	60	1769.0	1764.0	4.930×10^5	4.4615×10^5	6.24×10^9
480	111.8	2/21/58	2:30	99,513	60	1659.0	1654.0	4.622×10^5	4.1342×10^5	5.78×10^9

NOTES:

(1) Foil Numbers refer to positions on foil holder as shown in Figure 17.

(2) Counter Used: MMPR #1723

(3) Background: 5.1 c/sec

(4) All gold foils were irradiated from 1725 to 1800 on 1/30/58.

TABLE XVI

DATA FROM FLUX MEASUREMENTS IN "G" PORT USING COBALT WIRE

Cobalt Wire Number	Time Counted (3/3/58)	Weight (grams)	Counts	Seconds	Counts per Second	Counts/sec. Corrected for Background	Counts/Sec/ 100 mg.	Thermal Flux n/cm^2 Sec.
1	12:20 PM	0.0478	123,391	60	2057	2050	4288	1.38 x 10"
2	11:55 AM	0.0345	76,847	60	1281	1278	3704	1.20 x 10
3	12:05 PM	0.0261	68,334	60	1139	1133	4341	1.40 x 10"
4	12:30 PM	0.0372	100,594	60	1677	1672	4495	1.45 x 10"
5	12:34	0.0358	43,787	60	730	724	2022	6.54×10^{10}
6	12:37	0.0356	29,974	60	500	494	1388	4.49×10^{10}
7	12:42	0.0400	26,325	60	439	430	1075	3.48×10^{10}
8	12:45	0.0265	17,505	60	292	286	1079	3.48×10^{10}
9	12:50	0.0361	23,953	60	399	293	812	2.62×10^{10}
10	12:55	0.0356	23,099	60	385	279	784	2.54×10^{10}
11	1:00	0.0333	10,049	60	167	160	480	1.55×10^{10}
12	1:04	0.0365	15,369	120	128	122	334	1.08×10^{10}
13	1:17	0.0463	15,431	120	129	123	266	8.68×10^{9}
14	1:15	0.0283	9,886	120	83	77	272	8.79×10^{9}
15	1:20	0.0288	14,873	180	83	77	267	8.55×10^{9}
16	1:40	0.0298	14,191	180	78	73	245	7.95×10^{9}
Gold Foil 16	3/18/58-3:40 PM	0.0971	6,372	60	106	100	1.023×10^{4} (a)	7.12×10^{8}
Gold Foil 78	3/18/58-3:43 PM	0.0975	81,764	60	1363	1357	1.4039×10^{5} (a)	9.77×10^{9}
Gold Foil 84	3/18/58-3:45 PM	0.0993	84,132	60	1403	1397	1.4364×10^{5} (a)	9.93×10^{9}

(a) Saturated Activity, Corrected for Decay.

Notes:

(1) Cobalt wire numbers refer to position on the irradiation holder as shown in Figure 17.

(2) Counter Assembly MMPR #1723 used with a high voltage adjustment setting of 1340V.

(3) Backgroumd: 365 C/min.

(4) All cobalt wire was irradiated from 1653 to 1700 on 2/28/58.

TABLE XVII

DATA FROM FISSION PLATE FOIL MEASUREMENTS

Foil No.	Cadmium Covered	Time (9/17/58)	Weight (Mg.)	Total Counts	Counting Time (Second)	Counts/ 100 Mg.	Counts/sec/ 100 Mg.	Counts/second/ 100 Mg. after Background Correction	Saturated Activity Corrected for Decay	Corrected for Monitor Foil	Calculated Thermal Flux @ 100 KW	Cadmium Ratio
1	No	12:55 P.M.	103.3	54,413	60	52,675	878	873	1.09×10^{6}	1.09×10^{6}	7.80×10^{11}	9.2
2	No	12:45	102.9	57,781	60	56,153	936	931	1.17×10^{6}	1.17×10^{6}	8.16×10^{11}	8.1
3	No	12:39	109.3	31,069	60	28,425	474	469	5.87×10^{5}	5.87×10^{5}	4.24×10^{11}	10.6
4	(Monitor)	12:43	94.6	10,423	60	11,018	184	179	2.24×10^{5}	2.24×10^{5}		
5	No	12:32	102.8	35,583	60	34,614	577	572	7.16×10^{5}	7.16×10^{5}	5.03×10^{11}	8.2
6	No	12:34	97.7	43,175	60	44,191	737	732	9.14×10^{5}	9.14×10^{5}	6.38×10^{11}	7.8
7	Yes	12:56	94.6	5,909	60	6,246	104	99	1.20×10^{5}	1.20×10^{5}		
8	Yes	12:47	115.0	8,290	60	7,200	120	115	1.44×10^{5}	1.44×10^{5}		
9	Yes	12:57	100.2	3,068	60	3,062	51	46	5.57×10^{4}	5.57×10^{4}		
10	Yes	12:46	118.6	7,305	60	6,159	103	98	1.19×10^{5}	1.19×10^{5}		
11	Yes	12:37	89.1	3,893	60	4,369	73	72	8.72×10^{4}	8.72×10^{4}		
12	(Monitor)	1:15	95.7	16,682	60	17,432	290	285	3.36×10^{5}	-		
13	No	1:13	108.9	73,560	60	67,548	1,126	1,121	1.33×10^{6}	8.89×10^{5}	6.02×10^{11}	6.6
14	(Monitor)	12:49	108.8	873	180	-	Foil Dropped from Reflector During Run		-	-		
15	No	1:09	104.6	36,681	60	35,068	584	579	6.85×10^{6}	4.57×10^{5}	3.22×10^{11}	8.2
16	No	1:08	102.2	51,165	60	48,915	815	810	9.58×10^{5}	6.39×10^{5}	4.20×10^{11}	5.6
17	No	1:25	102.1	45,501	60	45,565	758	753	8.90×10^{5}	5.93×10^{5}	4.10×10^{11}	7.3
18	No	1:23	96.0	33,817	60	35,226	587	582	6.87×10^{5}	4.58×10^{5}	3.43×10^{11}	8.3
19	Yes	1:19	103.0	4,094	60	3,975	66	61	7.15×10^{4}	5.61×10^{4}		
20	Yes	1:29	99.6	3,866	60	3,882	65	60	7.04×10^{4}	5.54×10^{4}		
21	Yes	1:27	100.0	9,174	60	9,174	153	148	1.73×10^{5}	1.36×10^{5}		
22	Yes	1:20	114.3	6,412	60	5,610	93	88	1.03×10^{5}	8.10×10^{4}		
23	Yes	1:16	107.3	8,333	60	7,766	129	124	1.45×10^{5}	1.14×10^{5}		
24	(Monitor)	1:21	96.5	14,387	60	14,909	248	243	2.85×10^{5}	-		

NOTES:

Background: 1323 counts per 5 minutes

Voltage: 1190 volts

Scaler: Baird Atomic Glow Tube

Scintillation Detector

Model 810A

Foils Irradiated 9/12/58

See Reactor Log for Exact Times

TABLE XVIII

DATA FROM THRESHOLD FLUX MEASUREMENTS

I. Foil Data from a Stringer Placed Along "J" Port with the Fission Plate in Place on the East Face of the Core (See Section III-C) with the Reactor Operating at 100 KW.

A. Measurement of Na^{24} from Al^{27} (n,α) Na^{24} with a calibrated scintillation counter (Radiation Counter Labs Type 23-A)

Al Foil Number	Time when Counted(1)	Weight (grams)	Counts/Min	C/M Corrected for Background	Decay Correction ($e^{-\lambda t}$)	Total Flux Above 8.6 Mev(2) (n/cm^2 sec)
1	1513	0.0250	7,205	6,945	0.353	1.80×10^8
2	1520	0.0593	2,860	2,600	0.352	2.84×10^7
3	1537	0.0627	862	602	0.348	6.32×10^6
4	1619	0.0696	457	197	0.337	1.91×10^6

B. Measurement of Na^{24} from Mg^{24} (n,p) Na^{24} with a calibrated scintillation counter (RCL type 23-A)

Mg Foil Number	Time when Counted(1)	Weight (grams)	Counts/Min	C/M Corrected for Background	Total Flux Above 6.3 Mev(2) (n/cm^2 sec)
1	1518	0.0425	19,280	19,020	7.03×10^8
2	1525	0.0361	3,240	2,980	1.29×10^8
3	1543	0.0411	933	673	2.57×10^7
4	1640	0.0444	460	200	7.21×10^6

C. Measurement of Mg^{27} from Al^{27} (n,p) Mg^{27} with a Dual, 100 channel, pulse height analyser (Radiation Instrument Development Laboratory Modified Type 3300)

Foil Number	Time when Counted(1)	Weight (grams)	ΔE Setting	Height at Peak	Decay Correction ($e^{-\lambda t}$)	Flux Above 5.3 Mev(2) (n/cm^2 sec)
1	1506	0.0250	0.0183	4.06×10^3	0.1045	1.07×10^{10}

NOTES: (1) All foils were irradiated on 8/15/58 from 1504 to 1641. However, the foils were counted on 8/16/58 and Hence "Time when Counted" refers to this date.

(2) Refers to reactor operation at 100 KW

II. Foil Data from a Probe Placed Between #43 and #47 (See Figure 26, Section III) with the Fission Plate on the East Face and the Reactor at 100 KW.

A. Measurement of Mg^{27} from Al^{27} (n,p) Mg^{27} with a dual, 100 channel, pulse height analyzer (Radiation Instrument Development Laboratory)

Al Foil Number	Weight (grams)	Time when Counted(1)	Length of Count (Minutes)	Corrected Height at Peak(2)	ΔE Setting	Decay Correction ($e^{-\lambda t}$)	Total Flux Above 5.3 Mev(4) (n/cm^2 sec)
1	0.0344	1709	1	1.01×10^4	0.0183	0.0252	1.06×10^{10}
2	0.0378	1707	1	1.16×10^4	0.0183	0.0290	1.52×10^{10}
3	0.0425	1705	1	1.08×10^4	0.0183	0.0338	1.34×10^{10}
4	0.0398	1702	2	1.57×10^4	0.0183	0.041	7.03×10^9
5	0.0423	1659	2	0.328×10^4	0.0183	0.051	1.43×10^9

B. Measurement of Na^{24} from Al^{27} (n,α) Na^{24} with a calibrated scintillation counter (RCL Type 23-A).

Al Foil Number(3)	Time when Counted(1)	Counts/Min	C/M Corrected for Background	Decay Correction ($e^{-\lambda t}$)	Total Flux Above 8.6 Mev(4) (n/cm^2 sec)
1	2025	141,060	140,800	0.828	1.24×10^9
2	2027	140,590	140,330	0.827	1.86×10^9
4	2029	110,670	110,410	0.825	1.63×10^9
6	2031	70,130	69,890	0.824	8.64×10^8
7	2033	12,230	11,970	0.823	1.80×10^8

C. Measurement of Na^{24} from Mg^{24} (n,p) Na^{24} with a calibrated scintillation counter (RCL Type 23-A).

Mg Foil Number	Weight (grams)	Time when Counted(1)	Counts/Min	C/M Corrected for Background	Decay Correction (e-λt)	Total Flux Above 8.6 Mev(4) (n/cm^2 sec)
1	0.0428	2035	158,260	158,000	0.823	5.34×10^9
2	0.0316	2036	239,620	239,360	0.822	7.43×10^9
3	0.0348	2038	216,120	215,860	0.820	6.89×10^9
4	0.0306	2040	96,200	95,940	0.817	3.5×10^9
5	0.0357	2041	25,825	25,565	0.816	7.98×10^8

NOTES: (1) All foils were irradiated on 8/13/58 from 1523 to 1619. "Time when Counted" refers to this same date.

(2) Corrected for the Na^{24} contribution.

(3) Weights are the same as for Table II A.

(4) All values are for reactor operation at 100 KW

III. Foil Data from a Probe Placed in the Center of the Fission Plate with the Reactor at 100 KW

A. Measurement of Mg^{27} from Al^{27} (n,p) Mg^{27} with the I.D.L. 100 channel analyser.

Al Foil Number	Weight (grams)	Time when Counted(1)	Length of Count (Minutes)	Corrected Height at Peak(2)	ΔE Setting	Decay Correction (e-λt)	Flux Above 5.3 Mev(3) (n/cm^2 sec)
1	0.0414	1721	2	1.81×10^4	0.019e	0.070	1.06×10^{10}
2	0.0665	1718	2	3.96×10^4	0.0196	0.0872	1.16×10^{10}
3	0.0393	1714	2	3.06×10^4	0.0196	0.116	5.42×10^9
4	0.0130	1711	2	5.69×10^3	0.019e	0.145	2.25×10^9
5	0.0656	1708	2	7.30×10^3	0.019e	0.180	4.63×10^8

B. Measurement of Na^{24} from Al^{27} (n,α) Na^{24} with the RCL scintillation counter.

Al Foil Number	Weight (grams)	Time when Counted(1)	Counts/Min	C/M Corrected for Background	Decay Correction (e-λt)	Total Flux Above 8.6 Mev(3) (n/cm^2 sec)
1	0.0414	1258	27,550	27,290	0.395	1.19×10^9
2	0.0665	1300	48,970	48,710	0.395	1.32×10^9
3	0.0393	1302	13,350	13,090	0.396	6.5×10^8
4	0.0130	1304	2,180	1,920	0.396	2.66×10^8
5	0.0656	1315	2,620	2,360	0.397	6.46×10^7

C. Measurement of Na^{24} from Mg^{24} (n,p) Na^{24} with the RCL scintillation counter.

Mg Foil Number	Weight (grams)	Time when Counted(1)	Counts/Min	C/M Corrected for Background	Decay Correction (e-λt)	Total Flux Above 6.3 Mev(3) (n/cm^2 sec)
1	0.0390	1345	45,500	45,240	0.379	5.15×10^9
2	0.0860	1347	35,160	34,900	0.379	5.96×10^9
3	0.0218	1348	14,990	14,730	0.380	2.74×10^9
4	0.0358	1350	10,040	9,780	0.380	1.21×10^9
5	0.0576	1354	2,590	2,330	0.381	1.79×10^8

NOTES: (1) All foils were irradiated on 8/13/58 from 1616 to 1646. Foils listed in Table III A were counted on 8/13/58, but all other foils were counted on 8/14/58.

(2) Corrected for the Na^{24} contribution.

(3) For operation at 100 KW.

APPENDIX B

SAMPLE CALCULATIONS

I. Calculation of the Combined Absorption Energy Transferred to a System by "Mixed" Neutron and Gamma Radiation

Assume that the following radiation flux exists at the point of interest:

$$\bar{\Phi}_S = 1 \times 10^{11} m/cm^2 \text{ sec}$$

$$\bar{\Phi}_F = 1 \times 10^{11} n/cm^2 \text{ sec } (\geq 0.5 \text{ Mev})$$

$$D_\gamma = 30{,}000 \text{ R/min}$$

The contribution due to gamma radiation may be converted to units of Mev/gm sec by means of Equation (11),

$$E_g^\gamma = 9.6 \times 10^5 D_\gamma$$
$$= 9.6 \times 10^5 \quad (3 \times 10^4 \text{ R/min}) \qquad (11)$$
$$= 2.88 \times 10^{10} \text{ Mev/gm sec}$$

The contribution due to slow neutrons is given by Equation (3),

$$E_g^S = \bar{\Phi}_S \frac{\Sigma_a^{H_2}}{\rho} E_\gamma \left(1 - e^{-\mu_\gamma \rho L}\right) \qquad (3)$$

For a n-heptane system contained in a 5.3ℓ reaction vessel, the following values are applicable:

$\sigma_a^{H_2} = 0.33 \times 10^{-24} \text{ cm}^2$ (Hughes, Reference 33)

$E_\gamma = 2.17$ Mev (Caulkins, Reference 10)

$\rho_{c_7} = 0.684 \text{ gm/cm}^3$

$\mu_\gamma \cong 0.026 \text{ cm}^2/\text{gm}$ (Assuming that the energy absorption coefficient for n-heptane is approximately equal to that for water, Fano, References 21 and 22)

ℓ = 10.8 cm (Approximating the vessel volume by a 5.3ℓ sphere)

Consider the following energy ranges,

ΔE_1 = 0.01 - 0.5 Mev, ΔE_2 = 0.5 - 1.0 Mev,

ΔE_3 = 1.0 - 1.5 Mev, etc., and assume that 40% of the fast energy contribution is from neutrons in the first energy range, 60% from neutrons in the second range, and that the contribution due to neutrons above 1 Mev can be neglected (See Caulkins, Reference 10).

Then, the following values are applicable for neutrons in the energy range 0.5 - 1.0 Mev:

N_{H_2} = 6.6 x 10^{22} atoms of hydrogen/cm^3 for n-heptane

$\sum_a^{H_2} = N_{H_2} \sigma_a^{H_2}$ = 2.18 x 10^{-2} cm^{-1} (Glasstone, Reference 24)

These values are substituted directly into Equation (3) giving,

$$E_g^s = 1 \times 10^{11} \text{ n/cm}^2\text{sec} \; \frac{2.18 \times 10^{-2} \text{ cm}^{-1}}{0.684 \text{ gm/cm}^3} \; 2.17 \text{ Mev} \; (1 - e^{-0.192})$$

$$= 7.9 \times 10^8 \text{ Mev/gm sec}$$

The fast neutron contribution can be calculated from Equation (9),

$$E_g^F = \bar{\Phi}_{Avg}(\Delta E_1) \; \sigma_{s,Avg}^{H_2}(\Delta E_1) \frac{N_{H_2} E_{Avg}}{\rho} \left(1 - \frac{1}{e}\right) \qquad (9)$$

$$+ \bar{\Phi}_{Avg}(\Delta E_2) \; \sigma_{s,Avg}^{H_2}(\Delta E_2) \frac{N_{H_2} E_{Avg}}{\rho} \left(1 - \frac{1}{e}\right)$$

+ . . . .

$\bar{\Phi}_{F,Avg} = 1 \times 10^{10}$ n/cm^2 sec

$E_{Avg} = 0.75$ Mev

$\sigma_{s,Avg}^{H_2} = 22 \times 10^{-24}$ cm^{-1} (Hughes, Reference 33)

$e = 2.718$ .....

$N_{H_2} = 6.6 \times 10^{22}$ atoms hydrogen/cm^3 for n-heptane

Direct substitution into Equation (9) yields,

$$E_g^{0.5-1.0} = 1 \times 10^{10} \text{ n/cm}^2 \text{ sec} \times 22 \times 10^{-24} \text{ cm}^2 \times \frac{6.6 \times 10^{22} \frac{\text{Atoms}}{\text{cm}^3} \; 0.75 \text{ Mev}}{0.684 \text{ gm/cm}^3} \left(1 - \frac{1}{2.718}\right)$$

$$= 9.84 \times 10^9 \text{ Mev/gm sec}$$

and, assuming as indicated above that

$$E_g^{0.1-0.5} = \tfrac{2}{3} E_g^{0.5-1.0}$$

then,

$$E_g^{0.1-0.5} = 6.53 \times 10^9 \text{ Mev/gm sec}$$

and the total contribution due to fast neutrons, E_g^F, is the sum of the contributions from these two energy ranges, or

$$E_g^F = 1.63 \times 10^{10} \text{ Mev/gm sec}$$

The total energy transferred to the n-heptane system can now be calculated from Equation (12):

$$E_g = E_g^\gamma + E_g^s + E_g^F \qquad (12)$$

$$= 4.59 \times 10^{10} \text{ Mev/gm sec}$$

$$= 2.86 \times 10^6 \text{ R/hr}$$

II. Calculations Necessary for Hydrogen-Heptane Runs

The following sample calculations are all based on the raw data exactly as recorded in the original data sheet from Run 14 (Table X).

A. Calculation of the Liquid Feed Rate and a Liquid Material Balance

The liquid feed rate based on the total pumping time of Run 14 is calculated as follows:

$$\frac{\text{Difference in L-1 level}}{\text{2.5 inches/liter}} \times 1000 \frac{\text{ml}}{\text{liter}} \times \frac{1}{\text{pumping time (min)}} = \frac{\text{ml C7}}{\text{min}} \tag{33}$$

$$\frac{31.1''}{2.5''/\ell} \times 1000 \frac{\text{ml}}{\ell} \times \frac{1}{61.9 \text{ min}} = 20.1 \text{ ml/min} \tag{34}$$

The liquid feed rate may also be calculated from measurements during the actual run time, e.g.,

$$\frac{\text{Difference in L-1 level}}{\text{2.5 inches/liter}} \times 1000 \frac{\text{ml}}{\ell} \times \frac{1}{\text{run time (min)}} = \frac{\text{ml C7}}{\text{min}} \tag{35}$$

$$\frac{15.7 \text{ inches}}{\text{2.5 inches/liter}} \times 1000 \frac{\text{ml}}{\ell} \times \frac{1}{31.9 \text{ min}} = 19.8 \frac{\text{ml}}{\text{min}} \tag{36}$$

Finally, the liquid rate is calculated from the actual liquid sample volume collected:

$$\frac{\text{Total ml product}}{\text{Run time (min)}} = \text{ml/min} \tag{37}$$

$$\frac{635 \text{ ml}}{31.9 \text{ min}} = 19.9 \frac{\text{ml}}{\text{min}} \tag{38}$$

The liquid rates calculated by these three independent methods agree within 1.5%.

B. Calculation of the Gas Feed Rate

The hydrogen feed rate for Run 14 may be calculated from spot readings of level gauge L-3 as follows.

L-3 Level (Inches)[a]	Corresponding Time (minutes)	Difference in L-3 ΔL-3	Difference in Time $\Delta\tau$	$\frac{\Delta L\text{-}3}{\Delta\tau}$ (inches/min)
38.3 ↓	0	-	-	-
31.1 ↓	10.3	7.2	10.3	0.70
25.6 ↓	18.2	5.5	7.9	0.70
20.8 ↑	25.5	-	-	-
24.0 ↑	30.2	3.2	4.7	0.68
25.2 ↑	31.9	1.2	1.7	0.70

a) Arrow indicates the direction that the level in L-3 is moving.

The average rate of level change in L-3 is 0.70 inches/min, and since, for this gauge, 1 in = 100 ml, this corresponds to 70 ml hydrogen/min at 520 psig and 82°F. This is converted to standard conditions (70°F and 1 atm).

$$\frac{70 \text{ ml}}{\text{min}} \times \frac{535 \text{ psia}}{14.7 \text{ psia}} \times \frac{530°\text{R}}{542°\text{F}} \times \frac{\text{Ft}^3}{28{,}320 \text{ ml}} = 5.2 \frac{\text{Ft}^3}{\text{hr}} \qquad (39)$$

The hydrogen off gas rate may be calculated from the wet test meter readings. Each reading is corrected to 70°F and 1 atmosphere.

Wet Test Meter No. 1: $$\frac{2.940 \text{ ft}^3}{31.9 \text{ min}} \times \frac{530°R}{542°R} \times \frac{29.64"}{30"} \times \frac{60 \text{ min}}{\text{hr}} = 5.34 \text{ ft}^3/\text{hr} \quad (40)$$

Meter No. 2: $$\frac{0.081 \text{ ft}^3}{31.9 \text{ min}} \times \frac{530°R}{542°R} \times \frac{29.64"}{30"} \times \frac{60 \text{ min}}{\text{hr}} = 0.149 \text{ ft}^3/\text{hr} \quad (41)$$

The total off-gas is the sum of 40 and 41, or 5.5 ft^3/hr. This is apparently 0.3 ft^3/hr larger than the gas feed. The difference is due to cracked hydrocarbons and possible measurement errors.

C. Calculation of the Hydrogen Ratio

The molal hydrogen feed rate is

$$\frac{5.2 \text{ ft}^3/\text{hr} \times 1 \text{ atm}}{0.7302 \frac{\text{ft}^3 \text{ atm}}{°R \text{ lb mole}} \, 530°R} = 1.38 \times 10^{-2} \text{ lb mole/hr} \quad (42)$$

The molal n-heptane feed rate is

$$1195 \frac{\text{ml}}{\text{hr}} \times 0.689 \frac{\text{gm}}{\text{cc}} \times \frac{1 \text{ lb}}{435.6 \text{ gm}} \times \frac{1 \text{ lb mole}}{100.20 \text{ lb}} = \quad (43)$$

$$1.82 \times 10^{-2} \text{ lb mole/hr}$$

Thus, the hydrogen rate, obtained by dividing (42) by (43), is 0.76 moles hydrogen per mole n-heptane.

D. Calculation of the Moles of Each Gas Product from the Off-Gas Composition

The compositions listed in Table IX are converted to cubic feet per hour for each component by multiplying the percentages for sample 1 by the throughput recorded by wet test meter number 1 and performing the same operation for sample 2 and wet test meter 2. The results from these calculations are then added component-wise to obtain the total product.

Component	Ft^3/hr from Sample 1 (% from table x 5.34 ft^3/hr)	Ft^3/hr from Sample 2 (% from table x 0.15 ft^3/hr)	Total Ft^3/hr	Moles / 100 moles C_7	Moles / Mole of CH_4
CH_4	0.0226	0.00182	0.0245	0.350	1.0
$C_2^=$	0.0189	0.00824	0.0272	0.392	1.12
C_2	0.0289	0.00133	0.0162	0.232	0.66
$C_3^=$	0.0168	0.00103	0.0271	0.388	1.10
C_3	0.0119	0.00649	0.0185	0.264	0.78
$C_4^=$	0.0033	0.00245	0.0273	0.390	1.10
C_4	0.0027	0.00140	0.0380	0.0544	0.16
$> C_4$	0.0059	0.00040	0.0634	0.0907	0.26

The column pertaining to moles per 100 moles of C_7 is obtained by the following conversion factor:

$$2.61 \times 10^{-3} \frac{\text{moles}}{Ft^3} \quad \frac{1}{1.82 \times 10^{-2} \text{ moles } C_7/hr} \quad \frac{100}{100 \text{ moles } C_7} = \tag{44}$$

$$14.3 \text{ moles/100 moles } C_7/(Ft^3/hr)$$

E. A Carbon Balance to Compare "Liquid Conversion" and n-heptane Decomposition

The chart from the partitioner analysis of the liquid product from Run 14 is shown in Figure 47. The total area under the curve (1302 units) was determined by a mechanical integrator built into the partitioner. Assuming that the peaks, starting nearest the injection point, correspond to C_1, C_2, C_3, etc., the following calculations may be performed:

Component in the Liquid Sample	Area Units Under the Respective Peak (1302 total)	Molal Percentage ($\frac{\text{Peak Area}}{1302}$ x 100)	Heptane Equivalent i.e., the Molal Percentage Times the Number of Carbon Atoms for that Component Divided by 7
C_1	1	0.077	0.011
C_2	2	0.154	0.044
C_3	7	0.538	0.230
C_4	9	0.692	0.394
C_5	5	0.384	0.272
C_6	2	0.154	0.132
		Total	1.083

and, since 98 mole % of the liquid is n-heptane, it is seen that 1.083 moles of n-heptane are decomposed per every 99 moles fed, or about 1.10 moles per 100 moles n-C_7 in the feed.

A similar analysis may be made for the gas product (see Table IX for the composition).

Component in the Gas Sample	Moles Per 100 Moles of C_7 Feed	Heptane Equivalent, i.e. the Moles/100 Moles C_7 Times the Number of Carbon Atoms for that Component Divided by 7
C_1	0.350	0.050
C_2	0.624	0.178
C_3	0.652	0.280
C_4	0.444	0.250
C_4^+	0.090	0.090
	Total	0.852

Hence, about 0.85 moles of n-heptane per 100 fed are decomposed to form gaseous products.

The total moles of n-heptane decomposed per 100 moles C_7 fed is the sum of the decompositions to form liquid and gas or 1.10 + 0.85 = 1.95 moles/100 moles C_7. This agrees to within several percent with the measured "liquid phase conversion" of 2.0 moles/100 moles C_7 for Run 14.

F. Calculation of the Average Residence Time

The volume feed rate of n-heptane (vapor phase) at the average reaction vessel conditions for Run 14 is given by,

$$1195 \frac{\text{ml } C_7}{\text{hr}} \frac{1 \text{ liter}}{1000 \text{ ml}} \times \frac{0.689 \frac{\text{gm}}{\text{ml}} \times \frac{1 \text{mole } C7}{100.2 \text{ gm}} \times 82.057 \frac{\text{ml atm}}{^\circ\text{K mole}} \times 667^\circ\text{K}}{18 \text{ atm}} \tag{45}$$

$$= 24.9 \ \ell/\text{hr}$$

The volume feed rate of hydrogen is,

$$5.2 \frac{\text{ft}^3}{\text{hr}} \times \frac{28.32 \text{ liters}}{\text{ft}^3} \times \frac{1 \text{ hr}}{60 \text{ min}} \times \frac{1 \text{ atm}}{18 \text{ atm}} \times \frac{667^\circ\text{K}}{394^\circ\text{K}} = 19.2 \ \ell/\text{hr} \tag{46}$$

The total volume feed rate under reaction vessel conditions is the total of (45) plus (46) or 44.1 ℓ hr. The reaction vessel volume is 5.3ℓ, hence the average residence time may be calculated as below:

$$\text{Average Residence Time} = \frac{5.3\ell}{44.1 \ell/\text{hr}} \times \frac{60 \text{ min}}{\text{hr}} = 7.2 \text{ min} \tag{47}$$

G. Calculation of the G Value

From Figure 30 it is seen that the difference in radiation and blank liquid conversion at the reaction conditions used in Run 14 is about 0.5%. Also, from Chapter III, the dose rate received inside the

reaction vessel with a nuclear reactor power of 100 kw is 1790 rep min. For a residence time of 7.2 minutes as calculated above, the G value is:

$$G = 0.005 \frac{\text{moles decomposed}}{\text{mole } C_7 \text{ fed}} \times 8.2 \frac{\text{gm-mole } C_7 \text{ fed}}{\text{hr}}$$

$$\times \frac{1}{7.2 \text{ min}} \times \frac{\text{min}}{1790 \text{ rep}} \times \frac{1 \text{ rep}}{83 \text{ ergs gm}}$$

$$\times \frac{\text{hr}}{1195 \text{ ml}} \times \frac{1}{0.689 \text{ gm ml}} \times 1.60 \times 10^{-6} \frac{\text{erg}}{\text{Mev}} \qquad (48)$$

$$\times \frac{\text{Mev}}{10^6 \text{ ev}} \times 6.024 \times 10^{23} \frac{\text{molecules}}{\text{gm-mole}} \times \frac{100}{100 \text{ ev}}$$

$$= 4.5 \times 10^3 \text{ molecules } C_7 \text{ decomposed } 100\text{ev}$$

H. Correction of G Values in Figure 42

The curve drawn with a solid line in Figure 42 is for a constant liquid feed rate of 1.1ℓ/hr. However, since the gas ratio is varied, the residence time is not constant.

The change of residence time with gas ratio at a liquid feed rate of 1.1ℓ/hr is shown in Figure 45, the residence time having been calculated as illustrated in Section F above. As shown in this figure, the residence time is cut from 17 to 11.5 minutes when the gas ratio is increased from 0 to 0.5. Then, assuming a straight line extrapolation of Figure 38, the G value would be decreased by a factor of 1.4 simply due to the decrease in residence time of 5.5 minutes (9.8 kilorep). Thus, at this point the corrected line (broken-line) is placed about 1.4 times as high as the solid line and corresponds to a G value for a residence time of 17 minutes. This procedure is repeated to complete the correct curve.

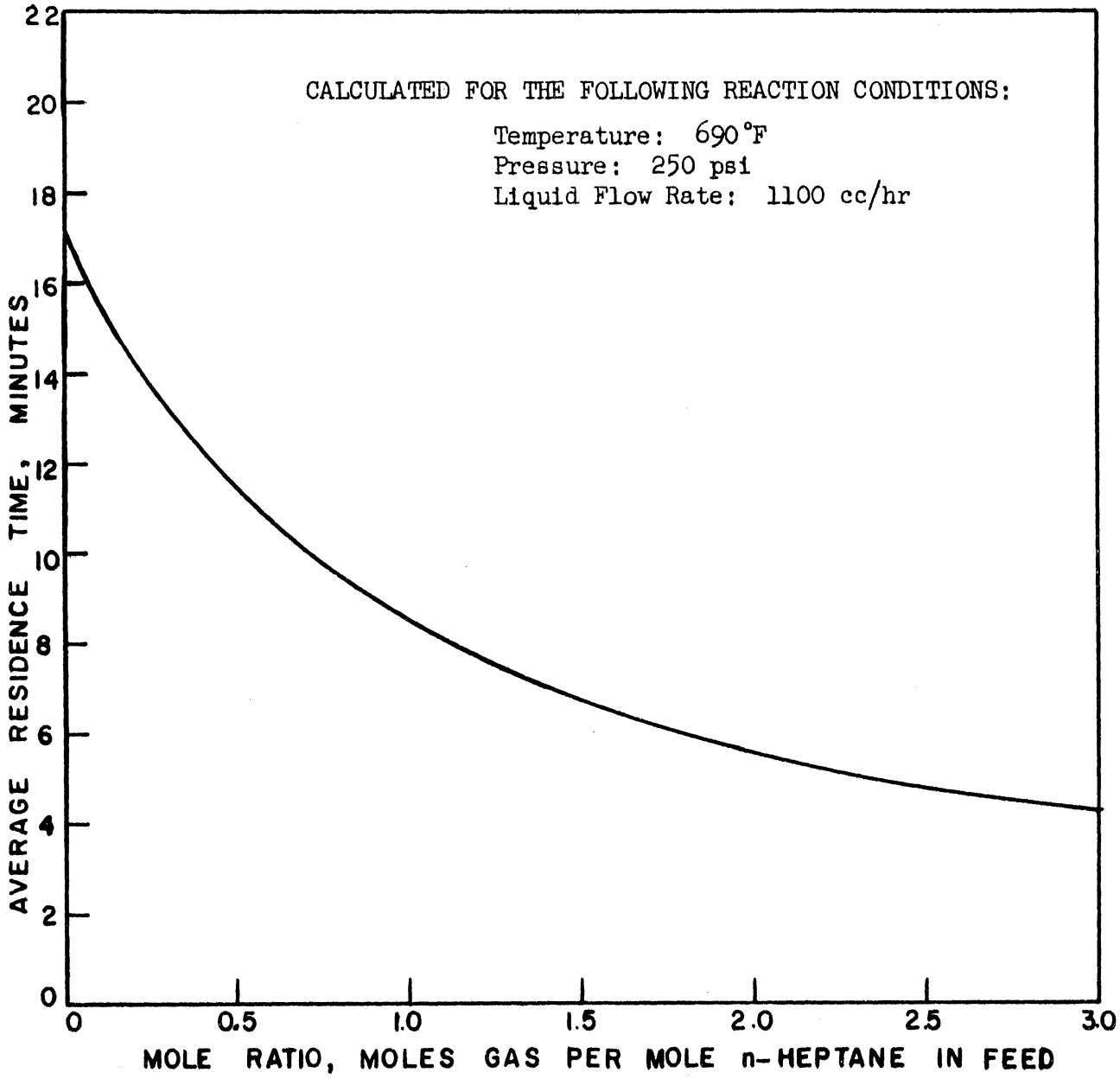

Figure 45. Average Residence Time Vs. Gas Ratio At a Constant Liquid Feed Rate of 1100 cc/hr

III. Calculation of the Phenol Production from Optical Density

The phenol concentration in a benzene and water system is given by Equation (13) taken from Reference 34.

$$\frac{\mu \text{ moles phenol}}{\ell} = 786\ [(AS-US)-(AB-UB)] \tag{13}$$

The optical density for the various samples changed with time after addition of the base, hence readings were taken at intervals of 2 minutes and extrapolated back to zero time or the time at which NaOH was added to the sample.

These extrapolated values for Run B-9, sample 4 turned out to be:

AS = 0.155

US = 0.045

AB = 0.008

UB = 0.002

and substituting these values directly into Equation (13) yields

$$\frac{\mu \text{ mole phenol}}{\ell} = 786\ [0.104] = 81.7$$

This corresponds to 39.9 kilorep as shown in Figure 18.

IV. Calculation of the Thermal Neutron Flux from Gold Foil Activation

For example, consider gold foil no. 453. From Table XV it is seen that

Foil Weight = 110.9 mg

Foil Activity Corrected for Background = 329 c/sec.

The saturated foil activity is[32]

$$A_{SAT} = \frac{A_o}{e^{-\lambda t_2}(1 - e^{-\lambda t_1})} \tag{49}$$

where A_o is the activity in counts per second at some time t_2 after the end of the irradiation period which lasted for a time t_1. λ is the decay constant for the foil under consideration.

Foil 453 was exposed for 35 minutes at 100 kw, removed at 1800 on 1/30/58 and counted at 1330 on 3/6/58. Hence, t_1 = 35 minutes and t_2 = 34.9 days.

The decay constant for gold is[23,32]

$$\lambda = \frac{0.693}{T_{1/2}} = \frac{0.693}{2.69} = 0.259 \text{ days}^{-1} \tag{50}$$

Direct substitution into (49) gives,

$$A_{SAT} = \frac{329 \text{ c/sec}}{e^{-0.259 \times \frac{35}{1440}} (1 - e^{-0.259 \times 34.9})} \tag{51}$$

$$= 4.2 \times 10^8 \text{ c/sec}$$

A_{SAT} is then correct for foil weight,

$$A'_{SAT} = \frac{100 \text{ mg}}{110.9 \text{ mg}} A_{SAT} \tag{52}$$

$$= 3.80 \times 10^8 \text{ c/sec} \quad 100 \text{ mg}$$

The cadmium ratio at this point is equal to:[63]

$$\text{C.R.} = \frac{\text{Bare Foil Activity}}{\text{Cd. Covered Foil Activity}} = \frac{\text{Activity of Foil 466}}{\text{Activity of Foil 439}} = \frac{4.41 \times 10^5}{2.91 \times 10^4} = 15.1 \tag{53}$$

Then, A^{th}_{SAT}, the specific saturated activity due only to thermal neutrons is given by,(63)

$$\begin{aligned} A^{th}_{SAT} &= A'_{SAT}\left(1 - \frac{1}{C.R.}\right) \\ &= 3.80 \times 10^8 \left(1 - \frac{1}{15.1}\right) \\ &= 3.56 \times 10^8 \text{ c/sec 100mg} \end{aligned} \tag{54}$$

But, it has been shown that for the scintillation counter used for these measurements and for this size gold foil, the thermal flux is related to A^{th}_{SAT} by(63)

$$\begin{aligned} \Phi_S &= 93.94\ A^{th}_{SAT} \\ &= 93.94\ (3.56 \times 10^8) \\ &= 3.34 \times 10^{10} \text{ n/cm}^2 \text{ sec} \end{aligned} \tag{55}$$

A small start-up correction is necessary since the foil "sees" some neutrons before the reactor hits the prescribed 100 kw. This correction was calculated by taking the area under the constant portion (100 kw) of the log N chart and dividing it by the total area under this chart. In the present case this fraction is 0.99, hence

$$\begin{aligned} \Phi_S &= 0.99\ (3.36 \times 10^{10}) \\ &= 3.33 \times 10^{10} \frac{\text{thermal neutrons}}{\text{cm}^2 \text{ sec}} \end{aligned} \tag{56}$$

V. Calculation of the Total Flux Above Threshold from Threshold Activation Data

The procedures used for calibrating the various counters are too envolved and lengthy to discuss in detail in this paper. The general procedure is outlined in Reference 28. Exact details will soon be published by Bullock and Wahlgren in a Michigan Memorial Phoenix Project report entitled "Fast Neutron Measurements in the Ford Reactor".

Using efficiencies obtained from these counter calibrations, it can be shown that(32,35,60)

$$\Phi_{\text{Mev}}(>5.3) = \frac{2.6 \times h}{e^{-\lambda t_2}(1 - e^{-\lambda t_1}) g\, \Delta t\, \Delta E} \tag{57}$$

$$\Phi_{\text{Mev}}(>6.3) = \frac{38.4\ (c/m)}{e^{-\lambda t_2}(1 - e^{-\lambda t_1})\, g} \tag{58}$$

$$\Phi_{\text{Mev}}(>8.6) = \frac{16.8\ (c/m)}{e^{-\lambda t_1}(1 - e^{-\lambda t_2})\, g} \tag{59}$$

where

Φ(>5.3 Mev), Φ(>6.3 Mev), and Φ(>8.6 Mev) represent the total neutron flux above 5.3, 6.3, and 8.6 Mev respectively,

h is the corrected pulse height from the 100 channel analyzer,

λ is the decay constant for the isotope under consideration,

t_2 is the time after irradiation until the foil is counted,

t_1 is the time the foil is actually irradiated,

g is the foil weight in grams,

Δt is the counting time in minutes,

ΔE is the energy band setting on the 100 channel analyzer,

c/m represents counts per minute, and the factors 2.6, 38.4, and 16.8 are conversion factors which include the counter efficiency.

For example, consider foil 1 from Table XVIII-IC. Data from the table is substituted directly into Equation (57) giving,

$$\Phi(>5.3) = \frac{2.6\ (4.05 \times 10^3)}{(0.1045)(0.99)(.0183)(2)(0.0183)} \tag{60}$$

$$= 1.07 \times 10^{10}\ \text{n/cm}^2\ \text{sec}$$

In a similar manner, data from foil 1, Table XVIII-1A, may be substituted directly into Equation (58), giving

$$\Phi(>6.3) = \frac{38.4\ (6945)}{(0.353)(0.0734)(0.0250)} \qquad (61)$$

$$= 1.80 \times 10^{8}\ n/cm^{2}\ sec$$

and, using data from Table XVIII-1B, the flux above 8.6 Mev may be calculated from foil 1 by direct substitution into Equation (59), i.e.,

$$\Phi(>8.6) = \frac{16.8\ (1.902 \times 10^{4})}{(0.352)(0.0720)(0.0425)} \qquad (62)$$

$$= 7.03 \times 10^{8}\ n/cm^{2}\ sec$$

APPENDIX C

HAZARD ANALYSIS FOR A HIGH TEMPERATURE AND PRESSURE BEAM-PORT EXPERIMENT

(Note: The following is a copy of a report submitted to the Ford Reactor Staff on May 28, 1958)

I. Introduction

The experiment considered in this analysis utilizes a flow system designed to handle hydrogen-heptane mixtures under maximum conditions of 900°F. and 1000 psi. Permission to insert this apparatus in "G" beam-port of the Ford Nuclear Reactor is requested. Feed rates of 0-5 liters per hour heptane and 0-48 standard cubic feet hydrogen per hour will be used. Figure 8, page 35 , indicates a schematic flow diagram while Figure 46, page 155 , shows the arrangement of the apparatus on the beam-port floor. A picture of the pressure vessel and beam-port plug is shown in Figure 10, page 44.

This report is divided into two main sections. A detailed listing of possible accidents is presented, followed by a discussion of the precautions taken to prevent these accidents.

II. Postulated Conceivable Accidents

Accidents may be divided into two major categories according to end results, i.e., accidents resulting in damage to the nuclear pile and accidents resulting in personal injury. The value of personnel safety is obvious, but the large investment tied up in the nuclear pile should be emphasized. An accident in an access beam-port might not only destroy expensive equipment but could also cause expensive and lengthy delays in the reactor operating schedule while repair work and decontamination are carried out.

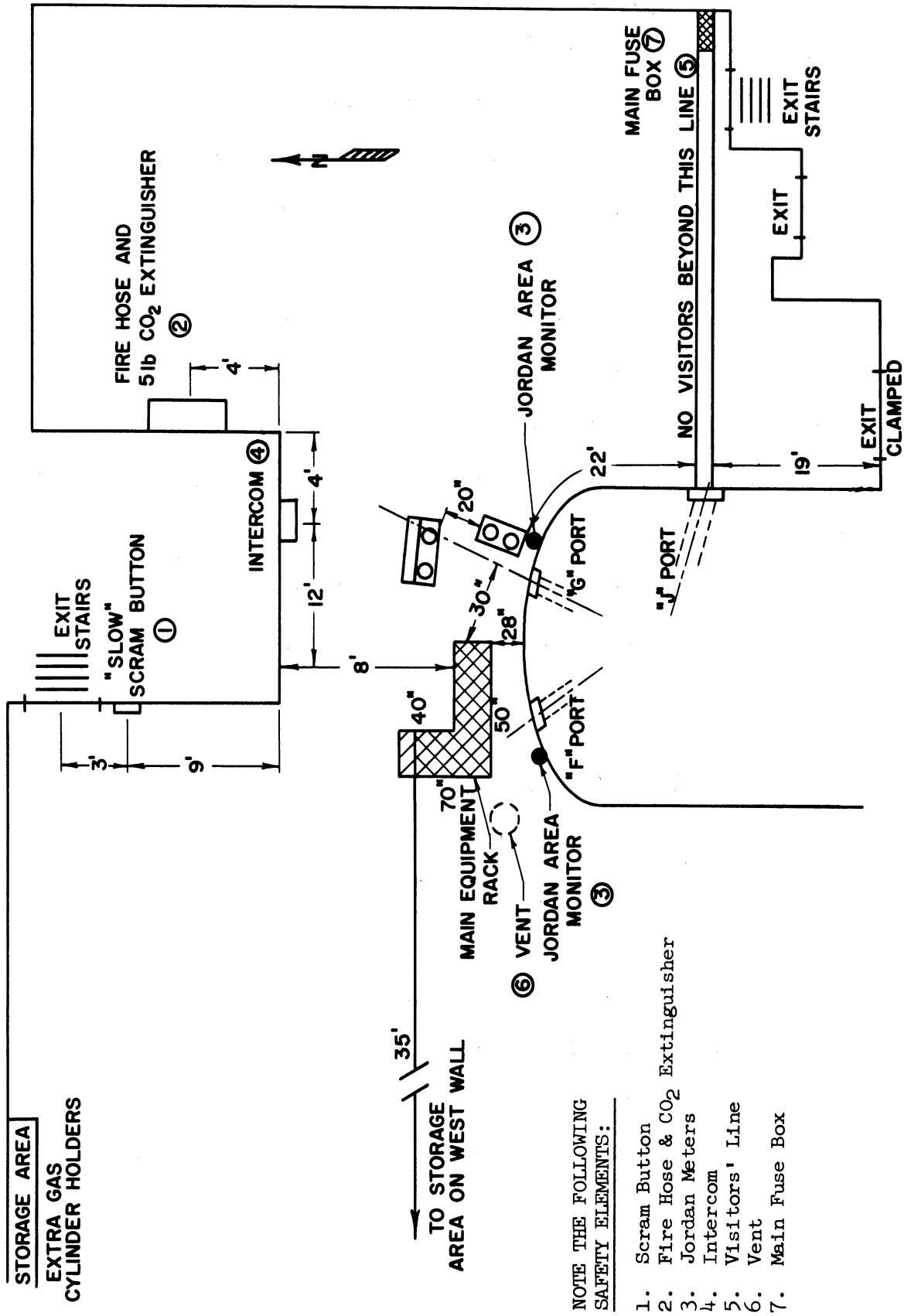

NOTE THE FOLLOWING SAFETY ELEMENTS:

1. Scram Button
2. Fire Hose & CO_2 Extinguisher
3. Jordan Meters
4. Intercom
5. Visitors' Line
6. Vent
7. Main Fuse Box

Figure 46. General Floor Plan and Apparatus Location for the Beam-Port Floor

A. Accidents Resulting in Pile Damage

1. Maximum Credible Accident

This accident could result from an in-pile explosion violent enough to cause the rupture of one or more fuel elements and at the same time jam the safety rods in an "up" position. Fission products released from the fuel rupture would contaminate the pool water, and reactor control would be lost without use of the safety rods. Actually, due to the negative temperature coefficient, a core melt-down is improbable, but excessive power levels and the resulting radioactivity problems are likely. Pool water flowing into the damaged beam-port would slowly leak out through the two 3/4" access tubes in the shielding plug. The leak would not be large (calculations indicate a drop of eleven feet in the pool water level in 4 hours), but the water would probably be contaminated as already indicated.

2. Postulated Conceivable Accident

Fortunately, a fuel element rupture is unlikely because the moderator elements serve as an explosion shield between the fuel elements and the beam-port.

It is probable that explosion damage would mainly be limited to the rupture of the beam-port liner. Once this occurs, a serious pool leak will take place through the access tubes in the shielding plug. There is a chance that such a leak might be stopped by forcing something like putty into the access tubes. If not, it would be necessary to move the reactor core to the south end of the pool and insert the divider doors.

3. The Excess Reactivity Accident

An accident commonly considered in connection with reactor experiments is the sudden removal of an experiment tying up a large amount of excess reactivity. Such an accident is unlikely in this case, since the reaction vessel involves only a small excess reactivity, and it is solidly anchored in the beam-port.

4. The Overheating Accident

There is little chance that local overheating due to the heated pressure vessel (700-900°F) could upset the pile nuclear characteristics. It is conceivable, but unlikely, that thermal stresses in the beam-port wall might result in a rupture of the liner.

B. Accidents Resulting in Personnel Injury

1. Out-of-Pile Fires and Explosions

The extremely volatile hydrocarbon-hydrogen mixture handled in the pilot unit is a potential fire and explosion hazard.

2. Radiation Exposure

Workers on the beam-port floor are confronted with numerous possible radiation hazards. Some of the more obvious of these include radiation leakage from the beam-ports, streaming during transferral operations, and radioactivity in the pilot plant product. A real danger lies in overlooking some unexpected source, for example, radiation from another experiment in the area.

III. Precautions and Safety Measures Used to Prevent Accidents

A. Summary of Safety Features

1. The vessel was designed with safety factors 1.5 to 2.0 times those listed in ASME Codes. Both mechanical and creep strength were considered.

2. The vessel was hydrostatically tested at room temperature to 3000 psi or three times the maximum operating pressure.

3. The vessel has been successfully used in eight runs outside of the reactor under maximum temperature and pressure conditions.

4. As indicated in Figure 7, two rupture discs are incorporated in the apparatus and set at 1400 and 1880 psi, respectively.

5. All tubing and fittings were purchased from "Autoclave Engineers" and recommended for 10,000 psi maximum or ten times operating pressure.

6. The reaction mixture of hydrogen and heptane does not represent an explosion hazard unless oxygen is present. Several precautions are used to insure the preclusion of oxygen.

a) A thirty minute nitrogen purge is always practiced before each run, and a reverse nitrogen purge is used at shutdown.

b) Any traces of oxygen are removed from the hydrogen feed stream by means of a palladium deoxo catalyst. Resulting water is then removed in a silica gel drier.

7. The possibility of plugging up the pressure vessel is lessened by appropriate use of strainers and filters.

B. Precautions to Prevent "External" Fires and Explosions

1. A detailed set of tested operating instructions and procedures have been written and are used for all experiments (Appendix D).

2. All tubing and fittings are rated at ten times operating pressure.

3. The entire unit was tested overnight at a pressure of 1000 psi of nitrogen. Leaks were eliminated until a pressure drop of less than 10 psi was observed.

4. All electric motors in operation during runs are explosion-proof, and all other conceivable spark sources have been eliminated or enclosed in a "fire screen".

5. No smoking is permitted in the area. As indicated in Figure 57, visitors are not permitted in the general area of the apparatus, thus, eliminating additional fire hazards.

6. Figure 57 shows the location of a fire hose and carbon dioxide extinguisher within 24 feet of the apparatus.

7. All exhaust fumes are vented to the forced air exhaust system. Calculations show that even under maximum H_2 flow conditions the hydrogen concentration in the vent system is about one-half the explosion concentration for hydrogen in air.

8. Safety glasses are worn during operation of the unit.

9. Only that amount of hydrocarbon necessary for a run is brought to the beam-port floor at any given time. Other hydrocarbon feed is stored in a safe location well-removed from the area.

10. The rupture discs are used to prevent pressure build-up.

11. The automatic pressure reducer valve installed in the apparatus is designed to "fail safe", i.e., open if the instrument air fails. The separate radioactive system has an air-to-open valve to prevent an escape of radioactive gases if the instrument air fails.

12. Interruption of cooling water to the unit will be picked up by the temperature indicator and the unit shut down.

C. Precautions to Prevent Radiation Exposure of Personnel

1. The beam-port area is monitored by the experimenter before each run.

2. The product is monitored continuously. If a high radioactivity appears, the unit will be shut off, and any chemicals in the pressure vessel will be run into special lead-covered storage tanks.

3. All gases, even from the rupture discs assemblies, are vented to the exhaust system and will be periodically monitored.

4. High grade, pure feed stock is being used to prevent possible impurities which might become radioactive and thus contaminate the product. For this same reason, stainless steel construction is used throughout.

5. A number of general features of the reactor aid the experimenter. First, the beam-port door closed-circuit described on page IV-31 of the "Reactor Handbook"(64) adds to the general safety of the beam-port floor. Several additional features are illustrated in Figure 57. The Jordan monitors are conveniently near the apparatus so as to be a great aid in radiation detection in the area. The intercom is about 17 feet away for easy communication with the reactor operator, and a "slow scram" button is only 17 feet distant. Appro-

priate exits are marked on Figure 57 also.

6. Film badges are worn at all times.

IV. Special Problems

Safe unloading of the assembly after exposure and removal to the storage area, 35 feet distant, represents a unique problem. Calculations indicate that the stainless steel pressure vessel may give off as much as 780 r/hr at 20 centimeters immediately after long irradiations. General procedures for handling the apparatus are presented in Appendix D.

V. Emergency Procedure

A. In-port Accident

1. Follow the emergency shut-down procedure listed on page 168.

2. Attempt to plug any pool leaks.

3. Follow emergency procedure listed in the "Reactor Handbook", page XV-1 (64).

B. External Accident

1. Turn off unit, using the emergency shutdown procedure, omitting step one.

2. Apply a carbon dioxide extinguisher if necessary.

3. Inform the reactor operator by intercom.

C. Procedure in Case of a Building Alarm

1. Follow the procedure in "Reactor Handbook", XV(64). Unit can be completely shut down in approximately 3 - 5 minutes.

2. In the case of a practice alarm, the unit will be shut down by a slower but more efficient procedure which requires a 15 minute nitrogen purge.

D. Suggestions for Future Safety Improvement

1. A health physicist should be required to monitor the "G" beam-port area at the start of each run and post warning signs.

2. Smoking should not be permitted anywhere on beam-port floor. Appropriate signs should be posted on all doors leading to area.

3. The swimming pool divider doors should be moved from the basement to the control room floor to speed emergency insertion.

4. Consideration should be given to the possibility of a fume hood at the face of the reactor.

5. Experimenters should be informed in advance if a practice building alarm is scheduled.

6. The beam-port floor exhaust fans should not be stopped for the purpose of a practice building alarm.

7. The reactor operator should be completely familiar with the possible hazards connected with the experiment in order not to be caught "off-guard" in an emergency.

8. The reactor operator should periodically check with the experimenter by means of the intercom system.

APPENDIX D

Operating Instructions for Pilot Plant

The unit may be operated in a number of ways depending upon the experiment under consideration. The two cases considered here are the basic operations of feeding a pure liquid hydrocarbon and feeding a mixture of hydrocarbon and some gas, in this case assumed to be hydrogen. All nomenclature refers to the flow diagram shown in Figure 7 and the list of equipment in Table 4.

I. Case 1: Pure hydrocarbon feed only (No hydrogen)

A. Preliminary Procedure

1. Monitor the beam hole area with a Juno.

2. Evacuate and label gas sample tubes. Clean and label liquid sample flasks.

3. Turn on temperature recorders TR-1 and TRC-2, press manual standardization lever, mark and date the chart.

4. Check pressure controller setting and turn on instrument air. Drain the instrument air wet traps.

5. Turn on pressure controller PRC-1, mark the chart and date.

6. Turn on cooling water to E-1, E-2 and E-3.

7. Place dry ice and alcohol in ice traps CT-1 through CT-3.

8. If either tank T-2 or T-3 is not in use, check all valves in the lines through valve 44, the appropriate tank, and valves 19 and 21 to assure a free path for a nitrogen purge.

a) If tanks T-2 and T-3 are in use, prepare all valves for a nitrogen purge through valve 41 directly to 26.

B. Nitrogen Purge Procedures

1. Set PRC-1 at the desired run pressure.

2. Set TRC-2 at the desired temperature control point.

3. Turn on all powerstats and set at desired levels.

4. With valves 26, 42, and 65 closed, adjust the nitrogen cylinder pressure reducer to a pressure of about 10 lbs. above the PRC-1 set point.

5. Adjust the nitrogen flow rate by means of valves 26, 42, and 65 if the feed path is through T-4 or T-5. If the nitrogen feed path is through valve 41, adjust the flow rate by valve 26 alone.

C. Run Procedure

1. When the reactor temperatures come within 100°F of the desired temperatures, stop nitrogen flow by closing valve 41 or valve 21. Open valve 40 to obtain a nitrogen blanket in R-3. Be sure the gas side of mixing valve 26 is closed and the liquid side open.

2. Start the hydrocarbon feed. If a pump is used, it is most important that the valving on pump P-1 (valves 13, 14, 15 and 16) or P-2 (11 and 25) are open. If atmosphere's feed pressure is used, be sure that the feed tank vent is open.

3. Set stopcocks S-5 and S-4 so that off gases are vented and do not pass through the cold traps or wet test meters.

4. Allow the unit to operate for 10-20 minutes after the reactor reaches run conditions of temperature and pressure.

5. At this point, the run proper may be begun. A run is defined as a set period of time during which run conditions are held reasonably constant, and appropriate measurements are obtained to permit an adequate

material balance. In order to obtain good balances, careful manipulation at the start and end of a run is essential. In general, those readings which are rapidly changing with time (wet test meters, liquid levels, etc.) should be read as close to the desired time as possible. Other variables such as temperature should be recorded only afterwards.

6. To start the run:

a) Note the time for the start of the run.

b) Switch stopcocks S-4, S-5 and close valve 54 so that gas flow is directed to the respective wet test meters. By-pass the gas sample tubes.

c) Mark the liquid level in R-3.

d) Record the feed tank liquid level and the water level in L-3.

e) Place the liquid sample flask R-4 in the system.

7. Periodically record all temperatures and pressures. Also record liquid levels. At least once during the run the atmospheric pressure, along with the wet test meter temperatures and pressures, should be recorded.

8. Gas samples are collected by placing evacuated sample tubes into positions GS-1 and GS-2. Then, gas flow is directed through these tubes for about 5-10 minutes to obtain a sample.

9. The following operation should be performed to complete a run:

a) Record the time when the liquid level in R-3 reaches the starting mark.

b) Repeat Step 3 above.

c) Stop pump.

d) Read liquid levels and record wet test meter readings.

10. The total volume of liquid sample collected should be recorded. All samples are placed in a cooler.

11. The volume of liquid caught in the cold traps should be measured and the liquid stored in a freezer.

12. Go directly into the normal shut-down procedure given in Section III. Steps 2 and 3 are omitted since a hydrogen feed is not used.

II. Case 2: Hydrogen and Hydrocarbon Feed

A. Preliminary Procedure

1. It is assumed that the gas feed tanks, T-4, 5 have been properly filled.

2. Care must be taken to insure the absence of air before H_2 is admitted to a hot system.

3. Repeat all steps of Section A, Case 1.

4. Check through H_2 panel board to insure a free path when flow starts. To avoid surging in the sight glass, valve 57 should only be open 1/4 turn.

B. Nitrogen Purge

5. Follow Steps 1 through 5, Section B, of Case II.

6. Continue N_2 purge for 20 minutes, then set H_2 press regulator at approximately 20 lbs. higher than PRC-1. Stop N_2 flow by closing valve 41 or 21.

7. To initially fill tanks T-4 and T-5 with hydrogen, open both 58 and 59 while the outlet valves are closed. Once operating pressure is reached in the tanks, again close 58 and 59.

8. Open valves 55, 59 and close valves 58, 56 or open valves 58, 56 and close 55, 59 depending on whether H_2 is to be forced from T-4 or T-5, respectively.

9. Regulate H_2 flow by valves 42 and 65 along with 26.

10. From this point on, Section C of Case 1 may be followed. However, now Steps 2 and 3 of the shut-down procedure are to be included.

III. Shutdown Procedures

A. Normal Shutdown Procedure

1. Turn off all powerstats.

2. Turn off H_2 feed by closing left side of mixing valve No. 26. Close 42 and 62. Turn off all gas cylinders.

3. Block pressure to T-4 and T-5 by closing valves 58 and 59 and opening 55 and 65.

4. Turn pump off. Close valves 13, 14, 15, and 16.

5. Slowly reduce pressure in reaction vessel by setting supply pressure on PRC-1 at 13 psi. Care must be taken to keep R-3 from overflowing during this process.

6. When liquid ceases to flow from unit into R-3 and pressure falls below 50 psi, close valve 32.

7. Start a reverse purge by setting N_2 regulator at 50 psi, open valve 40, and drain gas and any liquid out through 21 and 20.

8. Continue purge until temperatures drop below 200°F.

9. Close 40, 21, and 20. Turn N_2 off.

10. Turn off all electrical instruments, air, and H_2O.

11. Check TRC-1, TRC-2 for calibration stop.

B. Emergency Shutdown

1. The assistant operator should press the beam-port floor reactor scram button while Steps 2 through 4 are being performed.

2. Turn off electricity by throwing master switch on east wall of Phoenix Building.

3. Close valves 26 (both sides) and 32.

4. Turn gas cylinders off.

5. After emergency passes, start normal shutdown procedure.

IV. Radioactivity in Product

A. Radioactivity Control

1. If at any time the product activity level arises above 10 mr/hr, immediately turn PRC-2 on, close valve 28 and open 27 so that the product flows into shielded tanks R-1 and R-2.

2. If the activity remains at this level for 15 minutes, shut the unit down.

3. If the activity increases another 100 mr/hr at any time during this period, shut the unit down immediately.

APPENDIX E

HAZARD ANALYSIS AND INSTRUCTIONS FOR LOADING AND UNLOADING THE BEAM-PORT APPARATUS

I. Introduction

Section XIII of the "Ford Nuclear Reactor Handbook"(64) outlines the standard procedure for loading and unloading beam-port samples. However, due to the unique design of the present apparatus, certain modifications of this procedure are necessary.

II. Hazards During Loading and Unloading

A. Radiation Hazard to Personnel

1. Induced Radioactivity in Equipment

Preliminary calculations indicate that radiation levels as high as 780 r/hr at 20 cm, dropping to 190 r/hr in 24 hours, could be emitted from the stainless steel pressure vessel immediately after long periods of exposure. (The figure 730 r/hr assumes complete saturation, a condition which probably will never be reached. However, levels as high as 10 r/hr are likely and have been observed.) (See calculations in Appendix B.) In addition, the "ion end" of the beam-port plug will show a high activity immediately after irradiation, but since the activity dies fairly rapidly in Al, the major source of radiation and hence the major hazard will be the extremely "hot" pressure vessel.

2. Radiation from the Open Beam-Port

All movements of the beam-port apparatus will be performed with the reactor shut down. However, the core is still a powerful source of gamma rays. The gamma-intensity is a function of the history of the

reactor's operation, time after shutdown, and core position. In March 1958, levels as high as 5 r/hr were recorded at the entrance of G-port after the reactor had been idle over a weekend and with the core in beam-port irradiation position.

B. Possibility of Damage to Nuclear Reactor

1. Beam-Port Section

If a rough spot exists either on the apparatus being inserted or on the beam-port wall, the possibility exists that the resulting binding will separate the cone section of the beam-port from the pipe section embedded in the reactor shielding. As illustrated in Figure 14, the inner and outer sections of the beam-port are connected by means of a flange. It is this connection that presents a danger area, both from the point of view of possible leakage and the fact that it represents a discontinuity or rough spot in the smooth beam-port wall. Any damage would naturally result in a serious leak.

2. Rupture of End of Beam-Port

If the apparatus is forced too far into the beam-port or if it is too long, the end of the beam-port could conceivably be punched-out and a serious leak result.

C. Possibility of Damage to Apparatus

1. Welded Extension on Shielding Plug

The pipe segment welded on the beam-port shielding plug to support the weight of the pressure vessel (see Section II, item 3d) cannot take large stresses and could easily be broken off, especially at the weld.

2. Thermocouples, etc.

Thermocouples, electrical extension lines, etc., are vulnerable to damage, especially in the area between the plug and the pressure vessel (see Figure 11). It should be noted that any movement of the thermocouples would throw off their internal location and, thus, seriously impair results.

3. Dislocation of Pressure Vessel

The pressure vessel purposely is not securely fastened to the shielding plug so as to afford easy removal after it becomes radioactive. A hard knock could move it out of the guide grooves which hold its support legs in position and cause serious damage. Because of the close dimensions in the beam-port, it would be difficult to dislocate the vessel while it is in position; but care should be taken during transferral to the storage area.

III. Precautions

The best method of averting the possible accidents listed in Section II is believed to be the setting up and rigid adherance to a carefully thought-out loading and unloading procedure. Such a procedure is presented in Section IV.

IV. Loading and Unloading Procedure

A. Loading the Apparatus with the Handling Coffin

1. Enter time of loading into the nuclear reactor operating schedule.

2. Transferral immediately following long high power runs with the reactor may necessitate having the reactor staff move the core back from the beam-port irradiation position. Under ordinary conditions, this is not necessary.

3. Drain the beam-port as per Section XIII-1 of the "Reactor Handbook".(64)

4. At this point, a health physicist should monitor the door area and then remain on the beam-port floor throughout the remainder of the operation.

5. Follow steps 3-5 of XIII-2, "Reactor Handbook".(64) Note that it may be necessary to completely remove the water level sight glass from the reactor wall in order to get the coffin into proper location.

6. Follow Steps 1-6 of XIII-3, "Reactor Handbook".(64)

7. Using the grappling hook and hand force only, push the plug assembly out of the coffin and into the beam-port. Do not force the assembly if it binds. In most cases, binding is caused by improper alignment of the coffin. This is a very tedious adjustment, and usually many corrections are necessary to get the proper position.

8. Remove the coffin unit.

9. Place lead liner in position on the end of the shielding plug and bolt the aluminum cover flange into position.

10. Complete all tubing and electrical connections passing into beam-port.

11. Place any lead shielding in vestibule that is thought to be necessary.

12. Close lead door to within 1" of the bottom so as to allow for tubing and wires.

13. In order to operate the pile, it is necessary for the operator to defeat the safety interlock connected to the open beam-port door.

14. Place tape over the water-fill valve so that there is no possibility of accidental filling of the port.

15. Notify the reactor staff upon completion of this operation.

B. Unloading the Apparatus

1. Unloading is covered in detail on page XIII-2 of the "Reactor Handbook"(64), but one change has been found helpful. In most cases it is better to get the coffin into position in front of the port before the lead port door is opened; i.e., Step 2 should be placed after Step 5. Other additions already noted in Section A will, of course, also apply to unloading.

2. If it is necessary to remove the radioactive vessel from the plug, the recommended procedure is to first allow some time for cooling in the storage area. Then pull the shielding plug section into the coffin unit, leaving a gap of about 6" between the front of the coffin and the storage area wall. In this manner, the vessel itself is left in the storage port and the connecting pipes and wires are visible through the gap described above. These parts should not be too hot, and a person standing to one side of the coffin could easily cut the tubing and wires with a hack saw without ever being in a direct line with the radioactive pressure vessel. It might even be possible, though difficult, to break the tubing connections with long-handled wrenches. Once the tubing and wires are broken, the coffin should be pushed tightly against the wall. Then rotate the plug by means of the grappling hook 180° so that the aluminum support for the pressure vessel is above the vessel. The vessel should easily fall away from the support and the plug can now be pulled directly out, leaving the vessel in the storage port.

APPENDIX F

INITIAL CHECK-OUT OF THE PILOT UNIT

Several precautions were taken when the pressure vessel was first placed in the beam-port of the Ford Nuclear Reactor to insure safe operation.

First, a nuclear reactivity experiment was performed to be sure that the pressure vessel was not tying up a large amount of reactivity[24,32] To do this, the three safety rods were set at a constant position and the control rod setting was adjusted until the reactor barely went critical (indicated by a vertical line on the linear level recorder). The control rod position was recorded before and after insertion of the pressure vessel. Data from this experiment is shown below:

Safety Rod	Reading (inches)
A	13.74
B	13.62
C	13.98
Control Rod	
Before insertion	25.25 ± 0.02
After insertion	25.19 ± 0.02

Thus, the pressure vessel involved a maximum reactivity equivalent to p.1 inches of the control rod or 0.0019% k excess.[63] This was not considered large enough to present a serious safety problem.

In addition to the reactivity experiment, the unit was checked out by a series of low level runs intended to gradually and safely work up to the desired operating range. To do this, the pile was operated for several hours at power levels of 10, 50 and 100 KW. At each of these levels, a number of runs were performed with the chemical unit starting

in each case at low temperatures and pressures and gradually working toward the desired maximum conditions.

APPENDIX G

ANALYSIS TECHNIQUES FOR THE HYDROGEN-HEPTANE SYSTEM

I. Liquid Samples

All liquid samples were analyzed by means of a commercial "Fisher-Gulf Partitioner", type 11-130 (for details, see Fisher Scientific Co. Bulletin FS-255). A trimetacresyl phosphate - fire brick packing was used in the "Partitioner" column along with helium carrier gas. 0.2 ml samples were injected into the column by means of a capillary syringe. In order to pass the heavy, less volatile hydrocarbon through in a reasonable time, all liquid samples were run at 120°C, but the helium rate was varied from 25 to 50 ml/min depending on the accuracy of resolution desired. Each analysis required about 20 minutes at the higher flow rate.

A number of pure substances were run in the "Partitioner" in order to calibrate it under operating conditions, and retention times obtained from these runs are given in Table XIX. A plot of log retention time versus the number of carbon atoms is shown in Figure 47. Figure 48 shows a typical graph obtained from the "Partitioner".

Several general references dealing with the theory and use of partition chromatography as an analytic technique are included in the bibliography.(16,39)

II. Definition and Significance of Liquid Conversion

The terms "liquid phase conversion" and "liquid conversion" are used throughout this report to represent the mole percent cracked

TABLE XIX

RETENTION TIMES FOR THE FISHER-GULF PARTITIONER
(FOR 120°F, 41 c.c. HELIUM/MIN., AND A TRIMETACRESYL PHOSPHATE -- FIREBRICK COLUMN)

Substance	Time (min)	Relative times (ethylene = 1.0)	(n-pentane = 1.0)
methane	1.4	--	
propane	1.5	--	
propylene	1.6	1.0	
ethylene	1.6	1.0	
isobutane	1.7	1.06	
butane	1.9	1.09	
butene-1	2.1	1.31	
isopentane	2.1	1.31	
n-pentane	2.13	1.33	1.0
2,3 dimethylbutane	3.25	2.05	1.55
methylbutane	3.3	2.06	1.57
isohexane	3.4	2.12	1.62
n-hexane	3.75	2.35	1.78
methylcycopentane	4.6	2.88	2.19
2,2,4-trimethylpentane	5.0	3.20	2.38
acetone	5.5	3.44	2.62
isoheptane	5.75	3.6	2.74
n-heptane	6.25	3.91	2.98
iso-octane	9.13	5.7	4.35
methylyclohexane	9.38	5.87	4.46
n-octane	11.13	6.95	5.38
benzene	13.0	8.13	6.1
toluene	24.5	15.3	11.7

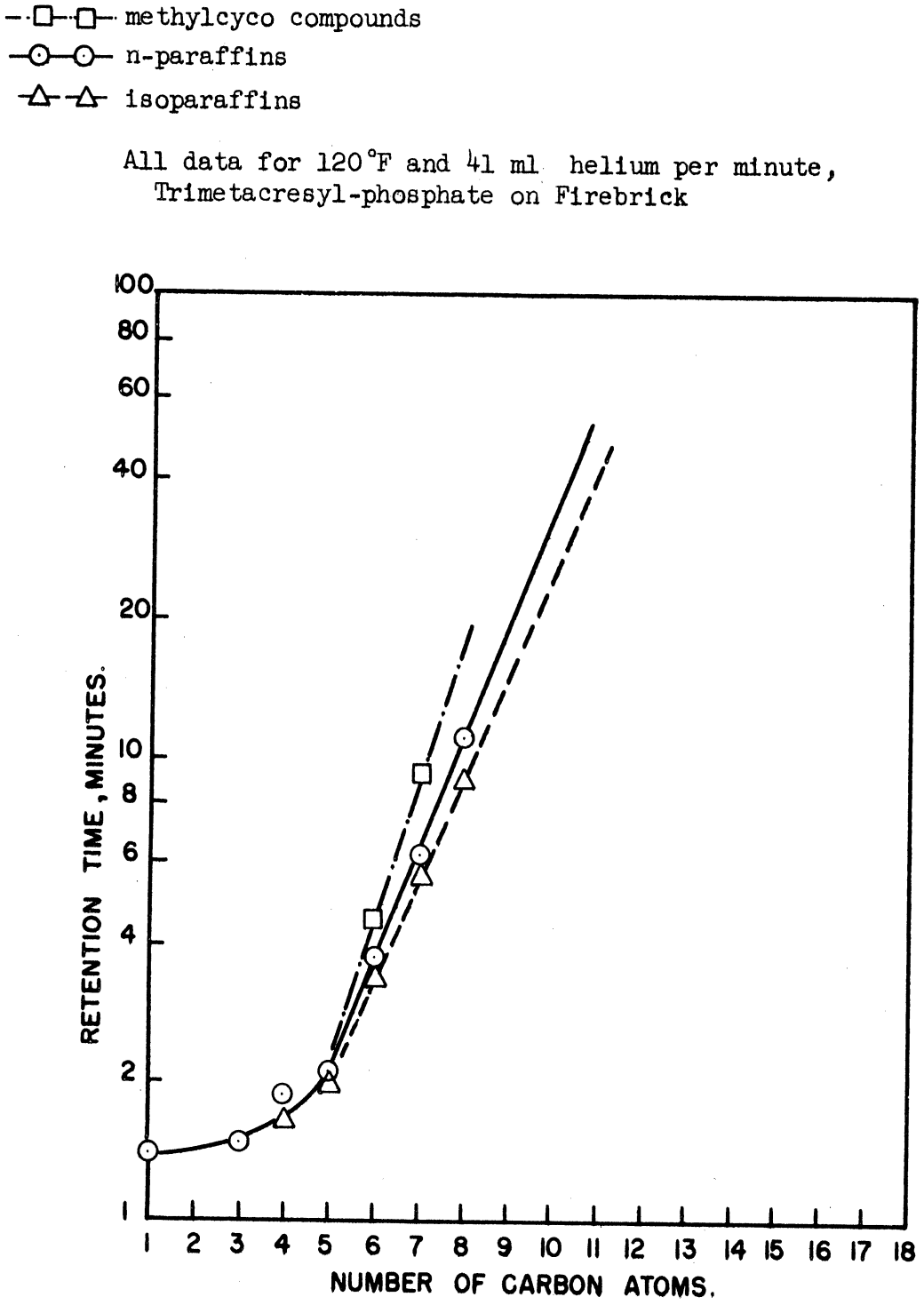

Figure 47. Fisher-Gulf Partitioner Calibration

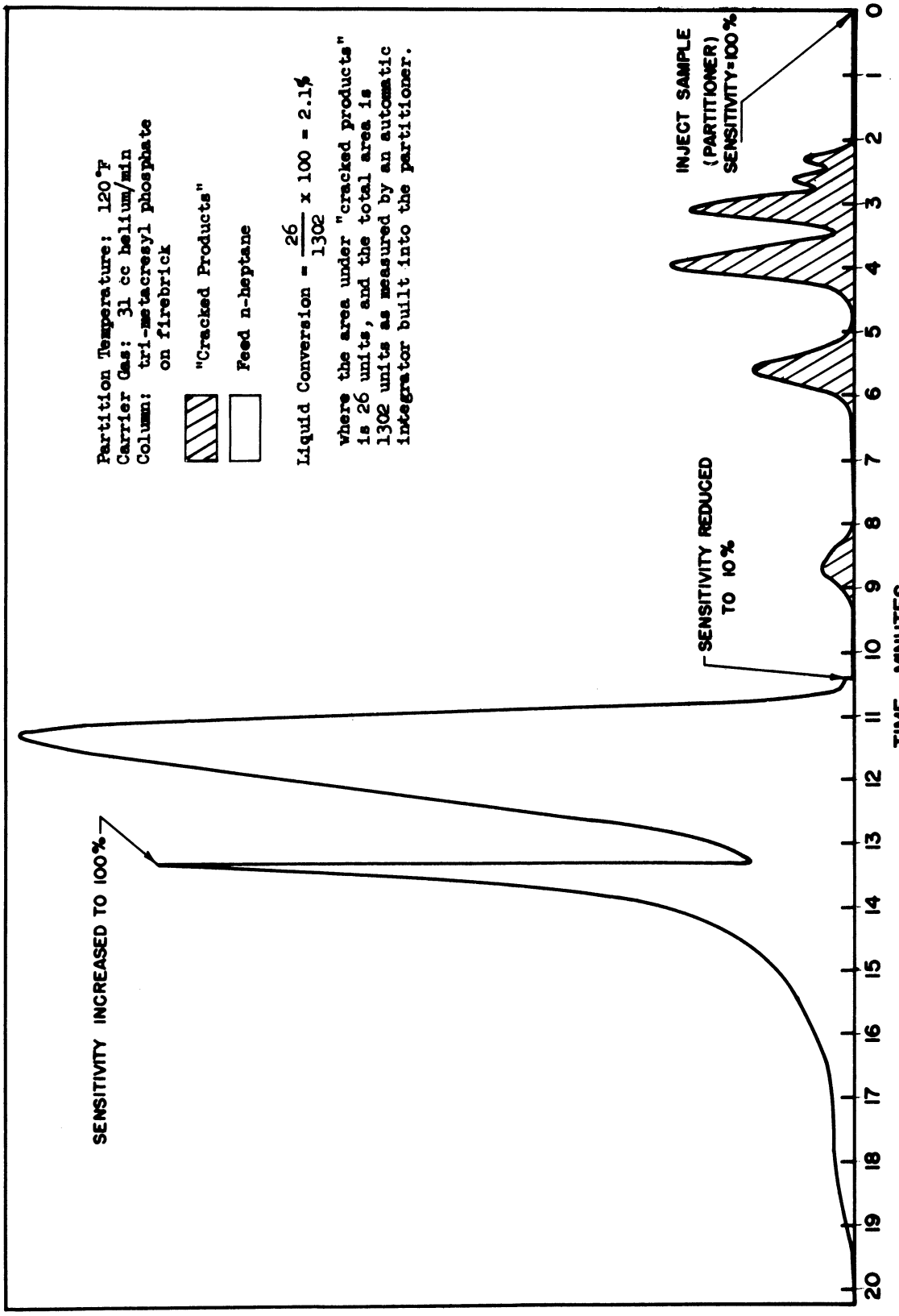

Figure 48. A Graph from the Analysis of the Liquid Sample from Run 14 Using a Fisher-Gulf Partitioner

hydrocarbons in the liquid product. This percentage was calculated from gas phase chromatography data by the following formula:

$$\frac{\text{Area Under Peaks Due to Cracked Hydrocarbons}}{\text{Total Area Under the Curve}} \times 100 = \% \text{ Liquid Conversion} \qquad (63)$$

Figure 48 shows a typical chromatography graph and calculation. The "peaks due to cracked hydrocarbons" are defined as any peaks which appear in the product analysis and not in the feed analysis. In all cases, a feed sample was run along with the product samples to insure that impurities were not present in the feed. The series of cracked hydrocarbons shown in Figure 48, all of which are lighter than heptane, are the only products detected from any run - i.e., any heavier hydrocarbons produced either coked out in the reaction vessel or were of such low concentration that they went undetected.

Ideally, both liquid and gas samples should be analyzed for every run, and the heptane conversion computed from a material balance. However, in the present work, a number of very low yield runs were performed with a high hydrogen to hydrocarbon ratio. This resulted in extremely dilute gas samples (i.e., only a trace of hydrocarbon product in a large volume of hydrogen). As already discussed, the only satisfactory method of analysis of these samples was with the mass spectrometer. Even so, the absolute amount of a given hydrocarbon in many very dilute samples could not be determined with great accuracy.

Thus, in order to get around these difficulties and to avoid the expense of analyzing gas samples from all 72 runs, the liquid

conversion was chosen as a measure of the actual conversion. It is an easy, cheap measurement, and was found to be fairly accurate.

The actual n-heptane conversion was computed from a material balance for runs where gas samples were taken in addition to liquid samples and where the conversion was high enough to allow reasonable accuracy in the calculation of the yield for individual components (see Appendix B). These calculations show that the liquid conversion is numerically equal to the normal heptane conversion for the present work. This means that for the sampling conditions and low conversions used in this work, the decomposition of one molecule of n-heptane produced, on the average, one molecule which remained in the liquid phase. It must be noted, however, that in order to make these material balances, certain assumptions were necessary about the identity of the various liquid peaks. In essence, it was assumed that all compounds with a given number of carbons (i.e., saturate, unsaturate, etc.) were lumped together under one peak in the chromatograph analysis. As seen from the observed retention times for pure substances, Table XIX, this appears reasonable, and the 6 peaks obtained in liquid analysis would correspond then to C_1 through C_6 hydrocarbons respectively. In light of these assumptions the correlation of liquid conversion to the actual normal heptane conversion is only considered good to $\pm$ 20%.

III. Gas Samples

All gas samples were analyzed by Mr. David Brown (Supervisor, Department of Chemical Engineering, Spectroscopic Analytical Laboratory) with an analytical mass spectrometer (Consolidated Electro Dynamics

Model No. 21-103-C). References covering general aspects of hydrocarbon analysis in this manner are included in the bibliography.[4,47]

For the low molecular weight hydrocarbons, the machine was calibrated with pure samples and average cracking patterns were assumed for the heavier compounds with the exception of n-heptane for which an actual sample was available. The mass spectrum of the unknown samples was then resolved by the standard technique of solving a system of simultaneous linear equations with an analog computer.

A number of checks of this procedure were made. "Pealing" (artichoke) and "lumping" techniques were used to check agreement. A synthetic mixture was analyzed to check out the analog matrix (Mass Spectrometer Log Book, Run 4575), and saturate to unsaturate ratios were re-checked with a gas chromatography unit (25 ft of coil with di-isodecyl-phthalate on firebrick).

In general, reasonable accuracy was obtained for most samples despite the very low percentages of hydrocarbons. However, some of the extremely low yield samples did show some large deviation. This difficulty was probably caused by the presence of relatively large amounts of heavier hydrocarbons and normal heptane in the samples. The mass spectrometer actually cracks these compounds in an analysis and, hence, the yields of the lighter hydrocarbons formed in this manner must be subtracted out of the total quantity recorded for each hydrocarbon. These differences are obviously less accurate for a high ratio of heavy to light hydrocarbon in the sample.

Future analyses might be obtained with increased accuracy if the samples were cut into suitable fractions before being run on the

mass spectrometer. One method of doing this is to trap fractions coming out of a chromatography unit and run them on the mass spectrometer.

APPENDIX H

REPRODUCIBILITY OF REACTION CONDITIONS

I. Temperature

Temperature control is extremely important in cracking experiments since the decomposition rate is a marked function of temperature. Ideally, reaction studies should be run under isothermal conditions. But as seen from Table VIII, a definite temperature profile was obtained along the length of the reaction vessel used in the present studies. This profile was mostly the result of operating the vessel at 250 psig instead of the design pressure of 1000 psig. (The reasons for the reduction in pressure were discussed in Chapter I). In fact, the preliminary runs, numbered 1 through 4, made before this pressure reduction, demonstrate a reasonably constant longitudinal temperature.

However, since radiation studies involve differences between radiation and blank runs, valid results can still be obtained if the temperature profile does not change from run to run.

Figure 49 compares temperature profiles for a typical series of runs. It is seen that radiation and blank runs have comparable profiles. A cross plot of this graph is presented in Figure 50 showing all thermocouple readings as a function of the reading for thermocouple No. 1. A linear plot is obtained showing that the profile is independent of the temperature level.

Temperature readings were recorded approximately every 5 minutes during a run (maximum variation $\pm$ 5°F), and the figures given in Table VIII for each thermocouple represent an average of all

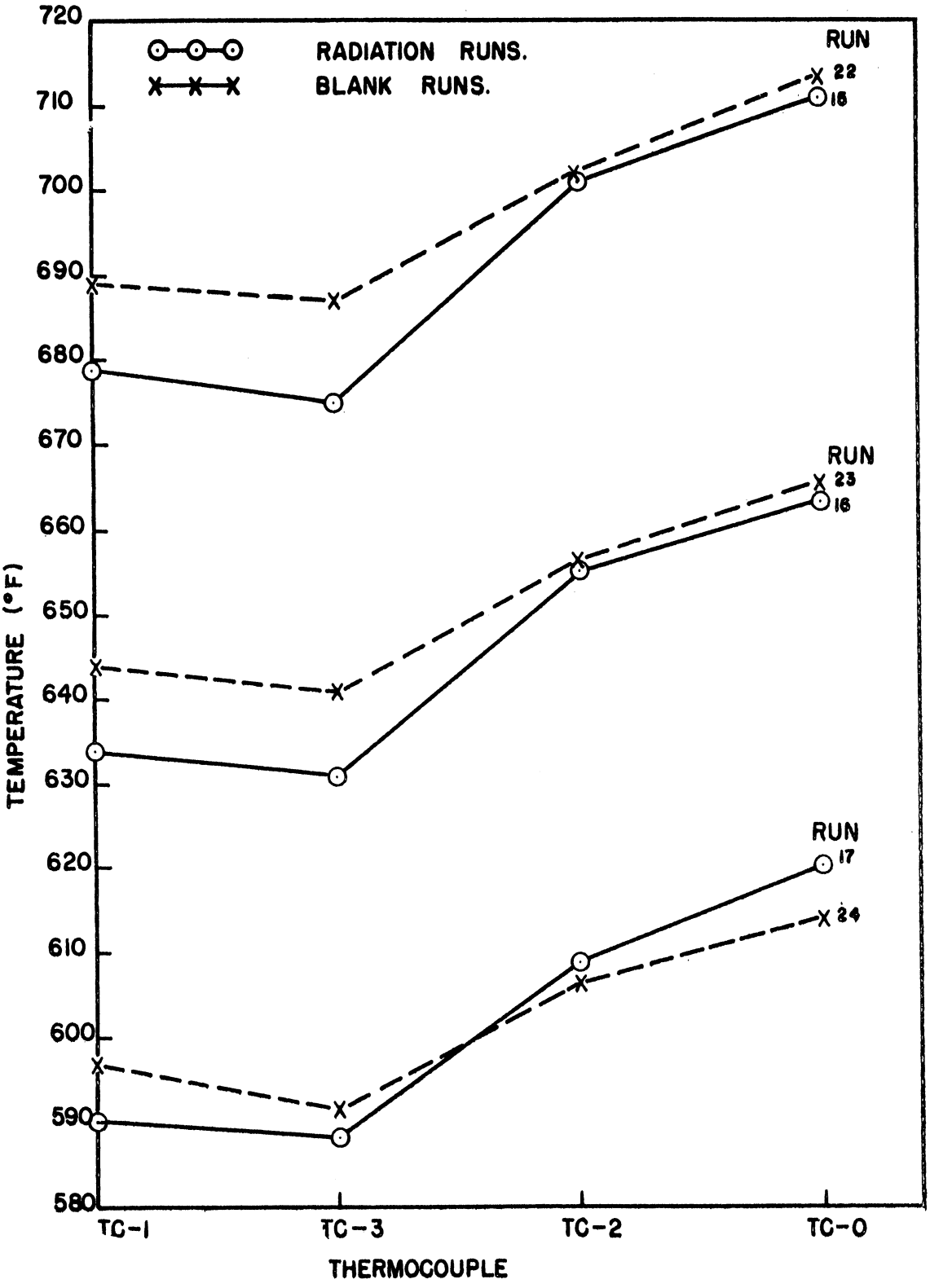

Figure 49. Comparison of Temperature Profiles for Radiation and Blank Runs

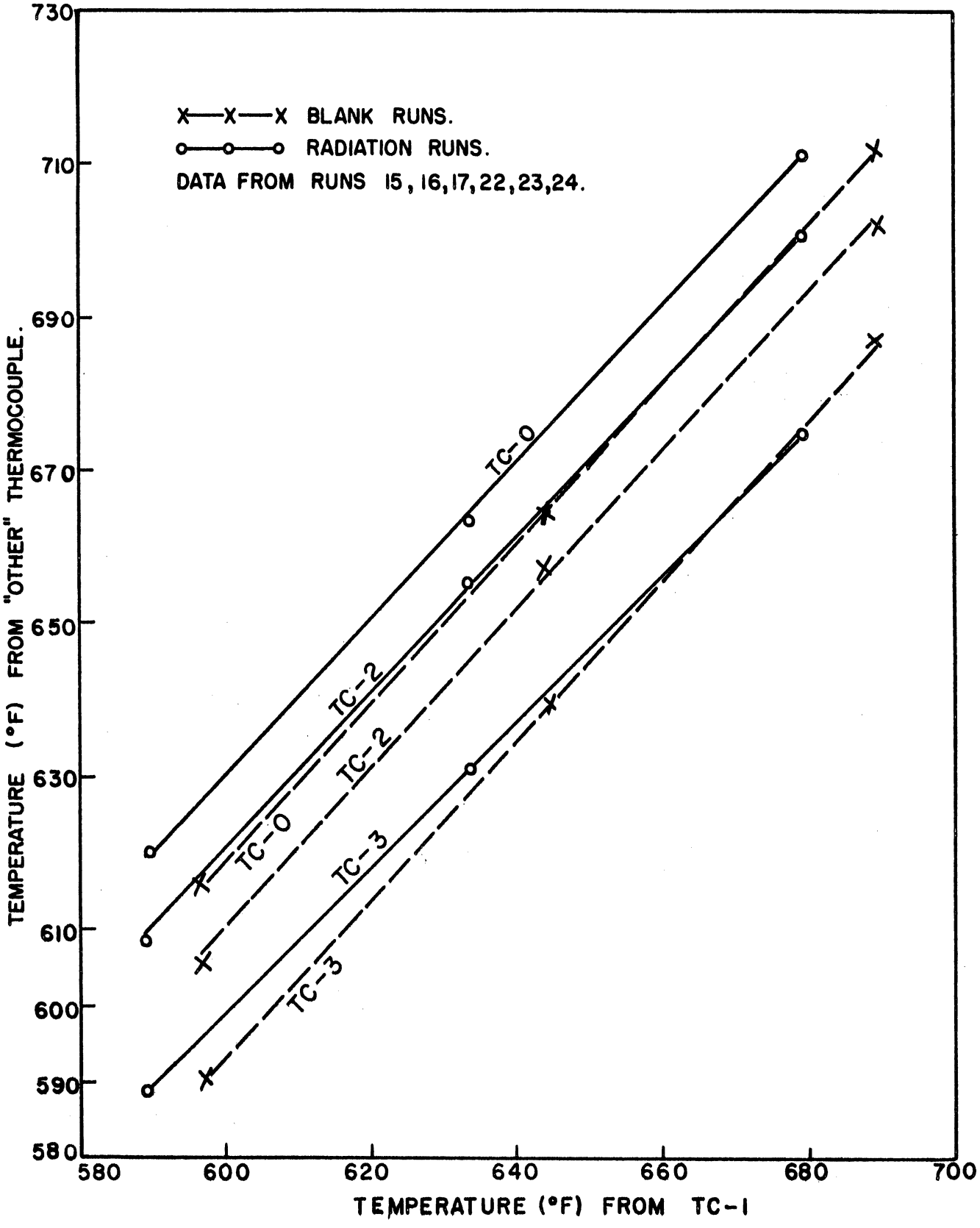

Figure 50. Comparison of Temperature Profiles at Different Temperature Levels

readings taken during a run. Since the four thermocouples located inside the pressure vessel (TC-0, TC-1, TC-2, and TC-3) were equally spaced along the length of the vessel, the average temperature for a run was computed by averaging their readings. The two thermocouples on the outside shell of the pressure vessel (TC-5, TC-6) and the thermocouple wired to the outside of the product outlet tube (TC-4) are not included in this average. Due to temperature gradients in the wall their readings are not representative of the fluid temperature. Also, because of their location near the external tape heaters, large variations in readings occurred with changes in the heat settings.

Since the temperature profile is relatively constant, the arithmetic average temperature is a valid basis for the internal comparison of a series of runs. However, since the reaction rate is not a linear function of temperature, the use of such an average introduces a small constant error in the absolute reaction yield for any given temperature. This error is not considered large enough to be significant in the present exploratory type work.

The validity of a thermocouple reading in a radiation field is always open to question. One possible source of error is the heating of the thermocouple bead due to radiation absorption. Another is actual radiation damage to the thermocouple materials. The thermocouples used in the present work were checked after run 72 by running steam through the pressure vessel with the nuclear reactor at 100 KW. Readings of 212 $\pm$ 3 °F were observed.

II. Pressure

The pressures listed have been averaged over the run time. Variations up to ± 10 psi occurred, mostly as a result of sampling operations. Theoretically, yields should not be a strong function of pressure so that these small variations would not be expected to seriously effect the accuracy of the results.

III. Reactor Power Level

The reactor power level was maintained at 100 ± 5 KW. Again, variations of this magnitude are not considered significant.

IV. Flow Rates

Variations of up to 5% occurred in the gas rate. The values presented in this report have been averaged over the time of the run.

Hydrocarbon flow rates were relatively constant throughout a given run due to the use of a metering pump. However, variations as high as 10% were measured from run to run.

APPENDIX I

SOME SUGGESTION FOR FUTURE WORK

I. Safety Features

A larger pressure vessel outlet line is recommended for future designs. This would permit a quicker pressure release in the event of a sudden pressure build-up than is possible with the present one-quarter-inch outlet. In order to install a larger outlet, however, the entire shielding plug must be redesigned with larger access tubes.

Additional safety might be achieved through the use of a pile scram interlock in conjunction with critical variables such as temperature and pressure. This interlock would automatically scram the pile if either the temperature or pressure in the reaction vessel exceeded some preset level. In general, though, care should be exercised in the selection of such interlocks. If a number of different experiments are tied into the reactor through interlocks, unless discrimination is used in selection of the interlocks, the pile operation may be impaired by unnecessary scrams.

II. Dosimetry

As pointed out in Chapter III, dosimetry techniques now available areinadequate for precise measurement of pile radiation. A more accurate technique and one which indicates an energy breakdown for gamma and neutron radiation is desirable. One promising line of research is concentrated on developing a chemical system such as benzene-water to which a neutron sensitive additive can be added.(34) For example, thermal

neutron utilization can be increased by the addition of a cadmium salt which will undergo a (n,γ) reaction.

A gas phase chemical dosimeter would be useful in conjunction with vapor phase cracking studies. It would closely duplicate the flow pattern, and hence residence time distribution for the system under study. If such a dosimeter is not developed, a residence time distribution study for the reaction vessel should be undertaken. This could be done with standard tracer techniques.

Some thought should be given to the possibility of making continuous flux measurements during a run. For example, a thermopile[32] or small ionization chamber[23] might be calibrated and placed directly into the beam hole with the reaction vessel. Actually, the flux for a given reactor core configuration is relatively constant throughout a run. However, if the core configuration is changed often (which is possible with the Ford Reactor) it would be easier to have an internal ionization chamber than recalibrate the port with gold foils, etc. for each configuration. Another possible method of obtaining continuous dose measurements would be to use a flow chemical dosimetry system in the pressure vessel cooling coil.

III. Unit Design

The present apparatus has proved, in general, to be very satisfactory. However, some minor changes should be considered if a new pressure vessel is built in the future. Experience has shown that the six-inch ports are much easier to load and unload than are the eight-inch ports. Also, since there are ten six-inch ports as opposed to only two

eight-inch ones, a larger variety of irradiation positions are available with the small ports. For these reasons, if construction problems are not too severe, there is a definite incentive to build a pressure vessel to fit the six-inch ports. In fact, as already discussed in Chapter II, if available, the ideal ports for flow irradiation experiments are the two six-inch through ports.

A future pressure vessel should be designed for isothermal operation. A temperature gradient developed in the present vessel during runs at pressures below the design pressure. Even though comparative results are possible if the gradient does not change, a gradient is undesirable because of the problem of calculating some average temperature which is actually representative of the reaction rate obtained. Apparently, the present vessel needed more insulation on the core end and additional wall heating capacity at this point. Probably the wall heating capacity should be increased but divided into sections which can be controlled separately.

The general philosophy of using a calrod heater inside the vessel for compactness and efficient heat transfer appears sound and might be included in future designs. Ideally, automatic control could be improved if two calrod heaters were used. One would have a high heat output and be on at all times during a run, although its output would be regulated manually by a powerstat. The second heater would only have a small output and would be connected to the temperature recorder controller. The on-off action of the small heater would afford control but not cause large fluctuations. This would be an improvement over the present set up where lengthly and tedious manual adjustments of the powerstats were necessary to gain a proper balance to minimize control flucuations.

IV. Other Approaches and Systems

Since the use of nuclear radiation to induce chemical reactions has only recently received widespread attention, many areas of research have yet to be investigated. Two general approaches, however, appear important at this stage of development. First, basic research aimed at a fundamental understanding of the interaction of radiation and matter to produce chemical reactions is needed. Secondly, an exploratory program aimed at developing methods for increasing radiation efficiency appears desirable.

Numerous fundamental aspects of radiation-induced chemical reactions have yet to be explored. For example, the comparative effects of various types of radiation, the effect of radiation energy level, and dose rate effects have not been thoroughly studied.

Obviously, extensive facilities are needed for comprehensive studies of this nature. Machine radiation sources are necessary in addition to reactor sources for some of this work. An interesting program possible at the Phoenix Memorial Laboratory would revolve around duplicating experiments using a reactor beam port, the cobalt-60 source, and the reactor thermal column. Perhaps one of the most interesting experiments would be to place a reaction vessel directly in the reactor core (a fuel element could be removed and the vessel inserted). However, thus far, safety considerations have prohibited this.

Although these facilities make a number of types of radiation available, there are some experimental difficulties in obtaining meaningful results. Perhaps the biggest problem is the difference in source intensity. For example, extremely long residence times would be required

in the thermal neutron column to obtain a significant yield because the dose rate is low. This practically rules out high-temperature work because the thermal-cracking would completely mask the radiation contribution. However, it might be interesting to perform some experiments about 50°F below the initial thermal-cracking temperature and use very long residence times.

It is apparent that in order to use radiation for economical chemical production, some method of increasing the radiation efficiency is needed. For reactions other than polymerization, the yields are much too low to warrent commercial interest. In a nuclear reactor, much of the radiation energy is not absorbed by the system or is ineffective in producing a reaction. One of the most promising approaches to increasing efficiencies has been the insertion of a fissionable material such as UO_2 directly into the reaction vessel.[27] This converts the comparatively ineffective thermal neutron flux to highly effective fission fragments. Previously fission fragment experiments have been restricted to relatively low temperatures. A logical extension would be to carry out high-temperature experiments similar to the present investigation with n-heptane.

Another possible method of increasing the utilization of thermal neutrons is the addition of some compound which will absorb thermal neutrons and in turn emit some form of effective ionizing radiation. Boron and cadmium are examples.

A solid such as cadmium can be used in the form of a plate or needles immersed in the reaction mixture or a metallic salt can be dissolved in the mixture. Needles do not afford as good distribution of the

absorber as direct solution of the salt, but the latter method results in the need of a purification step for the product. An interesting alternative would be to use a neutron absorbing gas. This would afford intimate mixing and the gas could easily be stripped from the liquid product.

Very low temperature irradiation represents another whole area of work which deserves investigation and which might afford a method of increasing radiation yields. It has been found that for some systems radicals formed during low temperature irradiation can essentially be stored at the reduced temperature and used for "seeding" a reaction. It might be possible to carry out n-heptane irradiation inside the nuclear reactor at -100°C, and then initiate a chemical reaction outside of the pile with the long-lived free radicals thus formed.

BIBLIOGRAPHY

1. Appleby, W. G., Avery, W. H., and Meerbott, W. K., "Kinetics and Mechanism of the Thermal Decomposition of n-Heptane," Journal of the American Chemical Society, 10, No. 10, 2279 (1947).

2. Babcock and Wilcox Design Blueprints for the University of Michigan Reactor, Job No. G.M.-46429.

3. Back, N., "Radiolytic Oxidation of Organic Compounds," Nucleonics, 51, No. 10, 478 (1955).

4. Barnard, G. P., Modern Mass Spectrometry, Institute of Physics, London (1953).

5. Bopp, C. D. and Sisman, O., "How to Calibrate Gamma Radiation Induced in Reactor Material," Nucleonics, 14, No. 1, 46 (1956).

6. British Patent Number 708901 Assigned to the Standard Oil Company of New Jersey, May 12, 1954.

7. Burton, Milton, "An Introduction to Radiation Chemsitry," Journal of Chemical Education, 28, No. 8, 404 (1951).

8. Burton, Milton, "Radiation Chemistry," Journal of Physical and Colloid Chemistry, 52, 564 (1948).

9. Burton, Milton, "Effects of High-Energy Radiation on Organic Compounds," Journal of Physical and Colloid Chemistry, 51, 611 (1947).

10. Calkins, V. P., "Radiation Damage to Nonmetallic Materials," Chemical Engineering Progress Symposium Series, 50, No. 12, 28 (1954).

11. Charlesby, A., "Irradiation of Long-Chain Polymers," Nucleonics, 51, No. 10, 477 (1955).

12. Charlesby, A., "The Cross Linking and Degradiation of Paraffin Chains by High-Energy Radiation," Proceedings of the Royal Society of London, A222, No. 1148, 60 (1954).

13. Charlesby, A., "The Effect of Ionizing Radiation on Long-Chain Olefins and Acetylenes," Radiation Research, 2, No. 1, 96 (1955).

14. Charlesby, A., "Review of Atomic Radiation Treatment of Polymers," Radiation Research, 2, No. 8 (1955).

15. Chemical and Engineering News, "The Atom's Role in the Chemical Industry," p. 919 (Feb. 27, 1956).

16. Chemical and Engineering News, "Gas Chromatography Growing," p. 1692 (April 9, 1956).

17. Colichman, E. L. and Gercke, R. H. J., "Radiation Stability of Polyphenyls," Nucleonics, 14, No. 7, 50 (1956).

18. Collinson, E. and Swallow, A. J., "Review of the Effect of Ionizing Radiation on Organic Compounds," Quarterly Reviews, 9, No. 4, 311 (1955).

19. Dewhurst, H. A., "Radiation Chemistry of n-Hexane and Cyclohexane," Journal of Chemical Physics, 24, No. 6, 1254 (1956).

20. Dondes, S. and Harteck, P., "Producing Chemicals with Reactor Radiations," Nucleonics, 14, No. 7, 22 (1956).

21. Fano, U., "Gamma Ray Attenuation, Part I," Nucleonics, 11, No. 8, 8 (1953).

22. Fano, U., "Gamma Ray Attenuation, Part II," Nucleonics, 11, No. 9, 55 (1953).

23. Fehr, E. B., "Neutron Detectors for High Temperature Applications," Nuclear Engineering and Science Conference, Preprint 123, Chicago, Illinois, (March, 1958).

24. Glasstone, S., and Edlund, M. C., The Elements of Nuclear Reactor Theory, D. Van Nostrand Company, Inc., New York, 1952.

25. Greensfelder, B. S. and Voge, H. H., "Catalytic Cracking of Pure Hydrocarbons," Industrial and Engineering Chemistry, 37, No. 6, 514 (1945).

26. Hammond, P. R., "Chemical Processing in Intense Radiation Fields," Nucleonics, 51, No. 10, 474 (1955).

27. Harteck, P., and Dondes, S., "Producing Chemicals with Reactor Radiation," Nucleonics, 14, No. 7, 22 (1956).

28. Heath, R. L., Scintillation Spectrometry and Gamma-Ray Spectrum Catalogue, AEC Research and Development Report, IDO-16408 (July, 1957).

29. Heitler, W., The Quantum Theory of Radiation, Oxford University Press, London, England (1954).

30. Henley, E. J., Barr, N. F., Thompson, S., and Johnson, E. R., "Scale-up of Radiation Effects," Chemical Engineering Progress, 54, No. 6, 69 (1958).

31. Honig, R. S. and Sheppard, C. W., "An Experimental Comparison of the Chemical Effects of Deutrons and Alpha Particles on Methane," Journal of Physical Chemistry, 50, No. 2, 119 (1946).

32. Hughes, D. J., "Pile Neutron Research," Addison-Wesley Publishing Company, Inc., Cambridge, Mass., 1953.

33. Hughes, D. J. and Harvey, J. A., "Neutron Cross Sections," BNL 325 (July, 1955).

34. Johnson, T. R., "The Effect of Nuclear Radiation on the Benzene-Water Systems," Ph.D. Thesis, Department of Chemical Engineering, University of Michigan, Ann Arbor, Michigan, 1958 (to be published).

35. Kaplan, I., Nuclear Physics, Addison-Wesley Publishing Company, Inc., Cambridge, Mass., p. 326 (1955).

36. Keenan, V. J., Atlantic Refining Company, Research and Development Department, Private Communication (April 25, 1958).

37. Krentz, F. H., "Radiolysis of Liquid n-Hexane and Solutions of Anthracene in n-Hexane," Nature, 176, 1113 (1955).

38. Lemmon, R. M. and Tolbert, B. M., "Radiation Decomposition of Pure Organic Compounds," Radiation Research, 3, No. 1, 52 (1955).

39. Lichtenfels, D. H., Fleck, S. A., and Burrows, F. H., "Gas-Liquid Partition Chromatography," Analytical Chemistry, 27, 1510 (1955).

40. Lucchise, P. J., Tarmy, B. L., Long, R. B., Baeder, D. L. and Longwell, J. P., "High Temperature Radiation Chemistry of Hydrocarbons," Industrial and Engineering Chemistry, 50, No. 6, 879 (1958).

41, Magat, M., Prevost-Bernas, Mrs. A., Chapiro, A., Cousin, C., and Lander, Y., "Proposed Systematic Study of Radiation Effects," Discussion of the Faraday Society, 12, 98 (1952).

42. Manowitz, Bernard, "The Industrial Future of Radiation Chemistry," Nucleonics, 11, No. 10, 18 (1958).

43. Marion, J. P., Burton, M., "Radiolysis of Hydrocarbon Mixtures," Journal of Physical Chemistry, 56, No. 5, 560 (1952).

44. Martin, J. J., "The Use of Radiation to Induce Chemical Reactions," Chemical and Engineering News, 33, No. 4, 1425 (1955).

45. Martin, J. J., "Where We Stand in Radiation Processing," Chemical Engineering Progress, 54, No. 2, 66 (1958).

46. Martin, J. J, and Anderson, L. C., "A Review of Radiation Polymerization," Modern Plastics, 32, No. 3, 94 (1955).

47. Mitchell, J. J., "Mass Spectroscopy in Hydrocarbon Analysis," Section in Farkas, A., Physical Chemistry of the Hydrocarbons, 1, Academic Press, New York (1950).

48. Nucleonics, 12, No. 12, 62 (1955). "Storing Radiation Effects by the Use of Low Temperature Radiation Processes."

49. Nucleonics, 16, No. 9, 89 (1958). "Radiation Sources."

50. Prevost-Bernas, Mrs. A., Chaprio, A., Cousin, C., Landler, Y., and Magat, M., "The Radiolysis of Some Organic Liquids," Discussion of the Faraday Society, 12, 103 (1952).

51. Rock Island Arsenal Laboratory, "High Energy Radiation of Polymers, a Literature Review," OTS PB111529 (November, 1953).

52. Sachs, F., "A Literature Search - The Effect of Radiation on Organic Compounds," ORNL Y-904 (Aug. 18, 1952).

53. Schoeder, M. C., Daniels, D. J., Foley, and Filbert, R. B., Jr., "Design and Construction Criteria for In-pile Experimental Chemical Reactors," Battelle Memorial Institute. Presented at the Annual A.I.Ch.E. Meeting, Chicago, Illinois, December, 1957 (to be published).

54. Schuler, R. H., and Allen, A. O., "Radiation-Chemical Studies with Cyclotron Beams," Journal of American Chemical Society, 77, 507 (1955).

55. Sisler, H. H., Vanderwerf, C. A., and Davidson, A. W., General Chemistry, The MacMillan Co., New York (1949).

56. Sisman, O. and Bopp, C. D., "Physical Properties of Irradiated Plastics," ORNL 928 (June 29, 1951).

57. Sisman, O. and Bopp, C. D., "Physical Properties of Irradiated Plastics," ORNL 1373, 68 (July 23, 1953).

58. Snow, A. I., Uhl, G. A., and Lewis, J. G., "Effects of Gamma Irradiation on Some Hydrocarbon Reactions in a Flow System," Preprint from a paper presented at the Miami Meeting of the American Chemical Society, Symposium on Nuclear Technology in the Petroleum and Chemical Industries (1957).

59. Stephenson, R. S., Introduction to Nuclear Engineering, McGraw-Hill Book Company, Inc., New York, 2nd Edition, p. 347 (1958).

60. Trice, J. B., "Measuring Reactor Spectra with Thresholds and Resonances," Nucleonics, 16, No. 7, 81 (1958).

61. University of Michigan Reactor Advisory Committee, Personal Communication, June 6, 1958.

62. University of Michigan Reactor Advisory Committee, Personal Communication, July 8, 1958.

63. The University of Michigan Memorial Phoenix Project, "Initial Calibration of the Ford Nuclear Reactor," MMPP-110-1, Ann Arbor, Michigan, June, 1958.

64. The University of Michigan Memorial Phoenix Project Handbook, "The Ford Nuclear Reactor -- Description and Operation," Ann Arbor, Michigan, June 1957.

65. The University of Michigan Memorial Phoenix Project Pamphlet, "The Ford Nuclear Reactor," Ann Arbor, Michigan, November, 1956.

66. The University of Michigan Memorial Phoenix Project, "Reactor Operation Log." (This book is on file at the Phoenix Building, University of Michigan, Ann Arbor, Michigan).

67. Wahl, E. F., III, "Effect of Radiation on Chemical Reactions," M.S. Thesis, Department of Chemical Engineering, Massachusetts Institute of Technology, Cambridge, Mass. (1955).

68. Weber, E. N., Forsyth, P. F., and Schuler, R. H., "Radical Production in the Radiolysis of the Hydrocarbons," Radiation Research, 3, No. 1, 68 (1955).